Interactome study of the *Giardia intestinalis* nuclear localized cytochrome b_5

A Thesis Submitted to the Committee on Graduate Studies in Partial Fulfillment of the Requirements for the Degree of Master of Science in the Faculty of Arts and Science

TRENT UNIVERSITY

Peterborough, Ontario, Canada

Environmental and Life Sciences M.Sc. Graduate Program

May 2022

Abstract

Interactome study of the *Giardia intestinalis* nuclear localized cytochrome b_5

G. William Batoff

Giardia intestinalis is a waterborne enteric parasite that lacks mitochondria and the capacity for heme biosynthesis. Despite this, Giardia encodes several heme proteins, including four cytochrome b_5 isotypes (gCYTB5-I – IV) of unknown function. The aim of this thesis is to gain insight into the function of the Giardia cytochrome b_5 isotype III (gCYTB5-III) that is found in the nucleus, as first reported by our laboratory using immunofluorescence microscopy experiments with an isotype-III specific antibody. Nuclear localization of isotype-III is supported by two of my experiments: i) immunoblot analysis of crude cytoplasmic and nuclear enriched fractions of Giardia trophozoites; ii) association of gCYTB5-III with the insoluble fraction of Giardia lysates crosslinked with formaldehyde is reversed by DNase I treatment. To gain an understanding of the possible roles of gCYTB5-III, I performed immunoprecipitation (IP) experiments on lysates from Giardia trophozoites to identify its protein partners. Mass spectroscopy analysis of the immunoprecipitate identified proteins localized to the nucleus (RNA polymerase, DNA topoisomerase, histones, and histone modifying enzymes). Intriguingly, over 40% of the known mitosomal proteome, which functions in iron-sulfur (Fe-S) cluster assembly was also associated with gCYTB5-III. One of these proteins, the flavoenzyme GiOR-1, has been shown to mediate electron transfer from NADPH to recombinant gCYTB5-III. These IP results provide evidence that GiOR-1 and gCYTB5-III interact *in vivo*, and furthermore, suggest that some proteins in the mitosome could

interact with those in the nucleus. I also found that DNA stress, caused by low concentrations of formaldehyde (0.1 – 0.2%) resulted in the increased expression of gCYTB5-III. Collectively these findings suggest a role of gCYTB5-III in Giardia's response to DNA stress and perhaps the formation of Fe/S clusters.

Acknowledgement

I would first like to thank my supervisor, Dr. Janet Yee, for giving me the opportunity to complete my M.Sc. in her lab, and her constant support and advice throughout the course of my project. I would also like to thank Dr. Steven Rafferty for helping me with biochemically related topics but more importantly, providing a patient ear to bounce ideas off through experimental design. I am grateful to my supervisory committee, Dr. Huber, and Dr. Saville for their valuable advice in deciding the direction of my research. I would also like to thank Dr. Dolezal for his collaborative efforts and expertise on the mitosome.

I would like to thank the members of Dr. Yee and Dr. Rafferty labs, with special mention to Guillem Dayer, who I picked up the project from, and taught me many of the techniques applied, and Kyla Bruce for assisting me with my later work. Finally, I would like to thank my family for their constant support both emotionally and financially: Mom, Dad, Brad, Aunt Mary, and Aunt Vanessa. A special thank you goes to my girlfriend Alex, who made sure I took care of myself and kept me from drowning in papers.

Table of Contents

List of Figures

List of Tables

List of Abbreviations

ALA	Aminolevulinic acid
ALAS	ALA synthase
BMH	Bismaleimidohexane
ChIP	Chromatin immunoprecipitation assay
CIA	Cytosolic iron-sulfur cluster assembly
CL	Crosslinked
Co-IP	Co-immunoprecipitation
CPOX	Coproporphyrinogen oxidase
CYTB5	Cytochrome b5
DSG	Disuccinimidyl glutarate
DSP	Dithiobis(succinimidyl propionate)
EMSA	Electrophoretic mobility shift assay
ER	Endoplasmic reticulum
FACT	Facilitates chromatin transcription
FAD	Flavin adenine dinucleotide
FECH	Ferrochelatase
Fe-S	Iron sulfur
FMN	Flavin mononucleotide
gCYTB5	Giardia cytochrome b5
GiGAP1	Giardia GAPDH
GO	Gene ontology
HA	Hemagglutinin
HA-III	HA tagged Giardia cytochrome b5 III
HMBS	Hydroxymethylbilane synthase
IFA	Immunofluorescent microscopy analysis
ISC	Iron sulfur cluster (mitochondrial Fe-S pathway)
MS	Mass spectroscopy
PBGS	porphobilinogen synthase
PBS	Phosphate buffer saline
PBST	PBS containing tween detergent
PDI2	Protein disulfide isomerase
PI	Pre-immune serum
PPOX	Protoporphyrinogen oxidase
PV	Peripheral vacuoles
rIII	Recombinant Giardia cytochrome b5 III
RMSD	Root mean squared deviation
RT	Room temperature
SL	Supernatant lysate
SMPB	Succinimidyl 4-(p-maleimidophenyl)butyrate)
STD	Standard molecular weight marker
TBS	Tris buffer saline

TBST	Tris buffer saline containing Tween detergent
TX	Triton X-100
UROD	Uroporphyrinogen decarboxylase
UROS	Uroporphyrinogen synthase
UT	Untransfected
WL	Whole cell lysate

Introduction

1.1 Giardia intestinalis

Giardia is a waterborne unicellular protozoan parasite that causes the zoonotic disease giardiasis. The organism has a life cycle consisting of two forms, the infectious cyst and the motile trophozoite. The cysts can be found in freshwaters, soil, and fecally contaminated fruits and vegetables. Once ingested, cysts pass through the stomach and excyst, forming the free swimming trophozoite that propagate and colonize the upper intestine of an infected host (Lujan & Svärd, 2011). Giardia trophozoites can be grown in axenic laboratory cultures (Keister, 1983), and be induced to encyst by alteration of the medium composition (Gillin, Reiner, & Boucher, 1988). The genome sequence of several isolates of Giardia have been determined but the genome of the WB C6 isolate was the first one sequenced and is commonly used as the reference.

Although it is a eukaryote, Giardia lacks fully functioning mitochondria, and its ability to form ATP is not based on oxidative phosphorylation (Lujan & Svärd, 2011). Instead, Giardia obtains energy using anaerobic fermentative catabolic pathways, and while oxygen levels above 50 μM are lethal, it can tolerate the lower levels typically found in the upper small intestine, owing to the presence of several enzymes that reduce oxygen without coupling this to energy production. As a result, Giardia can be considered as a micro-aerotolerant anaerobe.

Another consequence of its lack of mitochondria is the inability of Giardia to make heme, as most of the steps for heme biosynthesis occur in this organelle. This does not, however, mean that Giardia does not require heme to thrive. To date, Giardia is

known to express at least five heme proteins: a flavohemoglobin that can detoxify nitric oxide to nitrate, and four cytochromes of unknown function.

While Giardia does not possess mitochondria, it does possess a derivative organelle known as the mitosome. While it cannot make heme, it has a central role in the formation of a second major class of iron-containing proteins that possess iron-sulfur (Fe-S) clusters (Tovar et al., 2003).

1.2 Mitosomes and Iron-Sulfur Cluster proteins

Approximately 2 billion years ago, a single endosymbiotic event lead to the establishment of the mitochondrion in eukaryotes cells (Margulis & Bermudes, 1985). In addition to their roles in oxidative respiration, mitochondria are required for a variety of metabolic tasks including the urea cycle, biosynthesis of heme, and Fe-S cluster assembly. *Giardia intestinalis* was considered among the few amitochondrial eukaryotes, until the mitochondrial IscS and IscU genes were discovered in the nuclear genome (Tovar et al., 2003). IscU is a soluble iron binding protein that acts as a scaffold protein in conjunction with IscS to form Fe-S clusters in the mitochondria of other eukaryotes (Lill & Kispal, 2000). The localization of the proteins encoded by these genes in Giardia identified a double-membrane organelle that is approximately 100 nm in diameter (Martincová et al., 2015). This organelle, referred to as the mitosome, is a reduced form of the mitochondria that is missing cristae and mitochondrial DNA. Furthermore, the mitosomes have lost the functions of cellular respiration, citric acid cycle, ATP synthesis,

and heme biosynthesis, leaving Fe-S cluster assembly as its sole known function (Jedelsky et al., 2011).

Proteins with Fe-S co-factors are needed in the mitochondria, cytosol, endoplasmic reticulum, and nucleus. The synthesis for Fe-S compounds for proteins in all cellular compartments share the same initial steps that occur in the mitochondrion in a pathway that is referred to as the ISC. However, the pathway in the mitochondrion later splits into two branches. One branch is to complete the Fe-S clusters needed for mitochondrial proteins such as ferredoxin, and those involved in the respiratory electron transport chain. The second brand is to create an unknown sulfur containing compound that is exported from the mitochondria via the Atm1 transporter to continue the Fe-S assembly in the cytosol (Lill & Freibert, 2020). The cytosolic part of the pathway is referred to as the cytosolic iron sulfur assembly (CIA) and is shown in Figure 1. This part of the Fe-S synthesis pathway involves eight core proteins -Tah18, Dre2, Nbp35, Cfd1, Nar1, Cia1, Cia2, and Met18 that are present in most eukaryotic cells. Cfd1 and Nbp35 form a hetero-tetrameric scaffold complex, which assembles the transient [4Fe-4S] cluster. To stabilize the formation of these [4Fe-4S], an electron transfer chain composed of the flavoenzyme Tah18 and the Fe-S carrying Dre2 is required. Tah18 facilitates electron transfer from NADPH to Dre2, which in turn can reduce a Fe-S cofactor of Nbp35 (Netz, Mascarenhas, Stehling, Pierik, & Lill, 2014). In the final step of the pathway, the targeting complex, with the assistance of the hydrogenase-like Nar1 protein delivers the Fe-S to proteins requiring this co-factor throughout the cell, including the nucleus. Therefore, the targeting proteins Cia1, Cia2 and Met18 (MMS19 in

human) could also be found in the nucleus (Balk, Aguilar Netz, Tepper, Pierik, & Lill, 2005; Ito et al., 2010).

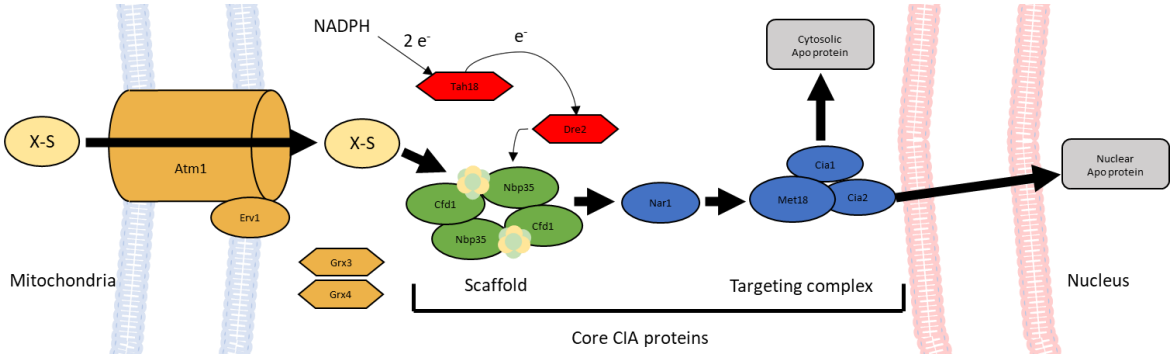

Figure 1: Representation of the current understanding of the cytosolic iron sulfur cluster assembly (CIA) in yeast. The CIA is essential for the insertion of iron sulfur (Fe-S) cluster into apo proteins in the cytosol, endoplasmic reticulum, and nucleus. The core CIA proteins are divided into two groups, the scaffold that stabilizes the Fe-S, and the targeting complex that is required for transport and insertion of the Fe-S into apo proteins. X-S is an unknown sulfur donor exported from the initial Fe-S assembly that originates in the mitochondra.

Giardia orthologs of proteins such as IscU, IscS, and Nfu, that are required in the initial steps for Fe-S cluster synthesis that occurs in the mitochondrion in other eukaryotes were identified in proteomic analysis of the Giardia mitosome (Jedelsky et al., 2011). Giardia also has orthologs of proteins, such as Nbp35, Nar1, and Cia2, that are required for continuation of the Fe-S synthesis pathway outside of the mitochondria / mitosome (Pyrih et al., 2016). Nevertheless, Fe-S assembly is not completely understood in Giardia since several of the proteins involved in this pathway in yeast and human are absent in Giardia (Jedelsky et al., 2011). One of these missing proteins is Tah18, which is a redox protein that supplies the electron required to stabilize the formation of the Fe-S cluster in the scaffold complex of the cytosolic iron-sulfur (CIA) assembly pathway (Paul

& Lill, 2015). However, a diflavoenzyme referred to as the Giardia oxidoreductase-1 (GiOR-1) was identified in the mitosomes (Jedelsky et al., 2011). GiOR-1 and Tah18 are both structurally and functionally similar to the cytochrome P450 reductases in that they contain a flavin mononucleotide (FMN) binding domain, a flavin adenine dinucleotide (FAD) binding domain, and could transfer electrons from NADPH to a variety of electron acceptors (Pyrih et al., 2014). Furthermore, GiOR-1 is able to rescue Tah18 knockdowns in *T. brucei* (Pyrih et al., 2016), which suggests that these enzymes are functionally equivalent. Another key protein missing in Giardia is an ortholog for Dre2, which is the redox partner for Tah18 (Fig. 1). As GiOR-1 is a potential ortholog of Tah18, it was first thought that a Giardia cytochrome could function in place of Dre2 in this crucial cellular reaction (Pyrih et al., 2014). However, this notion was later dismissed due to the lack of detection of cytochromes in the mitosomes. These issues further illustrate the incomplete knowledge about the Fe-S assembly in the mitosomes and in the cytosol in Giardia.

1.3 Heme

The importance of heme as a metallocofactor is highlighted by its abundance in almost all compartments of most eukaryotic cells (Swenson et al., 2020). It plays a vital role in the transport and storage of gases (O_2, NO), as well as electron transfer and chemical catalysis involving these gases. As a signalling molecule, heme assists in oxygen sensing, iron homeostasis, oxidative stress responses, mitochondrial respiration, biogenesis, mitophagy, apoptosis, cell-cycle progression and proliferation (Hamza &

Dailey, 2012; Mense & Zhang, 2006; Severance & Hamza, 2009). These functions require heme to be delivered throughout the cell, but heme production and its transport need to be tightly regulated as free heme is hydrophobic and cytotoxic. The regulation and transport of heme, however, is poorly understood and current understanding of heme regulation is simply the balance of heme production to heme degradation (Hamza & Dailey, 2012).

With the exception of plants, the first step of eukaryotic heme synthesis (Fig. 2) is the production of aminolevulinic acid (ALA) in the mitochondrial matrix by the enzyme ALA synthase (ALAS). ALA is then transported by an unknown mechanism through both mitochondrial membranes to the cytosol. Here the enzyme porphobilinogen synthase (PBGS) combines two ALA molecules into porphobilinogen. Hydroxymethylbilane synthase (HMBS) forms the linear tetrapyrrole, hydroxymethylbilane, from four porphobilinogen molecules. Uroporphyrinogen synthase (UROS) inverts and cyclizes the linear tetrapyrrole into Uroporphyrinogen III, and with the decarboxylation of the pyrrole acetic acid side chains by uroporphyrinogen decarboxylase (UROD) coproporphyrinogen III is produced. Coproporphyrinogen III is transported back into the intramembranous space of the mitochondria, where it is oxidized to protoporphyrinogen IX by coproporphyrinogen oxidase (CPOX). The final two steps of heme biosynthesis occur in the mitochondrial matrix, where protoporphyrinogen IX is further oxidized to protoporphyrin IX by protoporphyrinogen oxidase (PPOX). Finally, ferrous iron is inserted by ferrochelatase (FECH) to yield heme *b*, which can be converted to heme *a*, *c*, or *o* (Swenson et al., 2020). The production of heme within a

cell is mainly regulated by the expression, stability, and localization of ALA synthase (Munakata et al., 2004; Yamamoto, Hayashi, & Kikuchi, 1982, 1983). The release of heme *b* from ferrochelatase limits the rate at which heme can be distributed (Hamza & Dailey, 2012).

Degradation of heme is catalyzed by heme oxygenase, which oxidizes and breaks the protoporphyrin ring to yield biliverdin and carbon monoxide and liberates free ferrous iron. Biliverdin is further oxidized to bilirubin, while iron is retained for further use by the organism, as ferric iron has low solubility in water. This scarcity of biologically available iron is important in the metabolism of many pathogens, which obtain iron from their hosts (Trypanosomes (Mach & Sutak, 2020), Plasmodium (Kassebaum et al., 2014), Leishmania (Huynh, Sacks, & Andrews, 2006), Trichomonas (Figueroa-Angulo et al., 2012)). Leishmania and *Trypanosoma cruzi* do not possess the enzymes for heme biosynthesis and instead sequester all needed iron and heme from a parasitized host, and it has been suggested that these parasites have developed novel pathways for heme sequestration and homeostasis (Agarwal et al., 2013; Flannery, Renberg, & Andrews, 2013; Krishnamurthy et al., 2005; Patel, Singh, Basu, & Mukhopadhyay, 2008; Singh et al., 2003; Tripodi, Menendez Bravo, & Cricco, 2011). Orthologs for any heme biosynthesis enzymes also seem to be absent in the genome of Giardia, and nothing is known about its ability to acquire, transport, process, and use this cofactor which it presumably obtains from its host (Rafferty & Dayer, 2015).

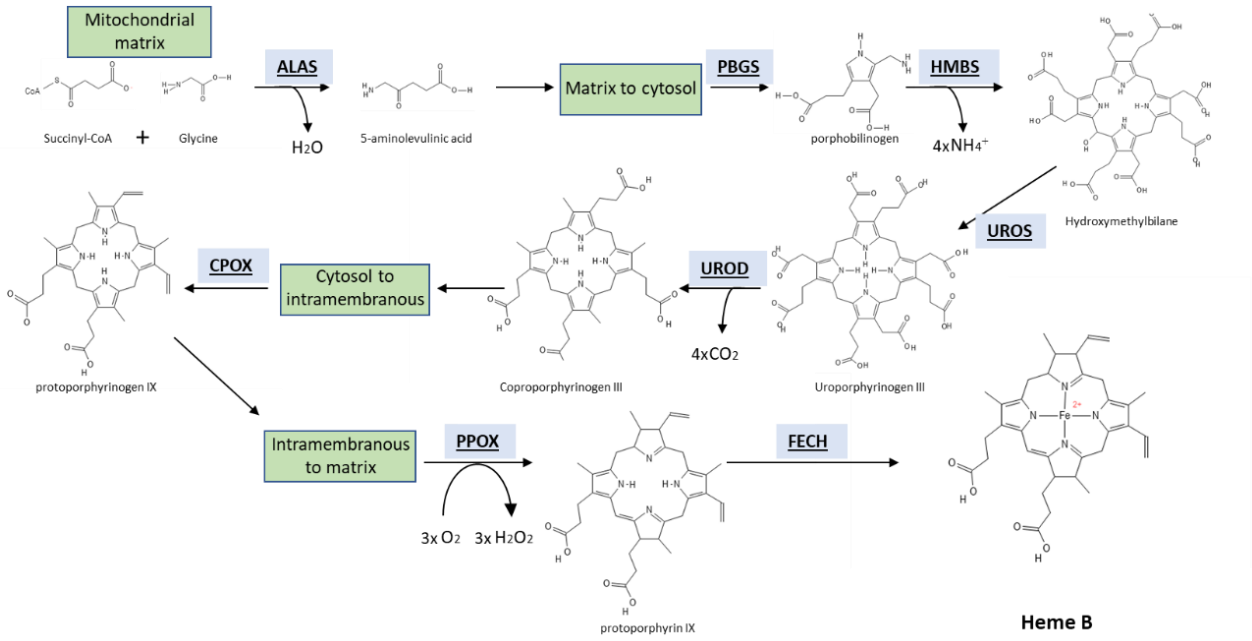

Figure 2: A diagram displaying the heme biosynthesis pathway that occurs in the mitochondria of Humans. Localization changes are highlighted by green boxes, enzymes by blue boxes. ALAS (aminolevulinic acid synthase), PBGS (porphobilinogen synthase), HMBS (Hydroxymethylbilane synthase), UROS (Uroporphyrinogen synthase), UROD (uroporphyrinogen decarboxylase), CPOX (coproporphyrinogen oxidase), PPOX (protoporphyrinogen oxidase), FECH (ferrochelatase).

1.4 Giardia Cytochromes

The analysis of the Giardia genome revealed a lack of genes encoding proteins of the respiratory chain and enzymes for heme biosynthesis (Rafferty & Dayer, 2015). Anaerobic parasitic eukaryotes such as Giardia are expected to have only a few heme-containing proteins compared to aerobic eukaryotes, as most heme proteins are involved in oxidative phosphorylation (the mitochondrial respiratory chain), oxygen transport to the respiratory chain (hemoglobins) or the use of oxygen in biosynthetic reactions (the cytochrome P450s). Despite lacking these functions as well as lacking the

enzymes required for heme biosynthesis, Giardia has five heme-containing proteins. One is a flavohemoglobin that acts as a nitric oxide dioxygenase that combines NO, O_2 and an electron to yield nitrate (NO_3^-), and which protects the organism from nitrosative stress. The remaining four proteins are isotypes of the electron transfer protein cytochrome b_5, referred to as the gCYTB5-I, II, III and IV. The ability of Giardia to take up extracellular heme has been demonstrated by the increased heme content in Giardia that overexpressed gCYTB5-IV (Pyrih et al., 2014), although the mechanism of cellular heme uptake is unknown. Giardia and other parasites such as *Encephalitozoon*, *Antonospora*, and *Nematocystis* have retained an unusually high number of cytochrome b_5 isotypes of unknown function (Kořený, Oborník, & Lukeš, 2013). Therefore, the study of these proteins in one parasitic protist may reveal their roles in others.

Cytochromes are proteins that use heme for electron transfer, in which the iron cycles between ferrous (Fe^{2+}) and ferric (Fe^{3+}) oxidation states as the heme alternately accepts an electron from a donor and transfers it to an acceptor. The electron donors and acceptors are usually other redox proteins. Cytochromes facilitate rapid electron transfer as oxidation-state dependent conformational changes in the protein structure are minimal. The specificity of electron transfer depends on complementarity between the surface of the cytochrome and its redox partners, which form a transient docking complex before electron transfer occurs. Specificity is also influenced by the subcellular localization of the cytochrome and its partners (Rafferty & Dayer, 2015).

Cytochromes are distinguished from each other by the type of heme they bind, such as heme *a*, *b*, *c*, or *o*. Even cytochromes that bind the same type of heme can vary

widely in structure and in the number of heme groups they bind, and cytochrome nomenclature is developed further by the addition of subscripts to the heme type to reflect this. For example, the four Giardia cytochromes are members of the cytochrome b_5 family (Lederer, 1994). The canonical cytochrome b_5 structure consists of 6 helices and 5 ß-strands that compose the core cytochromes *b*5 heme binding domain, with a pair of invariant histidine side chains acting as ligands to the heme iron (Fig. 3).

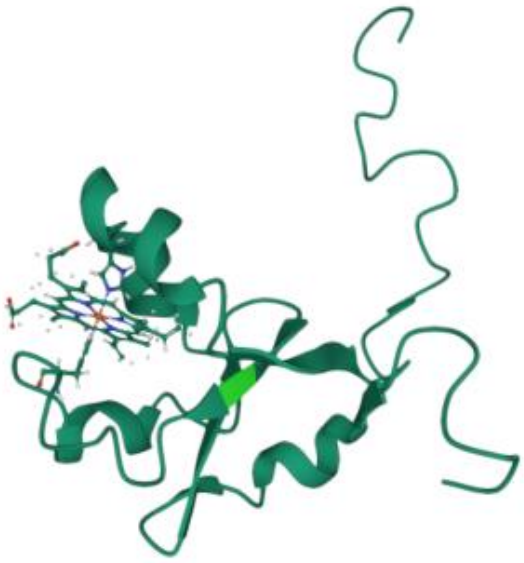

Figure 3: Structural representation of human microsomal cytochrome b_5 (Nunez-quintana, Truan, & Van Heijenoort, 2006). Axial histidines residues at H44 and H68 are shown, and C-terminal transmembrane domain is the unstructured portion going up away from the core cytochrome *b*5 domain.

Based on their sequences, especially those around the invariant histidine ligands, cytochrome b_5 proteins are classified into three types (Pyrih et al., 2014). Type-I cytochromes b_5, which have a C-terminal hydrophobic alpha helix that acts as a membrane anchor, are the most well characterized. This type includes mammalian CYTB5A, which is anchored to the membrane of the endoplasmic reticulum, and mammalian CYTB5B, which is anchored to the mitochondrial outer membrane facing the

intermembrane space. CYTB5A is involved in the redox pathways of fatty acid desaturation and electron transfer to the cytochrome P450 monooxygenases. A soluble splicing variant of CYTB5A, which lacks the c-terminal membrane anchor, is expressed in erythrocytes and functions in reducing oxidized hemoglobin back to its functional state (Vergeresb & Waskell, 1995). CYTB5B transfers electrons from membrane-bound NADH:cytochrome b_5 oxidoreductase on the mitochondrial outer membrane to cytochrome *c* of the respiratory chain, leading to the formation of ATP by oxidative phosphorylation.

Far less is known about the roles of Type II cytochromes b_5, which includes all four Giardia gCYTB5s. These have the same invariant pair of histidine ligands (H44 and H68, numbered as in mammalian CYTB5A) as Type I, but differ in the sequences that flank the ligands, and they lack the membrane anchor. Whereas acidic residues surround the histidine ligands in Type I, uncharged residues are found in Type II. As noted above, complementary charge interactions on the surface of redox proteins helps determine the specificity of electron transfer, and this difference between Type I and Type II cytochromes b_5 is likely significant in this regard.

There is only one known member of the Type III cytochromes b_5, which is found in the fungus, *Neurospora crassa*. Similar to the Type II cytochromes, it lacks the membrane anchor and acidic residues near the invariant ligands, but it has further sequence differences around these residues that set it apart.

Structural and biochemical studies of recombinant versions of the gCYTB5s expressed and isolated from *E. coli* have been performed by the Rafferty lab. UV-visible

spectroscopy, and resonance Raman spectroscopy of these proteins are consistent with low spin, histidine coordinated heme (Yang, Pazdzior, Yee, & Rafferty, 2016). These findings are typical of all cytochrome b_5; however, the reduction potentials of these proteins are strikingly lower than those of the well-characterized CYTB5A and CYTB5B of mammals (Pazdzior et al., 2015). The reduction potential of a redox-active molecule is a measure of its preference to be in the oxidized or reduced state relative to a reference redox reaction such as the standard hydrogen electrode, which is assigned a reduction potential of 0 mV. The thermodynamically favourable direction of electron transfer will be from the molecule with the lower reduction potential to one of a higher reduction potential, with the numerical difference between the reduction potentials of these molecules being proportional to the free energy change for the electron transfer reaction.

The reduction potential of cytochrome b_5 in mammals range from -100 to +78 mV, with most in the range of ~ 0 mV (Alam et al., 2012). The reduction potentials of the Giardia isotypes are much lower: -171 mV, -140 mV, and -153 mV, for gCYTB5-I, II, and III, respectively, indicating a greater preference to be in the oxidized state (Pazdzior et al., 2015). This preference is due to the polar residues within the heme binding pocket as shown by the increased reduction potential of gCYTB5-I when these residues were mutated to non-polar residues (Yang et al., 2016). Although this information can help determine directionality in biochemical reactions that may involve the gCYTB5s, no biological reactions or interacting partners for these proteins have yet been found.

To begin investigating the known function of the gCYTB5, our laboratory obtained specific affinity-purified antibodies prepared against each of the gCYTB5 isotypes, with epitopes in the N-terminus for isotypes II and III and the C-terminus for isotype I. Since this thesis work was completed, an antibody raised against the N-terminal half of gCYTB5-IV has also been prepared, although the laboratory has only begun to use it. The specific binding of these antibodies was confirmed via western blot analysis of the endogenous proteins from Giardia lysates alongside recombinant versions of each respective protein as a positive control (Sajer, 2019). The antibodies have also been used in immunofluorescence microscopy (IFA) to determine subcellular localization of each isotype, which detected gCYTB5-I in the nucleolus, gCYTB5-II in the peripheral vacuoles, and gCYTB5-III within the nuclei (Dayer, 2017).

Based on their localization, their low reduction potentials, and scarcity of identified redox partners in the Giardia genome, the gCYTB5s are unlikely to have the same functions of those of the well-studied CYTB5A (endoplasmic reticulum) and CYTB5B (mitochondrial inner membrane) isotypes of other eukaryotes. Giardia lacks a respiratory chain, which CYTB5B funnels electrons into, and it also lacks cytochrome P450 monoxygenases and acetyl-coenzyme A desaturases, the electron acceptors for CYTB5A. The only potential interacting partner for the gCYTB5s found to date is the mitosomal protein GiOR-1. GiOR-1 is a member of the cytochrome P450 reductase enzyme family, whose electron transfer partners include CYTB5A in other species, and GiOR-1 can transfer electrons to gCYTB5s in assays using purified recombinant proteins (Pyrih et al, 2014). However, none of the gCYTB5 have been localized to the mitosomes

by immunofluorescence or been detected in proteomic analysis of the mitosomes (Dagley et al., 2009; Dolezal et al., 2005; Elias et al., 2008; Jedelsky et al., 2011; Kunz et al., 2017; Lill & Kispal, 2000; Martincová et al., 2015; Pusnik et al., 2009; Pyrih et al., 2016; Pyrihov et al., 2018; Rada et al., 2009; Regoes et al., 2005; Rout, Zumthor, Schraner, Faso, & Hehl, 2016; Šmíd et al., 2008; Tachezy, Sánchez, & Müller, 2001; Tovar et al., 2003). Therefore, the functions of the gCYTB5s remain a mystery. One way to solve the mystery would be to identify the proteins that the gCYTB5s interact with *in vivo*.

1.5 Co-immunoprecipitation to study protein interactions

Co-immunoprecipitation (co-IP) coupled with mass spectrometry (MS) has become a popular method to identify *in vivo* protein-protein interactions (Gingras, Gstaiger, Raught, & Aebersold, 2007). In this procedure, a protein of interest is isolated or immunoprecipitated from a cell lysate through its recognition by an antibody that is linked to a bead so that the protein bound to the antibody and bead can be recovered as a pellet when the sample is centrifuged. Any proteins that interact with the protein of interest could also be recovered in the immunoprecipitate (Free, Hazelwood, & Sibley, 2009). An adaptation of the co-IP is to use magnetized beads so that proteins bound to these beads could also be separated from the unbound proteins by placement of the tube containing the sample against a specialized magnetic stand. The proteins in the immunoprecipitate are then digested with a protease and short sequences of the resultant peptides are determined by mass spectroscopy. A theoretical digestion of all

the proteins encoded in the organism's genome provides the blueprint to identify the proteins recovered in the sample.

The most difficult part of performing a co-IP is in the preservation of the protein interactions throughout the procedure, which is particularly difficult for weakly or transiently interacting proteins. Therefore, the employment of crosslinking *in vivo* allows these interactions to be maintained by introducing covalent bonds between the proteins within the cell prior to cell lysis (Smith, Friedman, Yu, Carnahan, & Reynolds, 2011). The addition of a crosslinking step in the co-IP of gCYTB5-III would be especially helpful because the electron transfer reaction between this protein and its partners would likely be transient. The addition of a crosslinker would also allow the use of harsher cell lysis buffers and more stringent washes during the co-IP procedure (Lubec & Afjehi-Sadat, 2007; Smith et al., 2011).

1.6 gCYTB5-III, a nuclear cytochrome b_5

The antibody raised against the N-terminus of gCYTB5-III has been used in immunofluorescent microscopy to determine that this protein is localized solely to the nucleus of Giardia (Dayer, 2017). This is very interesting because the only other case of a nuclear localized cytochrome is the re-localization of cytochrome *c* from the mitochondria to the nucleus where it interacts with apoptosis protease activating factor-1 in response to apoptosis (Henshall et al., 2001). Other proteins that bind heme within the nucleus are transcription factors, such as, Hap-1 (yeast), and Bach-1 (human) that help regulate heme homeostasis (Swenson et al., 2020). We cannot rule out the

possibility that gCYTB5-III may function as a transcription factor; however, *in vitro* DNA binding assays has been attempted in the Yee lab unsuccessfully, and bioinformatics studies did not identify any potential protein structural motifs (*i.e*., zinc-fingers, helix-loop-helix, bZiP) that are likely to bind DNA within the flanking regions of this protein. Furthermore, the redox reactions cytochromes b_5 are known to participate in have no known function in gene regulation. Thus, the function and interacting proteins of gCYTB5-III may be completely novel.

The goal of this thesis is to determine interacting partners through the application of co-immunoprecipitation coupled with mass spectroscopy, to investigate the function of the nuclear localized gCYTB5-III.

Experimental procedure

2.1 Giardia intestinalis cell culture and collection

Giardia intestinalis trophozoites (ATCC#50803 WB clone C6) were cultured in 16 mL glass culture tubes at 37°C in complete TYI-S-33 medium as previously described (Gillin et al. 1996). Media was supplemented with cysteine (2 g/L final concentration) and ascorbic acid (0.1 g/L final concentration) and antibiotic-antimycotic (2.5 mL/L, Hyclone). A Giardia cell line expressing a hemagglutinin (HA) tagged gCYTB5-III (referred to as HA-III) was supplied by Dr. Jan Tachezy's lab in the Czech Republic, and a Giardia cell line with a HA-tagged pseudouridine synthetase CBF5 gene integrated into the genome was supplied by Dr. Adrian Hehl's lab in Switzerland. Since the HA-tagged gCYTB5-III gene in the HA-III cell line is ectopically expressed from a plasmid containing a puromycin resistant cassette, these cells were grown under puromycin selection (54 µg/mL final concentration). To collect the cells, tubes of Giardia cultures were cooled in ice water for 10 minutes to detach adherent cells and then centrifuged at 1200 x g for 15 minutes (all centrifugations are at this setting unless stated otherwise). Cell counts were determined with a ViCell XR® cell viability analyser (Beckman Coulter).

2.2 Immunofluorescence microscopy

Immunofluorescence microscopy was used to examine the cellular localization of proteins in Giardia trophozoites. The primary antibodies used for these studies were

either custom antibodies that recognize the endogenous proteins or antibodies that recognize the HA-tag on epitope tagged proteins expressed in Giardia (Table 1).

Polylysine was used to treat coverslips to aid in cell adhesion. Coverslips coated with polylysine (300 µL of a 50 µg/mL solution) were incubated at 37 ℃ for 1 – 2 h, rinsed with water, and then dried overnight at room temperature (RT). Giardia cells were collected and counted as described in Section 2.1. 100 µL of cells at 4.0 x 10^7 cells/mL was spread over the treated slides and incubated in a 37 ℃ humidity chamber for 30 minutes. To each coverslip, 100 µL of fresh 4% formaldehyde dilute in PBS was carefully added into each cell suspension before incubating for 15 minutes at RT. The solution is pipetted off and 200 µL of quenching buffer (0.1 M glycine in PBS) was added to the coverslips for 10 minutes at RT. This is followed by 3x 300 µL PBS washes, incubating 5 minutes per wash.

Next, 200 µL of blocking / permeabilization buffer (0.1% Triton X-100, 20 mg/mL BSA in PBS) was added to the coverslips followed by incubation at 37 ℃ for 30 minutes. This buffer was removed, and primary antibody diluted in antibody buffer (0.05% Triton X-100, 5 mg / mL BSA in PBS) was added to each coverslip (Table 1). Following primary antibody incubation, washing was performed as stated above, and a dilution of a secondary antibody (anti-rabbit or anti-mouse antibodies) conjugated to a fluorophore was applied to coverslips (Table 1). Following secondary antibody incubation, washes were performed as stated above with two additional washes with Millipore grade water. Cover slips were placed onto slides with 5 µL of mounting medium (Vectashield with DAPI), sealed with nail polish and imaged on a Leica Fluorescent Microscope DM 6000B.

Table 1: Dilutions and incubation conditions of antibodies applied in immunofluorescent microscopy. All antibodies were dilute in an antibody buffer (0.05% Triton X-100, 5 mg / mL BSA in PBS) before being applied to Giardia cells on cover slips.

Antibody	**Type**	**Dilution**	**Incubation**
Anti-gCYTB5-III (produced in rabbits)	Primary	1 : 1500	overnight at 4 ℃
Anti-HA (produced in mice)	Primary	1 : 400	overnight at 4 ℃
Anti-rabbit-Cy3 (produced in goats)	Secondary	1 : 200	1 hour at RT
Anti-mouse-FITC (produced in goats)	Secondary	1 : 200	1 hour at RT

2.3 Cell lysis

Cells were resuspended in 15 µL of alkaline RIPA buffer (75.0 mM NaOH, 80.0 mM glycine (pH 10.6 @ 25 ℃), 150 mM NaCl, 1.0% NP40, 0.1% SDS) per milligram of packed cell pellet and supplemented with a protease inhibitor cocktail (PIC, BioShop Cat# PIC001) to 1X final concentration, 1 µg/µL Leupeptin and 1 mM EDTA. Non-crosslinked cells become visibly lysed within 5 minutes of their resuspension in the alkaline RIPA lysis buffer while crosslinked cells require pulse sonication (1 second per pulse) until the sample become transparent. In both cases, cells are then incubated on a rotisserie for 30 minutes at 4 ℃ to ensure complete lysis. To remove cell debris, lysates were centrifuged at 14 000 x g and the supernatant was used for analysis. Protein concentration of the supernatant is determined by Bradford assay. For analysis of the proteins in the pellet, the pellet remaining after the removal of the supernatant was

resuspended in 1x SDS-PAGE loading buffer in a volume equal to that of the volume of the supernatant removed.

2.4 Cell fractionation

The goal of this procedure is to gently disrupt the plasma membrane without disrupting the membranes of the organelles so that the cytosolic proteins can be isolated in a separate fraction from the proteins associated with membranes and organelles. Untransfected Giardia (UT) or transgenic HA-tagged CBF5 cell lines were collected as described in Section 2.1, and the packed cell pellet containing approx. 1 x 10^8 cells was resuspended in 500 µL PBS and centrifuged at 2000 x g for 10 minutes. The supernatant was removed, and the pellet was washed twice with 500 µL PBS. The washed cell pellet was resuspended in 300 µL hypotonic lysis buffer (10 mM HEPES, 1.5 mM $MgCl_2$, 10 mM KCl), followed by two freeze thaw cycles. NP40 is added to the samples at a final concentration of 0.2% and incubated for 30 minutes at 4 ℃. The samples were centrifuged at 2000 x g for 10 minutes and supernatant was removed and designated as the cytosolic fraction.

The cell pellet was grinded with a microfuge pedestal 20 times. Cells were then resuspended in 300 µL hypotonic lysis buffer and cell disruption was monitored via examination of aliquots of the sample under a light microscope. After each grinding cycle, the sample was centrifuged, and supernatant was removed. The cell pellet was further grinded with a pedestal. This cycle was repeated until ≥ 80% of cells in field of view appeared sickle or irregular shaped (both occur). The cell pellet was then washed

as stated above and protein released in each wash was evaluated by Bradford reagent (10 µL of wash supernatant, and 200 µL of Bradford reagent). Washes continued until no further change in the intensity of the blue colour of the supernatant was perceivable by visual inspection. The final pellet upon completion of the last wash was lysed with alkaline lysis buffer and designated as the organelle fraction.

2.5 Western blot

Western blotting was used to analyze the presence and expression of the Giardia cytochromes b_5. These proteins are small (14.5-15.5 kDa) and therefore require conditions that favor the retention of proteins of this size on the membrane. The protocol used followed that previously described (Gaechter, Schraner, Wild, & Hehl, 2008). Protein concentrations were determined by the Bradford assay (Bradford, 1976). Prior to SDS-PAGE, 50 µg of protein were mixed with 5 µL of 4x loading buffer to a final volume of 20 µL and heated at 65 ℃ for 20 minutes. SDS-PAGE was performed with 14% polyacrylamide gels electrophoresed at 120 V through the stacking gel and 150 V through the separating gel.

For the transfer of the proteins from the gel to the membrane, semi-dry electroblotting was used. This protocol has been applied using both nitrocellulose and PVDF membranes with a pore size of 0.2 µm (AmershamTM ProtranTM nitrocellulose Cat# 1060044 or Bio-Rad Immun-Blot PVDF Cat#1620177). PVDF membranes required activation by incubation in 100% methanol for 1 min, before it is rinsed in water and equilibrated in Towbin buffer (25 mM Tris, 192 mM glycine, 2 mM $CaCl_2$, 20% methanol).

Nitrocellulose membranes could be equilibrated directly in Towbin buffer without the activation step. The gel, and filter paper are also equilibrated in Towbin buffer for 20 minutes prior to the set-up of the transfer sandwich. The addition of the calcium chloride in the Towbin buffer assists in neutralizing the SDS from the SDS-PAGE, increasing the stable fixing of the proteins to the membrane. The transfer was performed at a constant current of 0.1 A for 35 minutes in a BioRad Trans-Blot Turbo instrument.

Following electroblotting the membrane was rinsed with deionized water for 5 minutes. From this point, all membrane incubations are done in a 50 mL canonical tube on a rotisserie. When using nitrocellulose, a Ponceau stain was applied to the membrane for 20 min to visualize the total protein transferred to the membrane. After an image of the membrane was recorded (Bio-Rad ChemiDoc MP), the Ponceau stain was removed by washing in TBST before the membrane was transferred to blocking buffer (5% powdered skim milk reconstituted in 40 mM TBS with 0.01% Tween20 (TBST)) for a 1-hour incubation at RT. Since Ponceau staining is not effective with PVDF membranes, these membranes were placed directly after electro-transfer into blocking buffer. The membrane was then incubated with the primary antibody diluted in blocking buffer (1:5000 for all primary antibodies) overnight at 4 ℃. The membrane was then washed with TBST on an orbital shaker set to 60 RPM for 3 x 10 minute, with a change in the buffer every 10 minutes. The membrane was then incubated in secondary antibody diluted in blocking buffer (1:25000 for anti-rabbit HRP or 1:50000 for anti-mouse HRP) for 1 hour at RT, followed by three washes with TBST. Chemiluminescent substrate was

added to the membrane (BioRad Clarity Western ECL substrate), incubated for 1 minute, and then imaged on a Bio-Rad ChemiDoc™ MP imaging system.

2.6 *In vivo* crosslinking

For each set of co-IP experiments, 40 x 16 mL cultures were grown to 80% confluency (late log growth) or approximately 7.8 x 10^5 cells/mL. Culture tubes were incubated in ice water for 10 minutes, and then centrifuged @ 1200 x g for 15 minutes to collect the cell pellet. All centrifugations described in this section are performed with these parameters. After centrifugation, the supernatant was removed except for 0.5 mL. Cells were resuspended in the remaining 0.5 mL medium, pooled in a 50 mL conical tube, and centrifuged. All remaining culture medium was removed, and the cells were washed in 5 mL of PBS. Three 50 µL aliquots of the cell resuspension were taken for triplicate cell counts on the Beckman-Coulter Vi-Cell XR cell counter. Cells were then aliquoted into the required number of samples to be analyzed, and then the samples were centrifuged before removing the supernatant. For titration experiments, cell pellets were resuspended in 500 µL PBS with different concentrations of each crosslinker (SMPB and BMH: 0, 1, 3, and 5 mM; formaldehyde: 0, 0.1, 0.25, 0.5, 1, and 2%). Since the crosslinker titrations were done with 1/6 the number of cells, 3 mL of 3 mM BMH was used for co-IP application on the entire cell pellet (no aliquots). This maintains the same volume / crosslinker mass / cell mass ratio.

The cells were incubated in the crosslinker for 30 minutes at RT and then centrifuged to remove the supernatant containing crosslinker. Cells were then resuspended in a

buffer containing quenching agents. Glycine was added to a final concentration of 80 mM to quench formaldehyde, and L-cysteine was added to a final concentration of 40 mM to quench BMH. A mixture of the two reagents was applied to quench SMPB because it is heterobifunctional. Quenching occurred for 20 minutes at RT followed by removal of the quenching buffer and three washes with 40 mM TBS.

2.7 Co-immunoprecipitation

A detailed procedure for co-immunoprecipitation (co-IP) is presented in Appendix A. Briefly, the cell lysate was diluted in a 2x volume of 80 mM TBS (pH 7.2) 0.01% Tween 20. This reduced the pH to an acceptable 8.4 for co-IP, as the original pH 10.6 of the alkaline lysis buffer is not favorable for antibody binding.

Co-IP was performed following the manufacturer's protocol for the protein G-coated magnetic beads (Dynabeads, ThermoFisher cat # 10003D) with slight modifications. A 50 µL aliquot of beads was put in each of four 1.5-mL low protein binding microfuge tubes (Sarstedt cat # 72.706.600). Two of these tubes were designated to be used with the custom gCYTB5-III antibody, and the other two tubes were designated to be used for the control pre-immune serum (PI). For all supernatant changes, the tubes are applied to the DynaMag, magnetic stand (Cat#: 12321D). This is done immediately to remove storage buffer, then again after a wash with 200 µL of PBS 0.02% Tween (PBS-T) with gentle pipetting. The beads are then resuspended in 200 µL of PBS-T and the respective antibody was added. For experimental gCYTB5-III samples, 10 µg of gCYTB5-III antibody was added, and for the control PI sample, 5 µL (an equal

volume to the specific Ab) of pre-immune serum was added. The samples were mixed by gentle pipetting and then placed on a rotisserie and incubated for 30 minutes at RT.

After removal of the antibody solution, the beads washed with 1 mL of TBS 0.01% Tween with gentle pipetting to remove any residual unbound antibody. 1.2 mL of lysate is then added to the washed beads and mixed with gentle pipetting. Tubes were placed on a rotisserie overnight at 4°C. The lysate is removed the following day to be analyzed as the flow through (FT) and beads were resuspended in 1 mL of TBS + 0.5% Tween-20 and placed on rotisserie for 1 minute at RT. This supernatant is removed from the beads, and this is represented the first wash step (wash 1). Five more washes are done with 1 mL TBS + 0.5% Tween. One of the two experiment samples and control samples was eluted with 1x SDS-PAGE loading buffer to be analyzed via western blot. These samples were heated to 65 ℃ for 15 minutes prior to loading on an 14% SDS-PAGE gel. The other samples were washed three more times with TBS without Tween-20, as this detergent is not compatible with mass spectroscopy analysis. These samples were stored at -20 ℃ frozen without liquid to be sent for MS analysis pending western blot results.

2.8 Mass spectroscopy analysis

Beads from the co-IP were sent to SPARC BioCentre for Mass spectroscopy analysis (Sick Kids Hospital, Toronto). Trypsin was used to digest the proteins and release the peptides from the beads. The tryptic peptides were purified by 200 µL C18 stage tips (Thermo Scientific) and analyzed by Q-Exactive LC-MS/MS. The tryptic peptides from

each co-IP sample were separated on a 50-cm Easy-Spray column with a 75-µm inner diameter packed with 2 µm C18 resin (Thermo Scientific). The peptides were eluted over 120 min (250 nl/min) using a 0 to 40% acetonitrile gradient in 0.1% formic acid with an EASY nLC 1000 chromatography system operating at 50 °C (Thermo-Fisher Scientific). The LC was coupled to a Q-Exactive mass spectrometer by using a nano-ESI source (Thermo-Fisher Scientific). Mass spectra were acquired in a data-dependent mode with an automatic switch between a full scan and up to 10 data-dependent MS/MS scans. Target value for the full scan MS spectra was 1,000,000 with a maximum injection time of 120 ms and a resolution of 70,000 at m/z 400. The ion target value for MS/MS was set to 1,000,000 with a maximum injection time of 120 ms and a resolution of 17,500 at m/z 400. The first mass for the MS/MS was set to 140 m/z and the normalized collision energy was set to 27. Unassigned, as well as charge states 1 and >5 were ignored for MS/MS selection. Repeat sequencing of peptides was kept to a minimum by dynamic exclusion of sequenced peptides for 12 s.

Acquired raw files were analyzed by MS-Amanda Proteome Discoverer (Research Institute of Molecular Pathology, Vienna, Austria; version AmandaPeptideIdentifier in Proteome Discoverer 2.2.0.388), X! Tandem (The GPM, thegpm.org; version X! Tandem Alanine (2017.2.1.4)) and Sequest (XCorr Only) (Thermo Fisher Scientific, San Jose, CA, USA; version IseNode in Proteome Discoverer 2.2.0.388). All softwares was set up to search all predicted proteins in Giardia genome from giardiaDB 43rd release (Aurrecoechea et al., 2009). MS-Amanda Proteome Discoverer, and X! Tandem, was set up assuming the protease was nonspecific. Sequest (XCorr Only) was set up assuming

the protease was trypsin. MS-Amanda Proteome Discoverer, Sequest (XCorr Only) and X! Tandem were searched with a fragment ion mass tolerance of 0.020 Da and a parent ion tolerance of 10.0 PPM.

Scaffold (version Scaffold_4.9.0, Proteome Software Inc., Portland, OR) was used to validate MS/MS based peptide and protein identifications. Protein identifications were accepted if they could be established at greater than 95.0% probability and contained at least 2 identified peptides. Protein probabilities were assigned by the Protein Prophet algorithm (Nesvizhskii, Al et al Anal. Chem. 2003;75(17):4646-58). Proteins that contained similar peptides and could not be differentiated based on MS/MS analysis alone were grouped and marked with “protein grouping ambiguity”.

2.9 DNase I treatment of insoluble fraction from formaldehyde crosslinking

Giardia cells were collected as described in Section 2.1 and crosslinked with formaldehyde as described in Section 2.6. The crosslinked cells were divided in two microcentrifuge tubes so that cells in one tube were lysed with neutral lysis buffer (80 mM Tris-HCl (pH 7.4), 150 mM NaCl, 1.0% NP40, 0.1% SDS) and the cells in the other tube were lysed with an alkaline lysis buffer (80 mM glycine, 75 mM NaOH, pH 10.6, 150 mM NaCl, 1% NP40, 0.1% SDS). EDTA was left out of these procedures as it would inhibit DNase I activity. Lysis was carried out as described in Section 2.4, followed by centrifugation at 14 000 x g to removed cellular debris. The supernatant was taken for analysis by western blot.

Only the cellular debris pellet from the formaldehyde treated sample prepared by alkaline lysis was treated with DNase I. The pellets were resuspended in DNase I buffer (10 mM Tris-HCl (pH 7.6), 2.5 mM $MgCl_2$, 0.5 mM $CaCl_2$) and centrifuged again to wash away any remaining lysis buffer. Insoluble debris pellet was then resuspended in DNase I buffer and 1 unit of DNase I (NEB #M0303, 2 units/µL) was added followed by incubation at 37 ℃ for 30 minutes. The reaction was halted by the adding 1 M EDTA to a final concentration of 5 mM. These samples were once again centrifuged at 14 000 x g to removed debris, and supernatant was taken for analysis by western blot as “DNase Pellet Extract".

2.10 BLAST analysis for FACT orthologs

Histone H2a was the most enriched protein in the co-IP of gCYTB5-III. Since the yeast genome database (Cherry et al., 2012) provides excellent interactome data for each protein coded by the genome, all Interactome data demonstrating experimental physical interaction with histone H2a (gene code HTA1) was used to analyze the proteins found in the co-IP of gCYTB5-III (www.yeastgenome.org). Under gene code HTA1, “interactions” was selected and further refined to only include “physical interactions”. The interaction data was then transferred to a data mining program by selecting “analyze” and then “YeastMine” (https://yeastmine.yeastgenome.org). YeastMine was used to extract the sequences of the 285 proteins found to physically interact with H2a. The BLAST function in the Giardia database was then applied to each sequence extracted from the yeast genome to identify any orthologs to the proteins found to interact with

H2a in yeast. A list of potential orthologs was generated in Excel and the VLOOKUP function was applied to find common GiardiaDB accession number between the H2a interacting orthologs, and the eluate of gCYTB5-III co-IP. Proteins found in both the H2a-yeast interactome, and the co-IP of gCYTB5-III were then analyzed again with BLAST against the UniProt database to determine the likelihood these proteins were true orthologs of the original yeast proteins. Of the proteins that held up to the reverse BLAST, the most common grouping was FACT associated proteins.

RESULTS

3.1 Localization of gCYTB5-III by immunofluorescence microscopy

Previous work in our lab used Giardia cell lines transfected with plasmids that overexpressed HA-tagged versions of each of the Giardia cytochrome b5 isotypes to identify their interacting partners through co-immunoprecipitation (co-IP) experiments (Dayer, 2017). For protein localization studies, I performed Immunofluorescence microscopy analysis (IFA) on both untransfected Giardia (UT) and Giardia transfected with the HA-tagged gCYTB5-III (HA-III) with an antibody against a unique peptide in the flanking region of the endogenous protein (anti-gCYTB5-III) and an antibody against the HA tag (anti-HA). Nuclear localization was observed with the anti-CYTB5-III antibody in both the UT (column 1, Fig. 4) and HA-tagged gCYTB5-III cell lines (column 2, Fig. 4). However, IFA results with the HA antibody showed diffuse cytoplasmic fluorescence in both the untransfected and HA-gCYTB5-III cell lines (columns 3 and 4). The initial interpretation of these results is that the HA-antibody was ineffective in IFA for detecting HA-tagged proteins in Giardia. More recently, our lab obtained a Giardia cell line that contains a copy of a HA-tagged pseudouridine synthetase CBF5 gene integrated into the Giardia genome. When I used the HA antibody in IFA analysis of the HA-CBF5 cells, I observed the expected nucleolar localization of this protein (column 5) indicating that the anti-HA antibody can detect HA-tagged proteins in Giardia. The inability to detect the expected nuclear localization of the HA-tagged version of gCYTB5-III in IFA suggests that HA-gCYTB5-III is not a viable candidate as a bait protein for co-IP

experiments. Therefore, the objective of my research is to use the antibody against the endogenous gCYTB5-III protein in co-IP to identify its interacting partners.

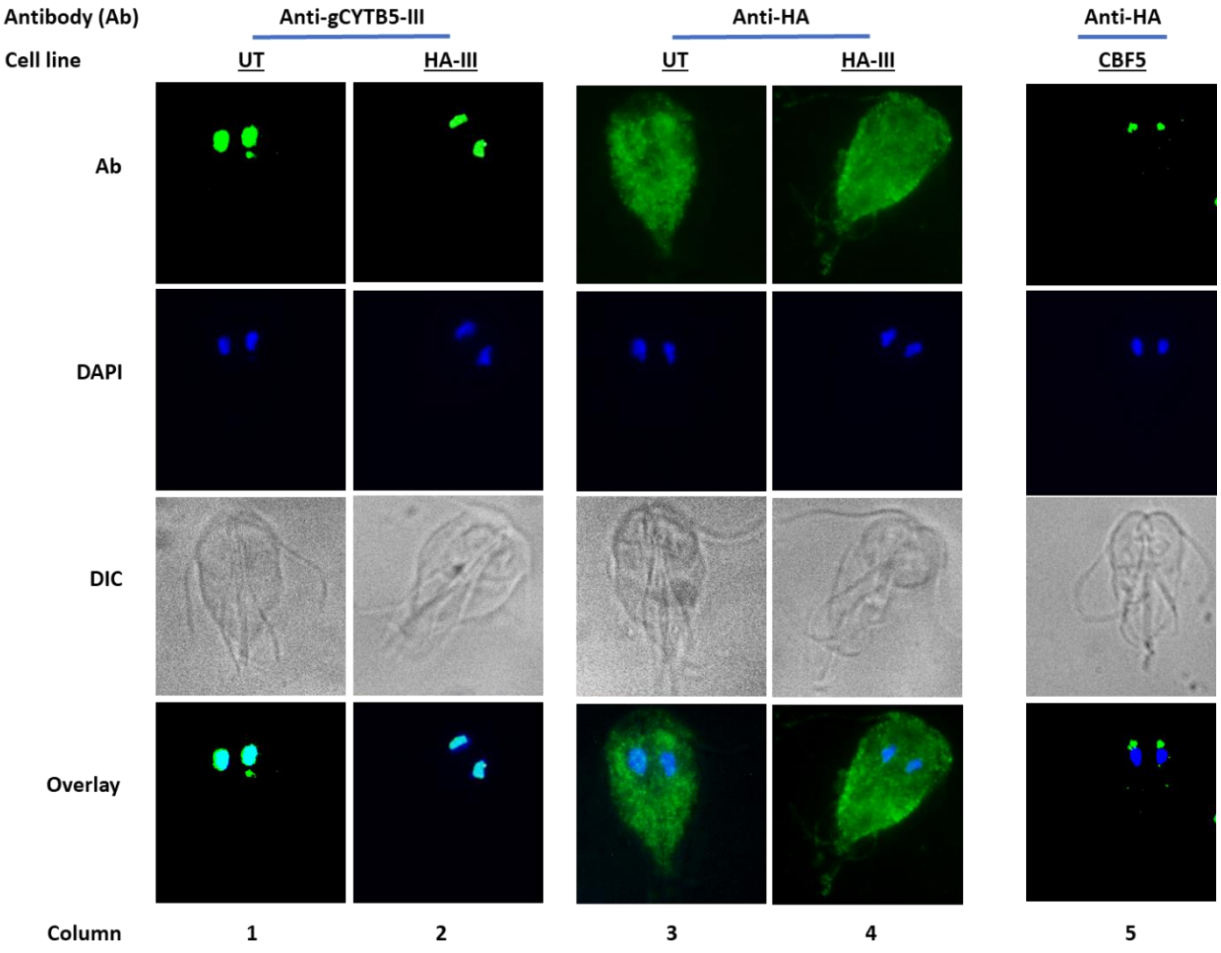

Figure 4: Immunofluorescent analysis for the localization of endogenous gCYTB5-III, HA-tagged gCYTB5-III, and HA-tagged CBF5 pseudouridine synthase. The cells lines and antibody applied are listed across the top. Immunostaining with the antibody against the endogenous gCYTB5-III (anti-gCYTB5-III) displays localization to the nucleoplasm of both cell lines (columns 1 and 2), highlighted by their complete overlay with DAPI staining of the DNA in both nuclei of each Giardia trophozoite. Immunostaining with the antibody against the HA-tagged gCYTB5-III shows diffuse fluorescence throughout the cytosol in both cell lines (columns 3 and 4). A cell line expressing a HA-tagged pseudouridine synthetase CBF5 was used as a positive control for detection of a HA-tagged protein with the anti-HA antibody (column 5).

3.2 Localization of gCYTB5-I, II and III by subcellular fractionation

The localization of each gCYTB5 isotype was previously established in our laboratory by immunofluorescent microscopy analysis (IFA) that used custom antibodies against peptides corresponding to sequences in the flanking regions unique to each isotype; these reflect the location of endogenously-expressed, untagged gCYTB5s (Dayer, 2017). This work showed that isotype I is localized to the nucleolus, isotype II to the peripheral vacuoles (PV), and isotype III to the nucleoplasm. To examine the localization of the three gCYTB5 by an independent method from IFA, I performed a crude fractionation of the cellular proteins, henceforth referred to as the organelle enrichment procedure, the workflow of which is outlined in Figure 6. In this procedure, Giardia trophozoites were lysed in a hypotonic buffer together with a freeze-thaw step that is followed by manual grinding by a pestle within a microcentrifuge tube. This was followed by the addition of 0.2% NP40, a nonionic detergent. My objective was to use the freeze-thaw step together with the detergent to disrupt the plasma membrane of the cells so that cytosolic proteins are released into the supernatant of the sample, while proteins within intact organelles and proteins tightly associated with membranes would remain in the cell pellet after centrifugation. The cell pellet was then washed extensively to ensure sufficient removal of cytosolic proteins. To monitor the efficiency of these washes, the blue colour intensity of Bradford reagent was used as a quick visual guide to determine the relative protein concentration in each wash (Fig. 5). Washes were performed until no further change in colour intensity was observed (washes 4 – 6, Fig. 5).

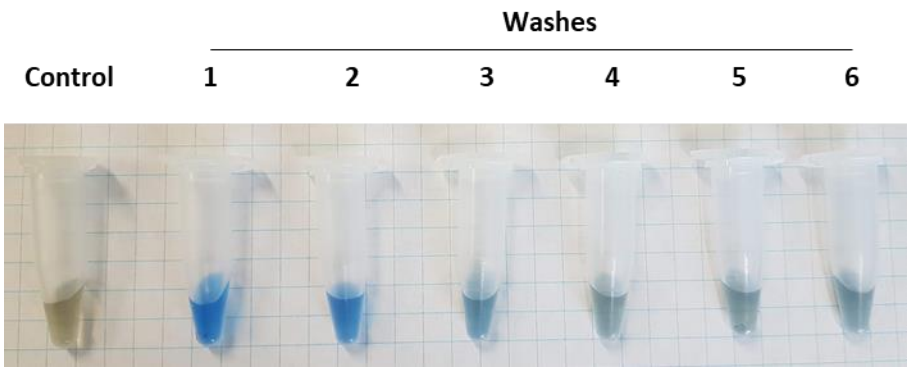

Figure 5: Bradford analysis of washes from organelle enrichment experiment. Tubes contain 200 µL of Bradford reagent and 10 µL of the PBS wash.

The initial supernatant should contain predominately cytosolic proteins (cytosolic fraction), while the pellet remaining after six washes should contain predominately proteins in the nuclei and in other organelles (organelle fraction). To examine the robustness of the organelle enrichment procedure, I used antibodies against proteins with known cellular localization to examine their presence in these fractions on western blots. PUP9296 is a protein with unknown function that is found in the Giardia mitosomes and an antibody against this protein is frequently used as a marker for this organelle in Giardia IFA (Martincová et al., 2015; Pyrihov et al., 2018; Voleman et al., 2017). Protein disulfide isomerase (PDI2) is a maker for the endoplasmic reticulum (ER) in Giardia (Gaechter et al., 2008). The results show that PUP9296 and PDI2 are both found within the expected organelle fraction (Fig. 6A).

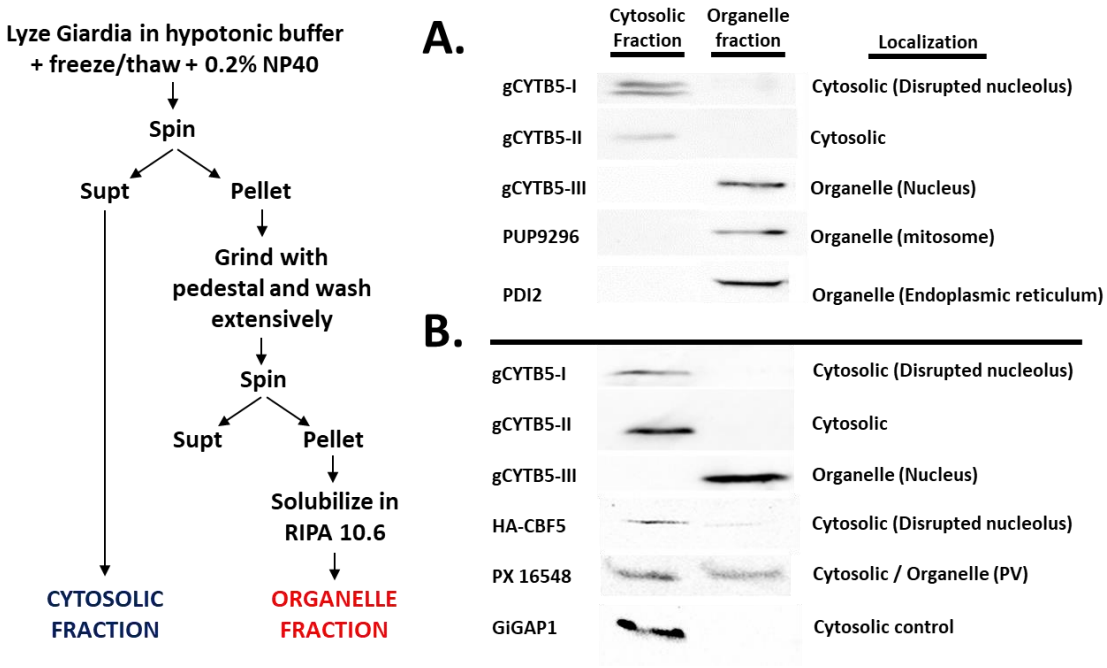

Figure 6: Western blot analysis of the organelle enrichment experiment. The outline of this experiment is shown on the left side of the figure and the western blot analysis is depicted on the right. The antibodies used to hybridize with the membrane are indicated by the labels on the left of the images. A) Organelle enrichment performed with untransfected cell line. The cytosolic fraction represents the proteins released into the supernatant after a freeze-thaw cycle and grinding of the cell pellet in PBS. The organelle fraction is the sample pellet solubilized in alkaline lysis buffer after the 6th wash to ensure all cytosolic protein was removed. B) Organelle enrichment performed on transgenic cell line expressing the nucleolar localized HA-tagged CBF5.

Antibodies against each of the gCYTB5 isotypes were used in western blot analysis of the fractions (Fig. 6A). The detection of gCYTB5-III in the organelle fraction is consistent with the IFA results showing its localization in the nucleoplasm. However, the detection of gCYTB5-I and gCYTB5-II in the cytosolic fraction are inconsistent with the IFA results that show gCYTB5-I in the nucleolus and gCYTB5-II in the PVs. Proteins associated with these structures are expected in the organelle fraction. Therefore, it is possible that the lack of detection of gCYTB5-I and II in the organelle fraction is due to

disruption of nucleolus and PVs during the initial cell lysis step. As pseudouridine synthetase CBF5 is a well-characterized nucleolar protein, I used the detection of HA-tagged CBF5 in the organelle fraction as a marker for the retention of the nucleolus in my fractionation procedure (Fig. 6B). The results show that although a small amount of HA-CBF5 is detected in the organelle fraction, the majority of HA-CBF5 is in the cytosolic fraction, suggesting that the nucleolus was disrupted during this fractionation procedure. The disruption of the nucleolus allowed proteins associated with this organelle to leak into the cytosolic fraction, including gCYTB5-I. The antibody against the PX 16548 protein has been previously used to localize the PVs in Giardia (Datta, Jana, Mondal, Ganguly, & Sarkar, 2018) and this antibody was used to evaluate the retention of the PVs in my fractionation procedure. The results demonstrate that proteins associated with the PV were also released in the cytosolic fraction. Finally, I used an antibody against Giardia GAPDH (GiGAP1), which is a protein used previously as a cytosolic marker in cellular fractionation studies in Giardia (Park, Kim, Shin, & Park, 2020) and noted that this protein was also exclusively detected in the cytosolic fraction in my study (Fig. 6B).

3.3 Recovery of gCYTB5-III in supernatant fraction of lysate

The lysis buffers used in the preparation of protein lysates for co-immunoprecipitation (co-IP) should not contain reducing reagent such as DTT and strong ionic detergents such as SDS, as these agents can denature or affect the binding of the

antibody applied in co-IP. I initially used a commercially available, proprietary lysis buffer (CelLytic Y, Sigma) that was commonly used for lysis of Giardia trophozoites in our lab. Although I was able to detect a low level of gCYTB5-III in the immunoprecipitate by western blot analysis, mass spectrometry analysis of the immunoprecipitate from these initial experiments showed no detection of the gCYTB5-III that was used as the bait protein (data not shown). As a result, I switched to using lysis buffers with known compositions so that I could control their composition to optimize recovery of the bait protein. I tested a standard lysis buffer for co-IP consisting of 25 mM Tris-HCl pH 7.4, and 1% NP-40, but only a small amount of gCYTB5-III was recovered in the supernatant (Fig. 7B, NP-40 sup. fraction) while most of this protein was retained in the cell debris pellet after centrifugation of the cell lysate (Fig. 7B, NP-40 pellet fraction). I also replaced NP-40 with Triton X-100 (TX) but this had no effect.

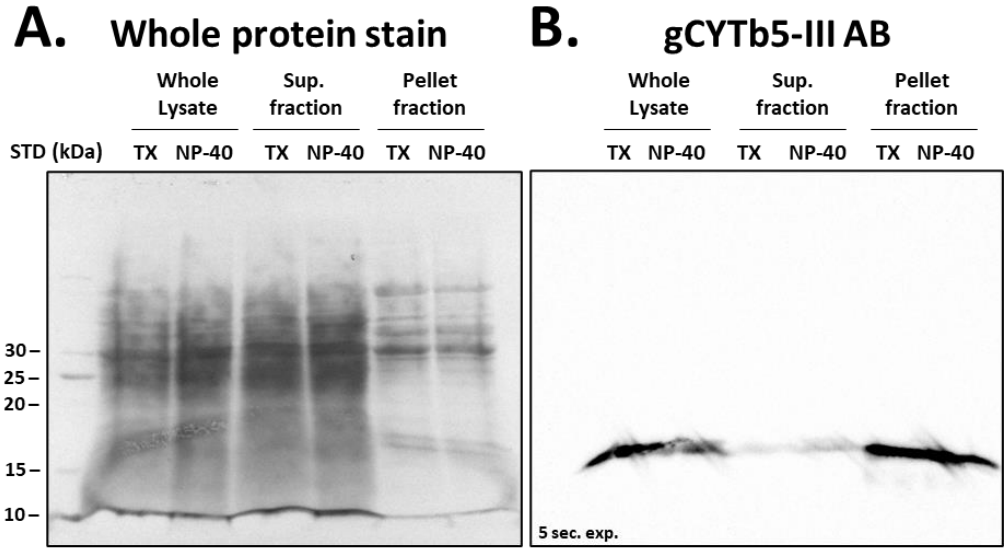

Figure 7: Western blot analysis of the recovery of gCYTB5-III in supernatant (Sup.) and pellet fractions of whole lysate prepared from lysis buffer containing Triton X-100 (TX) or NP-40. A) Ponceau stain to show the total protein in each lane that is transferred onto the membrane. B) Western blot results after hybridization of membrane with anti-gCYTB5-III antibody.

If the low recovery of gCYTB5-III in the supernatant was due to poor cellular lysis, the Ponceau stain should also indicate a deficiency of total proteins recovered in the supernatant (Fig. 7A). Since the Ponceau stain showed a good recovery of total protein in the supernatant, it is possible that gCYTB5-III is insoluble, resulting in its recovery in the pellet fraction. However, recombinant versions of gCYTB5-III produced in our lab are completely soluble (Yang et al., 2016), so I investigated other explanations for the poor recovery of gCYTB5-III in the supernatant after centrifugation of Giardia lysates.

One possible reason for the lack of detection of gCYTB5-III in the supernatant is that this protein is tightly associated with an insoluble membrane component. Since protein precipitation is an effective method to isolate insoluble proteins that interact with lipids from a sample, I tried a chloroform/methanol protein precipitation on Giardia whole cell lysates, but I was unable to solubilize the precipitated proteins in a buffer that is compatible for application in co-IP (RIPA buffers at pH 5.5, 7.4, 8.2 were tested). However, I was able to recover higher levels of gCYTB5-III within the supernatant when the precipitated proteins were resuspended in a lysis buffer with a pH of 10.6. When I used this alkaline lysis buffer to directly lyse Giardia cells without the protein precipitation step, the detection of gCYTB5-III was exclusively in the pellet fraction (data not shown). Next, I tested the addition of SDS to the alkaline lysis buffer. The addition of 0.1% SDS resulted in the 71% of gCYTB5-III in the supernatant from Giardia cells when compared to whole lysate (Fig. 6B). Increasing SDS concentration to 0.5% did not result in any further increase in gCYTB5-III retention so 0.1% SDS was used going forward.

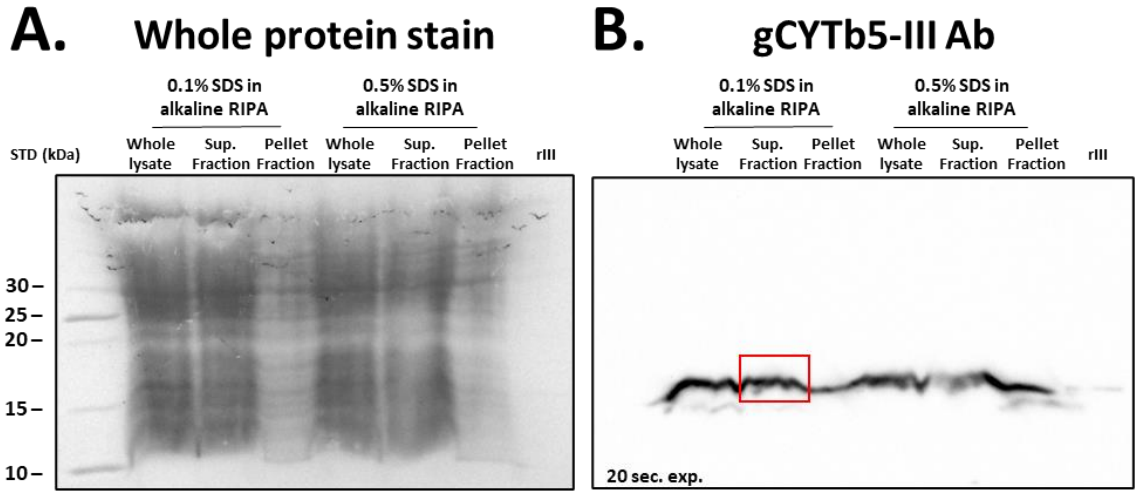

Figure 8: Analysis of gCYTB5-III recovery in cell lysates prepared with an alkaline lysis buffer with the addition of either 0.1% or 0.5% SDS. The whole cell lysate prepared with each lysis buffer was analyzed along with the supernatant and pellet fractions after its centrifugation. A) Ponceau stain displaying the total protein in each sample on the membrane. B) Western blot results from hybridization of the membrane with anti-gCYTB5-III antibody. A sample of recombinant gCYTB5-III (rIII) was included as a positive control.

3.4 *In vivo* crosslinking of gCYTB5-III

One major disadvantage to performing co-IP with a bait protein that has a low endogenous level of expression is that there will be a correspondingly low level of prey protein captured. This issue is further compounded if the interaction between the bait and prey protein is weak or transient. For my studies, I investigated the addition of a chemical crosslinker to covalently link interacting proteins to gCYTB5-III within the cells (*in vivo)* before the cell lysis step. This would stabilize transient or weakly interacting

proteins to gCYTB5-III. Giardia cell cultures were grown to exponential phase before the cells were collected and resuspended in PBS containing the crosslinker. Following crosslinking, the buffer containing crosslinker is removed and replaced by a buffer containing a quencher to inactivate all remaining crosslinker. The cells were then disrupted by the addition of the alkaline lysis buffer followed by sonication.

It is necessary to optimize the concentration of the crosslinking reagent that will be used for co-IP since insufficient crosslinking would be unable to stabilize the protein interactions while excessive crosslinking would result in problems in recovery of the protein complex and reduced accessibility of the antibody to the bait protein. Previous work with crosslinkers in co-IP experiments in Giardia used titrations of the crosslinking reagent to identify the minimal concentration that is required to crosslink at least half of the total protein of interest (Martincová et al., 2015; Pyrih et al., 2016; Rout, 2015; Zumthor et al., 2016).

I first evaluated the effect of *in vivo* crosslinking with the membrane permeable crosslinkers SMPB and BMH on the detection of gCYTB5-III in Giardia lysates by western blot. These analyses showed that the level of the free or un-crosslinked form of gCYTB5-III at ~15 kDa decreased with the increasing concentrations of each crosslinker (Fig. 9, band 1). In parallel, crosslinked, higher molecular weight complexes containing gCYTB5-III increased with increasing concentrations of crosslinkers (Fig. 9, bands 2 and 3). The results for the BMH crosslinker suggest the presence of at least two complexes containing gCYTB5-III; one at ~27 kDa (band 2) and another at ~40 kDa (band 3). Since 3 mM is the lowest concentration of BMH tested that gave a 60% decreased intensity of

band 1 while retaining the detection of bands 2 and 3, I chose this combination of crosslinking reagent and concentration to carry out my co-IP.

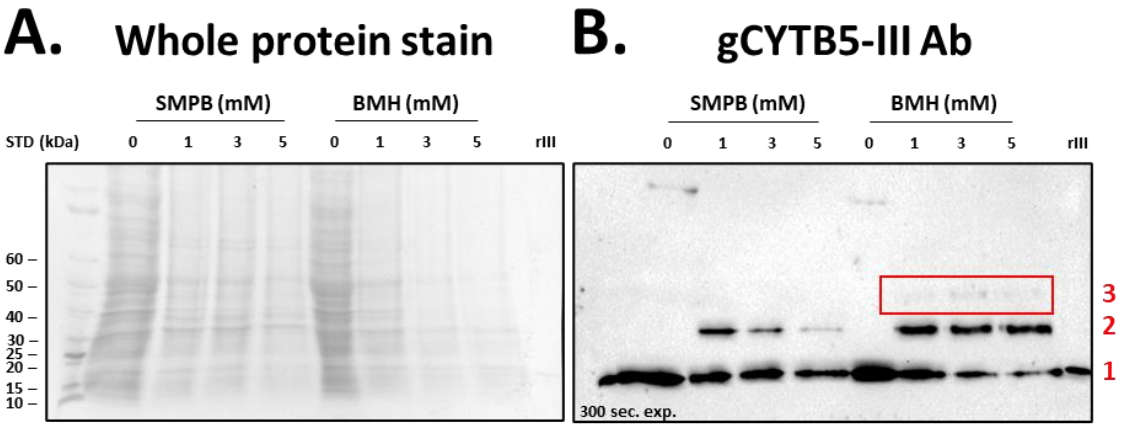

Figure 9: Analysis of lysates from Giardia cells treated with varying concentrations of SMPB and BMH crosslinkers. A) Ponceau stained membrane shows the total proteins in each lane of the blot. B) Western blot results with the gCYTB5-III antibody. The lowest molecular weight band (band 1) represents the free or un-crosslinked form of gCYTB5-III, and it co-migrates with the recombinant gCYTB5-III (rIII) shown in the last lane. Bands 2 and 3 represents higher molecular weight protein complexes containing gCYTB5-III that are captured by the crosslinkers. The highest molecular weight complex identified, band 3 (boxed in red), is only detected with BMH.

3.5 Co-Immunoprecipitation of gCYTB5-III

The main goal of my research was to identify interacting partners of gCYTB5-III by co-IP with the antibody against the endogenous protein. Since this antibody has not been used previously in co-IP experiments, I performed preliminary experiments to examine the recovery of gCYTB5-III by co-IP beads that are pre-incubated with this antibody. I compared the ability of these beads to capture a recombinant version of gCYTB5-III as the sole protein in a sample compared to their ability to capture endogenous gCYTB5-III from whole cell lysates (Fig. 10A). At this point of my research, I was considering using the whole cell lysate in the co-IP since centrifugation of this lysate

to obtain a soluble supernatant fraction would result in the majority of the gCYTB5-III being retained in the pellet. The results in Figure 8 show that the recovery of gCYTB5-III from the whole cell lysate (WL) is much less than that from the sample containing only the recombinant protein (rIII), which likely represents the maximum capacity of the co-IP beads and antibody combination. It is possible the interactions that caused the endogenous gCYTB5-III to persist in the non-soluble fraction of the lysate were interfering with the efficiency of the co-IP.

I then explored methods to obtain the gCYTB5-III in a soluble fraction; these efforts are reported in the section of my thesis on the "Recovery of gCYTB5-III in supernatant fraction of lysate". After establishing the new alkaline lysis conditions to allow the increased recovery of gCYTB5-III in the soluble supernatant fraction of the lysate, I observed increased recovery of this protein in the co-IP eluate (Fig. 10 WL eluate vs. SL eluate). The higher recovery of the gCYTB5-III bait protein in the immunoprecipitate with the protein lysate prepared from the new lysis buffer could be discerned by comparing the higher relative intensity of the gCYTB5-III band to the intensity of the antibody light chain (at ~25 kDa) in the SL eluate in Fig. 10B compared to the WL eluate in Fig. 10A.

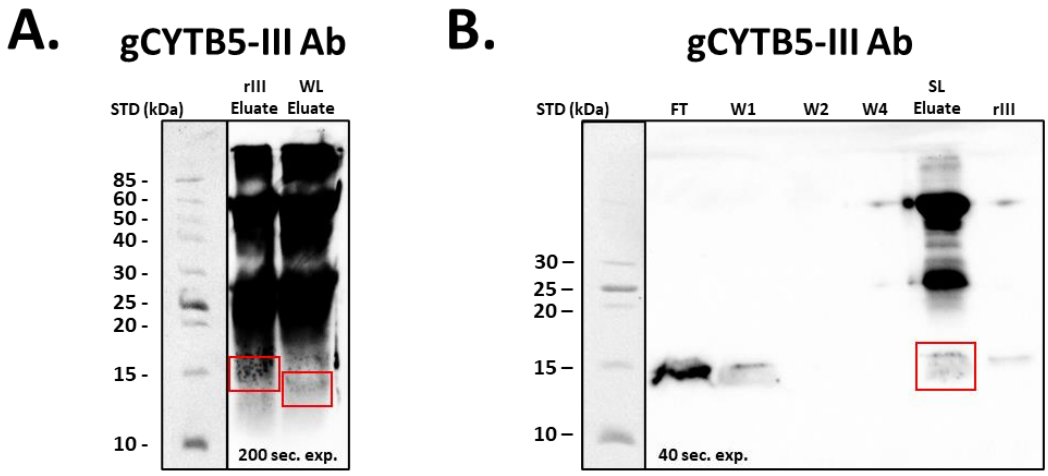

Figure 10: Western blot analysis of gCYTB5-III co-IP efficiency. A) Comparison of the co-IP capture of recombinant gCYTB5-III (rIII) as the sole protein in a sample compared to the capture of endogenous gCYTB5-III from whole cell lysate (WL). The eluted gCYTB5-III bait protein is indicated by red boxes. Note: The molecular weight of gCYTB5-III is slightly greater for the recombinant version of the protein due to presence of a hexahistidine tag. B) Western blot analysis of first attempt at co-IP with the supernatant recovered from centrifugation of Giardia lysates prepared with the alkaline lysis buffer. Flow through (FT) and washes (W1 – 4) are expected to contain mostly unbound proteins. The eluate from the supernatant lysate (SL) contains the band representing gCYTB5-III boxed in red. Recombinant gCYTB5-III (rIII) is included to confirm correct protein identification. Standard molecular weight marker (STD) is included as a colourimetric image overlay.

Furthermore, I also decreased the pH of the protein lysate prepared in the alkaline RIPA pH 10.6 lysis buffer before it was used in the immunoprecipitation assay by adding two volumes of 80 mM TBS (pH 7.2) to the supernatant recovered after centrifugation of the cell lysate. The resultant pH of the supernatant (pH 8.4) is more compatible with co-IP. This adjustment in pH resulted in higher recovery of gCYTB5-III as observed by comparing the intensity of the band representing gCYTB5-III at ~15 kDa to the band representing the antibody light chain at ~25 kDa in Figure 10A and Figure 10B.

Next, I examined the use of BMH crosslinking in co-IP. Two parallel co-IP samples were prepared: one sample with control lysate from untreated Giardia and the other sample with lysate from Giardia treated with the BMH crosslinker. Addition of the BMH crosslinker to the cells before the preparation of the protein lysate resulted in less monomeric gCYTB5-III recovered in co-IP compared to the lysate prepared from cells without its addition (Fig. 11A, red arrows). However, the results also show the appearance of an ~40 kDa complex (Fig. 11A, highlighted by the red box) in the BMH eluate that is absent in the control eluate. A complex of similar size was also observed in the BMH titration experiment (Fig. 9 band 3). This demonstrates that although there is reduced recovery of the monomeric gCYTB5-III protein, the IP was successful in capturing at least one crosslinked complex containing gCYTB5-III.

In mass spectroscopy analysis of preliminary Giardia co-IP experiments with the gCYTB5-III antibody, tubulin was the most abundant contaminant of the immunoprecipitate (data not shown). To address this, I increased the Tween-20 concentration in the washes from 0.01 % to 0.5 % to aid in the removal of tubulin and other contaminants in this experiment. The western blot results demonstrate the effective removal of tubulin from the eluate samples (Fig. 11B).

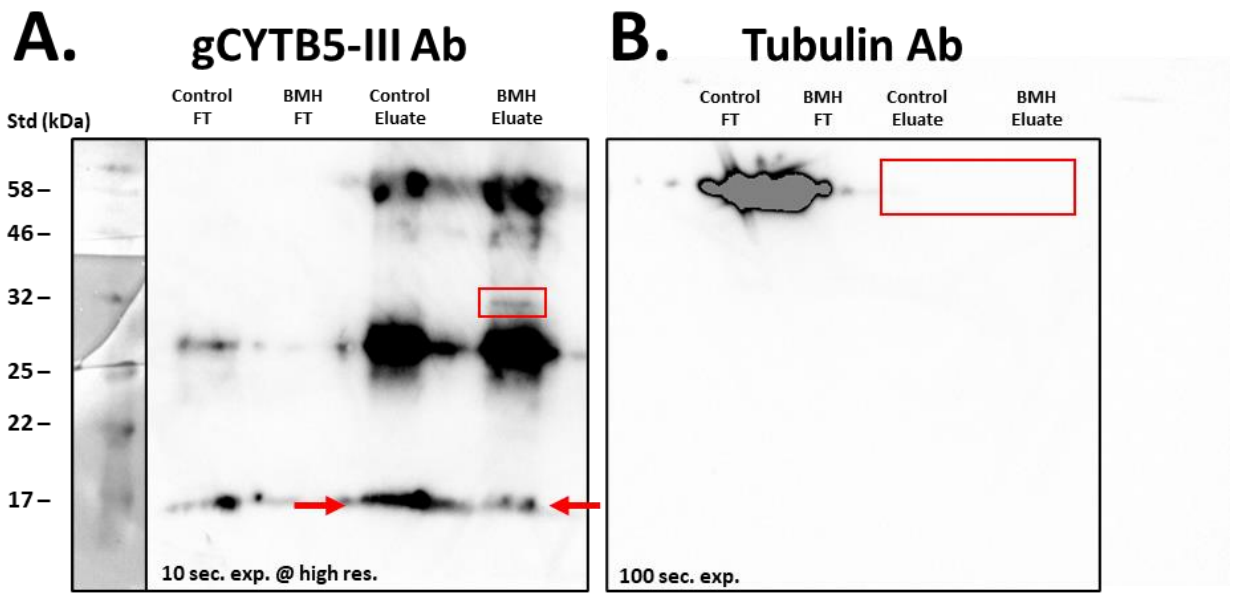

Figure 11: Western blot analysis comparing the co-IP results from non-crosslinked lysate (control) to BMH *in vivo* crosslinked cell lysate. A) Results of hybridization with the gCYTB5-III antibody. The position of the monomeric gCYTB5-III is indicated by an arrow and the ~30 kDa complex in the BMH eluted sample is indicated by the red box. Standard molecular weight marker is included as a colourimetric image overlay. B) Results of hybridization with the tubulin antibody. The absence of tubulin in the eluate for the control and BMH samples is indicated by the red box.

In preparation for my final co-IP experiment, the magnetic protein G beads for co-IP were initially incubated with either the antibody for gCYTB5-III or the pre-immune serum. The pre-immune serum is the blood serum of the host rabbit prior to its immunization with the peptide antigen. The antibodies in this control will have the same constant region as the gCYTB5-III antibody so that any proteins interacting non-specifically with the antibody structure, or constant region, will be accounted for in the pre-immune serum results and omitted as potential interaction candidates.

Giardia trophozoites were collected from cultures grown to exponential phase (4.7 x 10^5 to 7.8 x 10^5 cells / mL) and resuspended in PBS before incubation with the BMH

crosslinker. The cells were then resuspended in alkaline lysis buffer and immediately sonicated. The lysate was centrifuged to remove cellular debris and the supernatant was split into two samples: one sample was used for co-IP with the gCYTB5-III antibody and the second sample was used for co-IP with the pre-immune rabbit serum as a control. Furthermore, the immunoprecipitate (eluate) from each co-IP sample was divided so that half was analyzed by western blot and the other half was analyzed by mass spectrometry for protein identification. The western blot shows that gCYTB5-III is recovered in the eluate when gCYTB5-III antibody is used but not when the pre-immune serum was used in the co-IP (Fig. 12). In addition, a band at ~40 kDa is present in the eluate of gCYTB5-III antibody but not in eluate with the pre-immune serum. The remaining half of the eluate from gCYTB5-III antibody and the pre-immune antibody were sent for MS analysis.

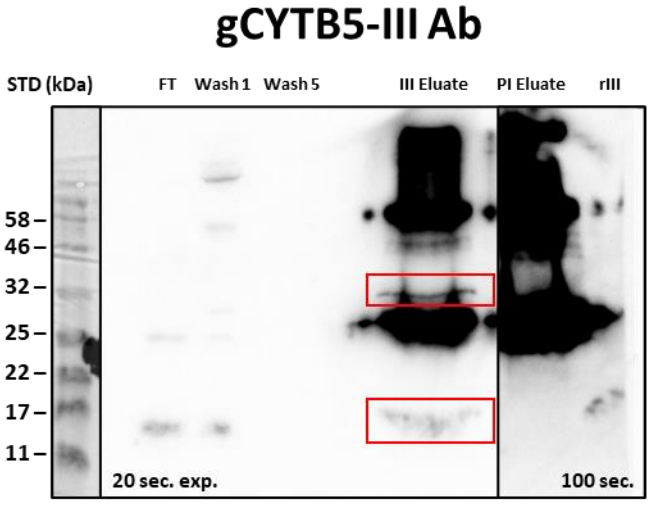

Figure 12: Western blot analysis of the co-IP experiment sent for analysis by mass spectroscopy. Standard molecular weight marker is included as a colourimetric image overlay. The presence of the free gCYTB5-III (~15 kDa) and the ~40 kDa complex are indicated by red boxes in the immunoprecipitate from the co-IP with the gCYTB5-III antibody. The blot from the co-IP with the pre-immune (PI) is purposely overexposed to show the absence of the free gCYTB5-III and the 30 kDa complex. A sample of recombinant gCYTB5-III (rIII) was loaded into the last lane as a marker for the location of this protein on the blot.

3.6 Identification of protein partners - Mass Spectroscopy

Co-IP eluate samples performed in parallel to those confirmed by western blot (Fig. 12) were sent for mass spectroscopy (MS) analysis and the peptides were matched against all predicted proteins from the Giardia genome (GiardiaDB ,43rd release, Aurrecoechea et al., 2009). A total of 1291 unique proteins, comprising 25984 spectra (individual peptides) were identified (Fig. 13). 182 proteins were unique to the gCYTB5-III immunoprecipitate, and a further 69 proteins were enriched 2-fold or higher in the gCYTB5-III immunoprecipitate compared to the pre-immune immunoprecipitate. Enrichment was determined by normalizing the number of peptides identified for each protein in the experimental sample over the number of peptides identified in the control, pre-immune immunoprecipitate.

44 of the 182 proteins unique to the gCYTB5-III immunoprecipitate, and 15 of the 69 proteins that are enriched in the gCYTB5-III immunoprecipitate have known or likely nuclear localization. These nuclear proteins include histones, transcription factors, and proteins involved in nucleosome remodeling. As gCYTB5-III was shown by IFA and organelle enrichment analysis to be associated with the nucleus, these nuclear proteins in the MS results are of particular interest.

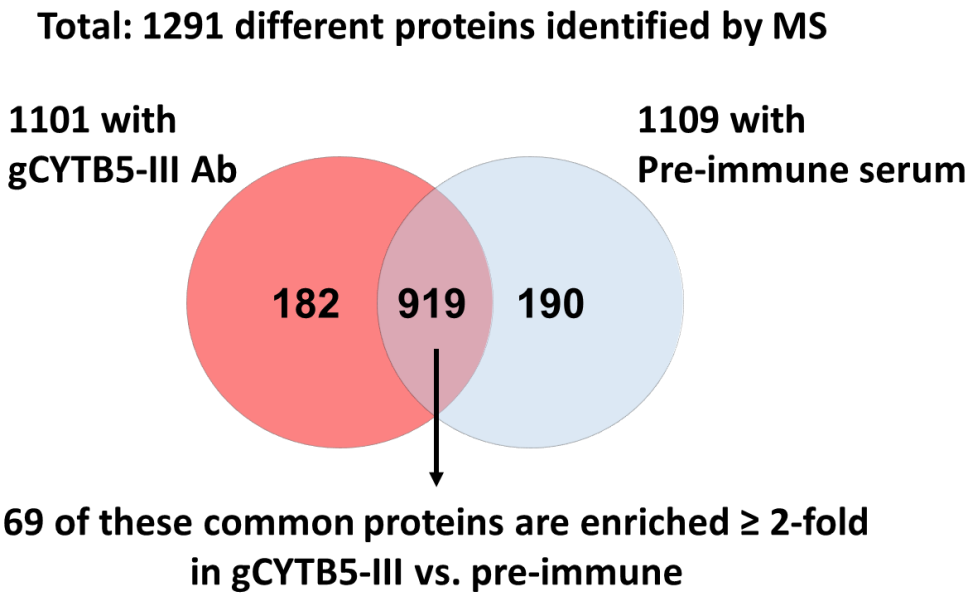

Figure 13: Diagram representing the proteins identified by the mass spectroscopy analysis of the IP samples. The results obtained found a total of 1291 different proteins. Of these, 919 are common to both samples, 182 were unique to the experimental sample and 190 proteins were unique to the pre-immune control. All the unique proteins (182) and only the common proteins that are enriched ≥ 2-fold in gCYTB5-III sample compared to the pre-immune sample (69) were considered proteins of interests.

Intriguingly, the MS analysis also identified 44% of the known mitosomal proteome among the proteins unique or enriched in the gCYTB5-III sample. These results are unexpected as gCYTB5-III is not localized to the mitosome, nor have mitosomal proteins been localized to the nucleus. The top 20 proteins identified in the unique and ≥2-fold enriched categories are shown in Table 2 and 3 respectively, with the nuclear proteins highlighted in green and the mitosomal proteins highlighted in orange.

Table 2: Top 20 Unique candidates for gCYTB5-III interacting partners. Highlighted in green are all expected or experimentally proven nuclear localized proteins. Highlighted in orange are experimentally proven mitosomal proteins. The reference to evidence for localization is listed under "Ref. Localization". Listed acronyms for localization evidence: S-Ab, IFA evidence using specific antibody; HA, IFA evidence using HA tagged protein; GFP, IFA evidence using GFP tagged protein; UniProt, based off of established localization of orthologs in other eukaryotes; NLS, nuclear localization signal identified via PSORT II.

			# Peptides		
Giardia DB accession #	**Annotation**	**MW (kDa)**	**III**	**PI**	**Ref. Localization**
GL50803_14581	Chaperone DnaK mitochondria HSP70	70	24	0	HA (Regoes et al., 2005)
GL50803_115245	Coiled-coil protein (possible importin)	124	24	0	NLS
GL50803_13922	hypothetical protein	114	16	0	
GL50803_9722	Protein 21.1	56	14	0	
GL50803_103891	Chaperonin 60	57	8	0	S-Ab (Regoes et al., 2005)
GL50803_91252	Nitric oxide synthase, inducible (GiOR-1)	67	8	0	S-Ab (Pyrih et al., 2016)
GL50803_16975	DNA topoisomerase II	168	8	0	UniProt
GL50803_15587	Protein 21.1	28	7	0	
GL50803_9478	GPP, processing peptidase (bMPP)	45	7	0	HA (Jedelsky et al., 2011)
GL50803_3762	Protein 21.1	82	7	0	
GL50803_17005	Protein 21.6	96	7	0	NLS
GL50803_14519	Cysteine desulfurase (IscS)	48	6	0	S-Ab (Tovar et al., 2003)
GL50803_15487	WD-40 repeat protein	106	6	0	GFP (Hagen et al., 2011)
GL50803_5593	Ribosomal protein L11	20	5	0	
GL50803_17587	CTP synthase	68	5	0	
GL50803_6933	hypothetical protein	134	5	0	
GL50803_8228	DNA-dependent ATPase, putative	145	5	0	UniProt
GL50803_89347	RNA polymerase II RPB1subunit	230	5	0	UniProt
GL50803_14821	HesB domain-containing proteins (IscA)	14	4	0	HA (Jedelsky et al., 2011)
GL50803_7309	Syntaxin-like protein 1	33	4	0	

Table 3: Top 20 enriched candidates for gCYTB5-III interacting partners. Highlighted in green are all expected or experimentally proven nuclear localized proteins. Highlighted in orange are experimentally proven mitosomal proteins. The reference to evidence for localization is listed under "Ref. Localization". Listed acronyms for localization evidence: S-Ab, IFA evidence using specific antibody; HA, IFA evidence using HA tagged protein; GFP, IFA evidence using GFP tagged protein; UniProt, based on the established localization of orthologs in other eukaryotes.

			# Peptides		
Giardia DB accession #	**Annotation**	**MW (kDa)**	**III**	**PI**	**Ref. Localization**
GL50803_7188	Hypothetical protein	116	19	3	HA (Martincová et al., 2015)
GL50803_27521 GL50803_14256	Histone H2A	14	43	7	UniProt
GL50803_2013	Glutaredoxin-related protein	22	10	2	HA (Rada et al., 2009)
GL50803_16317	Hypothetical protein	347	13	3	
GL50803_10370	ATP/GTP binding protein, putative	53	26	6	GFP (Hagen et al., 2011)
GL50803_17430	DRE4 protein	130	21	5	UniProt
GL50803_24662	L-serine dehydratase	57	8	2	
GL50803_16887	ATP-dependent RNA helicase HAS1	61	7	2	UniProt
GL50803_16328	DRAP deaminase	64	7	2	
GL50803_86681	Glutaminyl-tRNA synthetase	80	7	2	
GL50803_21321	High cysteine membrane protein Group 5	73	29	9	
GL50803_6633	Farnesyl diphosphate synthase	46	9	3	GFP (Hagen et al., 2011)
GL50803_42442	Transitional ER ATPase	90	9	3	
GL50803_15099	20S proteasome alpha subunit 4	23	6	2	UniProt
GL50803_28234	Adenylate kinase	32	6	2	
GL50803_6564	PcnA	33	6	2	UniProt
GL50803_16948	Nucleolar protein NOP2	55	6	2	UniProt
GL50803_101594	CCAAT-box-binding transcription factor	119	6	2	UniProt
GL50803_21444	Spindle pole protein	66	8	3	
GL50803_33989	hypothetical protein	35	8	3	

3.7 Evidence of gCYTB5-III interacting with DNA

During my evaluation of crosslinking reagents to stabilize protein interactions with gCYTB5-III, I also tested formaldehyde in addition to SMPB and BMH. When increasing concentrations of a crosslinker were added to Giardia cells, the level of free, un-crosslinked gCYTB5-III was expected to decrease, since increased sequestering of this protein in complexes with other proteins would reduce its monomeric form. This was observed for the titration with SMPB and BMH (Fig. 9). Although this trend was also observed for formaldehyde, there was an unexpected increase in the free form of gCYTB5-III at 0.1% and 0.2% formaldehyde relative to the untreated sample (Fig. 14). Due to the nuclear localization of gCYTB5-III, this finding is interesting as formaldehyde treatment is known to induce a DNA damage response (Anandarajan et al., 2020; Ciccia, McDonald, & West, 2008; de Graaf, Clore, & McCullough, 2009; Deans & West, 2011; Fink et al., 1996; Knipscheer et al., 2009; Mu et al., 2000; Noda et al., 2011).

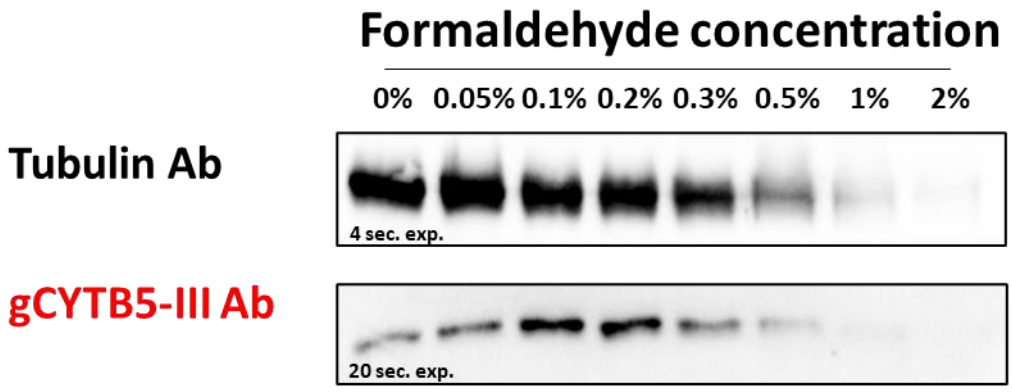

Figure 14: Western blot analysis of whole cell lysates prepared with neutral pH lysis buffer, from formaldehyde titration experiment. Giardia cells were treated with increasing concentrations of formaldehyde prior to lysis. Cells were crosslinked with the indicated concentration of formaldehyde for 30 min. and then quenched with 1 M glycine for 15 min. The samples were analyzed for gCYTB5-III in the lower panel and for tubulin in the upper panel.

Another interesting result was observed when I tested two types of lysis buffers on Giardia cells treated with increasing concentrations of formaldehyde. When a lysis buffer at neutral pH (7.4) was used, it was not possible to detect gCYTB5-III in the supernatant after centrifugation of the lysate (Fig. 15). In contrast, when a lysis buffer with an alkaline pH (10.6) was used, gCYTB5-III was detected in the supernatant of samples treated with 0 - 0.5% formaldehyde (Fig. 15). The highest recovery of gCYTB5-III with 0.1% and 0.2% formaldehyde is consistent with the previous results shown in Figure 14. The decrease in the detection of gCYTB5-III in the supernatant of the alkaline lysis samples treated with 0.25% or higher percentages of formaldehyde in Figure 15 is likely due to the sequestering of gCYTB5-III crosslinked in complexes by these higher percentages of formaldehyde. Note that there is also less free or un-crosslinked tubulin recovered in the supernatant from lysates from cells treated with 1% and 2% formaldehyde. The approximately equivalent level of tubulin recovered in the

supernatant from the neutral and alkaline lysis buffers suggests that both buffers were equally effective at disrupting the Giardia cells.

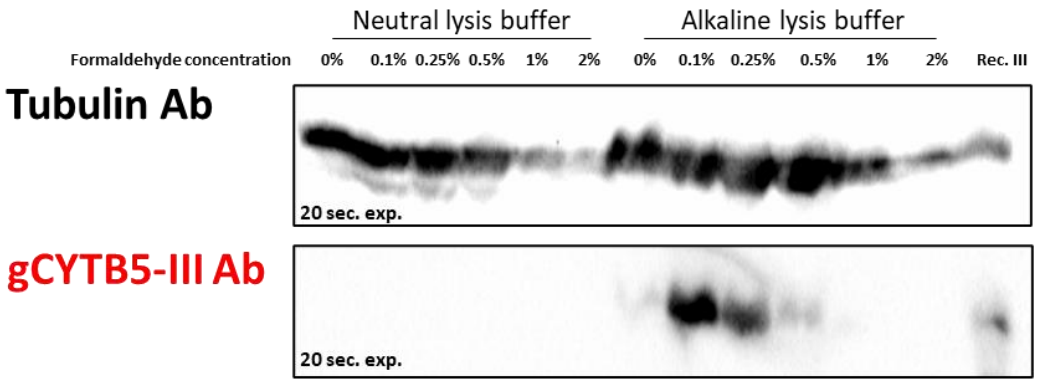

Figure 15: Western blot analysis comparing the supernatant of lysates prepared with either neutral or alkaline pH, from formaldehyde-treated Giardia cells. The supernatant samples were analyzed for gCYTB5-III in the lower panel and for tubulin in the upper panel. A sample of recombinant gCYTB5-III was loaded into the last lane as a marker for the location of this protein on the blot.

The low recovery of gCYTB5-III in the supernatant of the alkaline lysis samples of formaldehyde-treated Giardia may be due to the sequestering of gCYTB5-III in complexes with genomic DNA that would aggregate with the cell debris within the pellet after centrifugation of the cell lysate. Therefore, if gCYTB5-III were crosslinked to large molecules of genomic DNA, degradation of the DNA would release the protein and allow it to be recovered in the supernatant. To test this idea, I examined the effect of adding DNase I to the pellet. Figure 16 shows the outline of this experiment and the results. The Giardia cells were treated with varying concentrations of formaldehyde and then resuspended in alkaline lysis buffer. After centrifugation of the lysate, the presence of gCYTB5-III was analyzed in the supernatant without DNase treatment (Fig. 16,

Supernatant). Each pellet was then resuspended in DNase I buffer, treated with DNase I, and subjected to centrifugation. The recovered supernatants, termed DNase pellet extract, were then analyzed for the presence of gCYTB5-III (Fig. 16, DNase Pellet Extract).

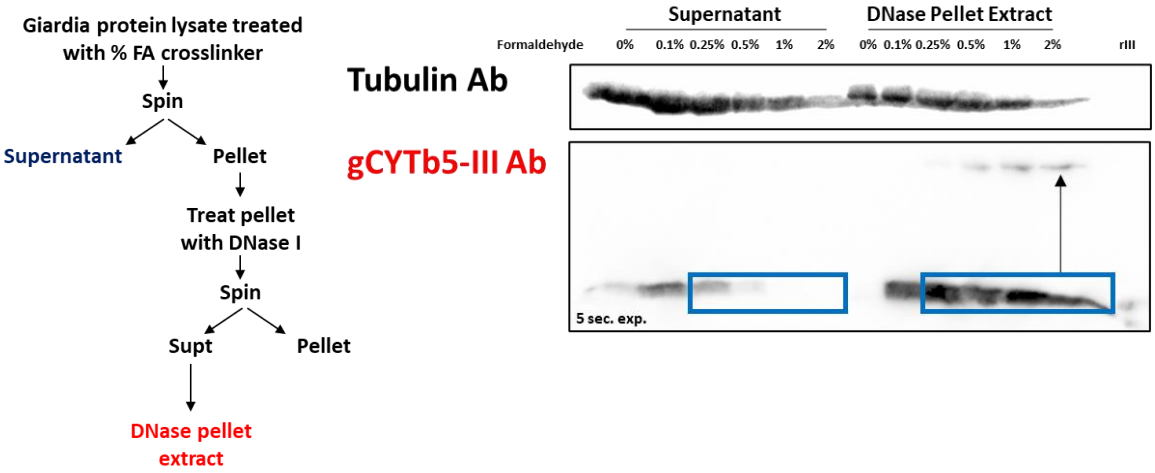

Figure 16: Western blot analysis of formaldehyde titration samples with and without DNase I treatment. The outline of this experiment is shown on the left and the results of the western blot analysis is shown on the right. Cells crosslinked with 0 – 2% formaldehyde were lysed with alkaline lysis buffer. The supernatant recovered after the initial centrifugation of the whole cell lysate is the supernatant without DNase I treatment. Each pellet was then resuspended in DNase I buffer and incubated with DNase I at 37℃ for 30 minutes. The supernatant recovered after the centrifugation of these samples are referred to as the DNase pellet extract. The lower panel shows the detection of gCYTB5-III, and the upper panel shows the results for the detection of tubulin. A sample of recombinant gCYTB5-III (rIII) was loaded into the last lane as a marker for the location of this protein on the blot.

The western blot results show that free gCYTB5-III was recovered in the DNase I-treated pellet extracts of the 0.1 – 2% formaldehyde samples (Fig. 16). Note that this increased recovery of gCYTB5-III in the pellet extract did not require the addition of SDS as observed in my previous experiment (Fig. 8). The decrease of free gCYTB5-III in the supernatant samples without DNase treatment coincides with an increase of free gCYTB5-III in the DNase pellet extract. In contrast, the recovery of tubulin is similar between the two samples for 0 – 1 % formaldehyde. Formaldehyde could crosslink

protein to protein as well as protein to DNA. Notably, 1 – 2% formaldehyde is commonly used to crosslink DNA-binding proteins to DNA In chromatin immunoprecipitation assays (ChIP). The total lack of recovery of free or monomeric gCYTB5-III in the supernatant of lysates prepared from Giardia cells treated with 1 – 2 % formaldehyde without DNase treatment suggest that all gCYTB5-III was crosslinked either directly or indirectly to DNA in these samples (Fig. 16, Supernatant). Incubation of these samples with DNase allow the release of gCYTB5-III from its association with DNA and is also associated with the appearance of an ~23 kDa band on the western blot. This 23 kDa band represents an increase of 8 kDa from the 15 kDa monomeric gCYTB5-III. Since a DNA fragment of ~8 kDa is ~200 bp, this shifted band could represent gCYTB5-III that is crosslinked to a 200 bp fragment of DNA, and the binding of gCYTB5-III to this DNA fragment may be protecting it from DNase digestion.

Discussion

Giardia intestinalis has four paralogues of a cytochrome b5 protein with unknown functions (Rafferty & Dayer, 2015). The goal of my research was to use co-immunoprecipitation (co-IP) to identify interacting partners of gCYTB5-III as a first step in determining the function of these proteins. I performed extensive preliminary work and troubleshooting before the final co-immunoprecipitation experiment with gCYTB5-III. This preparatory work is discussed below in Section I, while I will discuss the results of the co-IP experiment in Section II.

Section I: Preparatory work before co-Immunoprecipitation

4.1.1 Immunofluorescent microscopy

We obtained a Giardia cell line that is stably transfected with a plasmid that confers puromycin resistance and encodes an epitope-tagged gCYTB5-III that is expressed from a strong promoter of the Giardia ornithine carbamoyltransferase gene (GL50803_10311) (Pyrih et al., 2014). The epitope tag consists of two tandem sequences of hemagglutinin (2x YPYDVPDYA) at the N-terminus of gCYTB5-III. To identify potential interacting partners of gCYTB5-III, a previous student in our laboratory performed a co-IP with an anti-HA antibody on lysates prepared from this Giardia cell line, but the analysis of the immunoprecipitate did not identify proteins that are likely to be true interacting partners of gCYTB5-III. To seek a possible explanation for these results, I examined the localization of the HA-tagged gCYTB5-III (HA-gCYTB5-III) in the transfected

cells. My IFA results with an HA antibody in cells that overexpressed HA-gCYTB5-III showed staining throughout the cytosol of the Giardia trophozoites (Fig. 4 column 4). I observed the same staining pattern when the HA antibody was used in hybridization with the untransfected (UT) cell line (Fig. 4, column 3). In contrast, the use of the custom antibody raised against a unique peptide of gCYTB5-III in IFA showed that the endogenous protein localized to the nucleoplasm (Fig. 4 lanes 1 &2). The staining of the HA antibody in the transfected cells could be due to the cytosolic localization of the tagged protein or non-specific background staining by this antibody. Since the previous student was able to capture the HA-gCYTB5-III in the immunoprecipitate in the co-IP experiments performed on the transfected cell line (Dayer, 2017), it is likely that this cytosolic staining is due to mislocalization. The mislocalization of the HA-gCYTB5-III could be due to the overexpression of this protein, the disruption of a possible nuclear localization signal from the addition of 2x HA tag to the N-terminus of the protein, or a combination of both factors. The mislocalization of HA-gCYTB5-III and the inability of the previous co-IP to identify its likely interacting partners prompted me to repeat the co-IP experiments with a custom peptide antibody that recognizes the endogenous gCYTB5-III.

The peptide antigen used for the custom antibody is a unique 14 amino acid sequence located at the extreme N-terminus of the gCYTB5-III (see Fig. 23 in Discussion). The specificity of the custom anti-gCYTB5-III antibody is shown by the single band detected in western blot analysis (Fig. 7 and 8) and strong staining of the nucleoplasm in IFAs (Fig. 4). Co-IP against endogenous proteins is more reliable than using tagged

variants because no modifications have been made that could potentially interfere with the correct protein folding and its cellular localization.

4.1.2 Subcellular fractionation

To further study the cellular localization of endogenous gCYTB5-III as well as the two other cytochrome b5 isotypes (gCYTB5-I and II) for which our laboratory has custom antibodies against, I performed subcellular fractionation of Giardia trophozoites followed by western blot analysis of these fractions. Subcellular fractionations have been used to identify proteins enriched in the Giardia mitosome (Rout et al., 2016), as well as distinguishing organelle proteins from cytosolic proteins in Giardia (Jedelsky et al., 2011; Rivero et al., 2012; Tsaousis, Gentekaki, Eme, Gaston, & Roger, 2014) and in mammalian cells (Vashisht, Yu, Sharma, Ro, & Wohlschlegel, 2015).

I performed a crude differentiation fractionation of Giardia trophozoites and aimed to obtain a fraction containing only cytosolic proteins, and a fraction that contains proteins from all organelles including the nucleus. I first tested the success of my subcellular fractionation by using antibodies against Giardia proteins known to be associated with either the mitosome (PUP9296), ER (PDI2), peripheral vesicles (PX15548), nucleolus (CBF5), or the cytosol (giGAP1) in western blot analysis of the two cellular fractions. The mitosomal protein PUP9296 and the ER associated protein PDI2 were found as expected in the organelle fraction (Fig. 6A), and GAPDH protein (giGAP1) was found as expected in the cytosolic fraction (Fig. 6B). The detection of gCYTB5-III to

the organelle fraction (Fig. 6A and 6B) is consistent with the IFA localization of this protein to the nucleoplasm (Fig. 4). However, gCYTB5-I, gCYTB5-II, HA-CBF5, and PX 16548 were unexpectedly detected in the cytosolic fraction (Fig. 6A and 6B). These results would seem to contradict the IFA analysis that showed gCYTB5-I associates within the nucleolus and gCYTB5-II with the peripheral vacuoles (PV). Although the subcellular fractionation confirmed the nuclear localization of gCYTB5-III as well as the expected location of several control proteins, the inability of this technique to localize other proteins to their correct fractions showed the limitations of the subcellular localization protocol. It is likely that the two freeze thaw cycles in the initial lysis step of Giardia (see flowchart in Fig. 6) caused large ice crystal formation in the nuclei that resulted in premature lysis of this organelle, including the disruption of the nucleolus compartment. However, gCYTB5-III was retained even in the prematurely lysed nuclei due to its strong interaction with genomic DNA that remained in the nuclei.

4.1.3 Recovery of gCYTB5-III in soluble fraction of cell lysates

The first step in the co-IP is to prepare a cell lysate containing the bait protein and its interacting proteins. This involves the lysis of the cells followed by centrifugation of the lysate to pellet the cell debris so that proteins recovered in the supernatant could be used for the co-IP. One of the first challenges I encountered was the poor recovery of gCYTB5-III in the supernatant after the centrifugation of cell lysate. The use of a proprietary lysis buffer (CelLytic, Sigma) or a standard RIPA buffer at pH 8.0 resulted in

the recovery of proteins of a wide range of molecular weights in the whole lysate and supernatant (Fig. 7A), but western blot analysis showed that gCYTB5-III appeared almost entirely within the pellet fraction after centrifugation of the lysate (Fig. 7B). I investigated using the whole cell lysate (WL) without a centrifugation step in the co-IP procedure, but this was not successful as only a small proportion of gCYTB5-III was detected in the immunoprecipitate by western blot (Fig. 10A) and no gCYTB5-III was detected in the immunoprecipitate by mass spectrometry. One possible explanation for this poor recovery of gCYTB5-III is that the conditions causing gCYTB5-III to be present within the pellet fraction are also inhibiting gCYTB5-III from binding to the antibody when the whole lysate was used (Fig. 10A). Recombinant gCYTB5-III expressed in *E. coli* is a soluble protein based on prior work in our lab (Yang et al., 2016). Therefore, the retention of gCYTB5-III in the pellet fraction of Giardia lysate is likely not due to the insolubility of this protein itself but rather due to its association with a component of the cell pellet. To troubleshoot this issue, I investigated the use of different lysis buffer conditions to find one that would allow gCYTB5-III to remain in the supernatant after centrifugation of the whole lysate to remove the cellular debris in the pellet.

Several lysis methods and buffers have been used to prepare lysates from Giardia for co-IP (Table 4). This wide variety of procedures used by different laboratories suggests that it may be difficult to obtain an efficient and reproducible method to lyse Giardia trophozoites. These difficulties may be related to the extensive cytoskeleton network in Giardia that includes four pairs of flagella and the ventral disk (Holberton, 1981). One common method for the preparation of protein lysates from Giardia for co-IP

is to sonicate cells resuspended in an isotonic buffer (PBS) without the addition of any detergents or denaturing agents that would inhibit antibody binding to the bait protein. However, sonication can disrupt protein interactions and cause protein degradation (Pchelintsev, Adams, & Nelson, 2016). When I attempted to use sonication to prepare Giardia lysates, it yielded inconsistent results and caused some protein degradation. I next tried PBS with the addition of non-ionic detergent to aid in the lysis of the plasma membrane without disrupting antibody binding to the target protein. This buffer also was unsuccessful in retaining gCYTB5-III in the supernatant even after I substituted the non-ionic detergent with an ionic detergent and varied the pH from 7.2 to 8.0.

Table 4: Published lysis conditions for Giardia co-IP experiments.

Citation	**Detergent**	**Osmotic concentration**	**Reducing agent**	**Sonication**	**pH**
(Aggarwal, Merritt, & Nash, 1989)	1 % Triton	150 µM NaCl	No	No	7.2
(Touz, Kulakova, & Nash, 2004)	1 % Triton X-100	300 mM NaCl	No	No	8.0
(Dagley et al., 2009)	1% Digitonin	50 mM NaCl	No	No	7.4
(Krtkova et al., 2017)	0.1% Triton X-100	150 mM NaCl	0.05 mM DTT	Yes	7.5
(Rivero, Miras, Quiroga, Ropolo, & Touz, 2011)	1% Triton X-100	300 mM NaCl	No	No	8.0
(Rout et al., 2016)	1% IGEPAL 0.5% sodium deoxycholate	150 mM NaCl	No	Yes	7.4
(Zumthor et al., 2016)	N/A	150 mM NaCl	No	Yes	7.4
(Lujan, 1995)	1% Triton X-100 0.5% SDS 0.5% sodium deoxycholate	150 mM NaCl	No	No	N/A

I was unable to consistently recover gCYTB5-III in the supernatant fraction of the lysate until the pH of the lysis buffer was increased to 10.6 (Fig. 8). Notably, the regions flanking the core heme-binding domain of gCYTB5-III are charged at physiological pH. The N-terminal flanking region has a PI of 8.3 and the C-terminal flanking region has a PI of 9.6 (Fig. 17A, blue and red, respectively) (Alam et al., 2012). The lysine residues in these flanking regions are of particular interest due to their high PI of 9.74, which is the pH where the sidechain of lysine become deprotonated and uncharged. Therefore, it is interesting that the N and C terminal flanking regions contain two and three lysines, respectively, and are located on the surface of the protein (Fig. 17, B, dark blue). The increase of pH to 10.6 in the lysis buffer that is required to isolate gCYTB5-III (Fig. 8) would suggest that the positive charge of these lysine residues is important to the interactions that maintained gCYTB5-III within the pellet of the lysate. The use of a lysis buffer at pH 10.6, would remove the charges of these lysines and their role in ionic interactions, which would aid in the release of gCYTB5-III into the supernatant (Fig. 8B).

Moreover, increasing the pH of the lysis buffer to 10.6 would cause double stranded DNA to denature, allowing the release of DNA associated proteins into solution (Ageno, Dore, & Frontali, 1969; Russev, Venkov, & Tsanev, 1974). Given this observation, and the nuclear localization of gCYTB5-III, it would seem likely that the interaction being abolished by the pH 10.6 lysis buffer is one with DNA. This could also have been achievable with a high salt concentration lysis buffer (400 – 600 mM NaCl) (Zemskov, Kang, & Maeda, 2002). An extraction of a crude nuclear pellet with a high salt buffer

(420 mM KCl) was previously used successfully to recover gCYTB5-III in our lab (Sajer, 2019). However, both high salt (420 mM KCl) and high pH (pH 10.6) would inhibit antibody binding to the bait protein in co-IP (Dejaegere, Choulier, Lafont, De Genst, & Altschuh, 2005). I was able to reduce the pH of the alkaline lysis buffer with the addition of 80 mM Tris buffer after removing cellular debris with no protein lost. I also attempted a high salt lysis and exchanged the buffer afterwards into a lower salt buffer by using an ultrafiltration column but found significant protein loss. It is possible to perform a 2.7-fold dilution of the high salt lysis buffer, but this would result in a lysate that has a protein concentration too low for co-IP experiments. Furthermore, the high salt buffer was less efficient, requiring a larger volume to cell ratio to achieve effective lysis in comparison to the alkaline lysis buffer. Upon consideration of these factors, I decided to move forward using the alkaline lysis buffer.

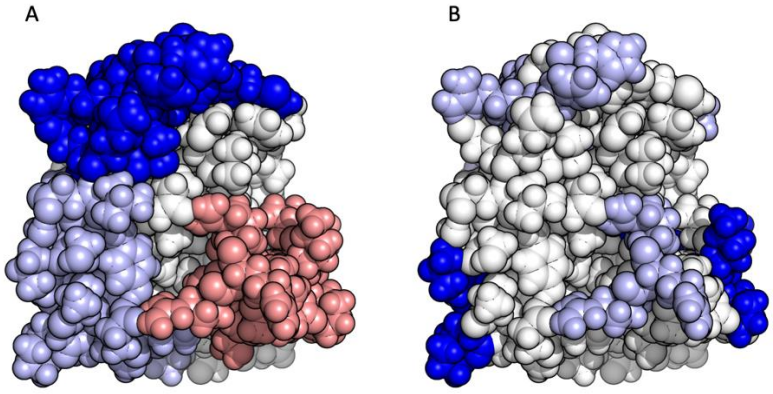

Figure 17: Structural model of gCYTB5-III prepared by the Rafferty/Yee lab using the I-TASSER program. Both panels show the protein in the same orientation. Panel A: The N-terminus is highlighted in blue, the C-terminus is in red, and the core cytochrome b_5 region is in white. The epitope of the custom antibody against gCYTB5-III is highlighted in dark blue within the N-terminal flank. Panel B: basic residues are highlighted in blue, with lysine residues in dark blue. The lysine residues would be neutralized under alkaline lysis buffer conditions.

4.1.4 *In vivo* crosslinking of gCYTB5-III

Cytochrome b5 is an electron transfer protein in other species, so if the Giardia gCYTB5-III has a similar function, its interaction with its protein partners would be rapid and transient (Meyer et al., 1995). In addition, the high pH (10.6) of an alkaline lysis buffer could disrupt the interaction of these proteins. Therefore, the introduction of chemical crosslinkers that would covalently link interacting proteins within Giardia cells would stabilize these interactions for the proceeding steps in the co-IP experiment.

The distance between reactive groups involved in the crosslinking is an important factor to consider in the choice of which chemical crosslinker to use in co-IP experiments. Although formaldehyde is the most commonly used chemical crosslinker for IP applications, it also has the shortest linker arm at 2 angstroms. For this reason,

formaldehyde is the crosslinker of choice in chromatin immunoprecipitation (ChIP) assays due to the tight junction between DNA and DNA-binding proteins. However, formaldehyde is not always effective. For example ELBA, a developmentally regulated chromatin insulator complex, could not yield a specific DNA sequence in ChIP assays when formaldehyde is used as the crosslinker despite ELBA's tight association with DNA; but the assay was successful when crosslinkers with longer arms (12 Å for DSP and 7.7 Å for DSG) were used (Aoki et al., 2014).

I first tested formaldehyde and DSP, as these crosslinkers were previously used successfully for co-IP in Giardia with non-nuclear proteins as the bait (Krtkova et al., 2017; Martincová et al., 2015; Pyrih et al., 2016; Zumthor et al., 2016). My results with these two crosslinkers were inconsistent and may be due to their reactions with primary amines that could have blocked the access of the antibody to the N-terminal epitope of gCYTB5-III. The primary amines are present in the first N-terminal amino acid and in the side chain of all lysines of a protein. In Figure 18 I have highlighted all primary amines in yellow to display their proximity to the epitope (blue). Therefore, I decided to try two other irreversible crosslinkers that contain maleimide groups, which react with sulfhydryl group of cysteine residues. I tested a heterobifunctional crosslinker (SMPB) that is reactive toward sulfhydryl groups on one end and primary amines on the other end, as well as a homobifunctional crosslinker (BMH) that is reactive toward sulfhydryl groups on both ends. As is the case with the DSP crosslinker used previously in other Giardia co-IP experiments (Martincová et al., 2015; Pyrih et al., 2016; Wade, Li, & M.

Wahl, 2013; Zumthor et al., 2016), both of these crosslinkers possess a long crosslinker arm (11.6 Å for SMPB and 13 Å for BMP) and are membrane permeable.

My results show that both SMPB and BMH are effective at capturing protein complexes containing gCYTB5-III (Fig. 9). These complexes increase with increasing crosslinker concentration (Fig. 9B, bands 2 and 3), while the level of monomeric gCYTB5-III decreases (Fig. 9B, band 1). The complex represented by band 2 formed with SMPB crosslinking diminishes from 1 to 5 mM SMPB, which suggests that this complex is being further crosslinked in a higher molecular weight complex that could not be detected in the western blot. This lack of detection could be due the formation of crosslinks that blocked the access of the antibody to the epitope on the gCYTB5-III protein, the resultant crosslinked complex was too large to enter the gel or transfer to the membrane, or it formed crosslinks to insoluble components so that it could not be recovered in the supernatant after centrifugation of the lysate. Furthermore, proteins must maintain their 3D structure to be successfully used in co-IP; thus, if a complex cannot be detected in a western blot where the protein is unfolded, it is likely that the epitope will also be obstructed in co-IP. Since 3 mM BMH contains the first complex (Fig. 9B, band 2) as well as a second complex (Fig. 9B, band 3), I chose to proceed with the BMH crosslinker for my experiments.

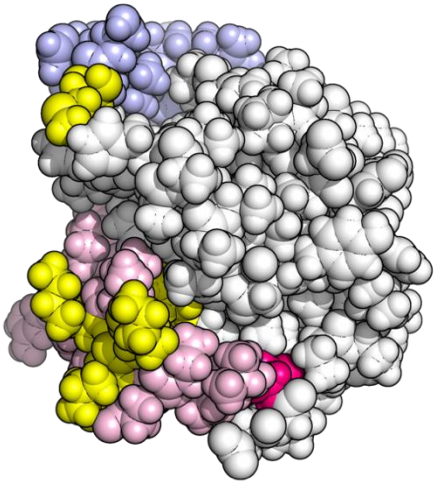

Figure 18: Structural model of gCYTB5-III prepared by the Rafferty/Yee lab using the I-TASSER program. The N-terminus in highlighted in light blue, the C-terminus in light red, and the core cytochrome b_5 region is in white. Highlighted in yellow are the primary amines (lysine and the amino terminus) that would be crosslinked by DSP, formaldehyde, and half of SMPB. Highlighted in magenta are the cysteines residues that would react with BMH. Of the two cysteine residues in the protein, only one of these are surface-accessible.

Section II: Interactome of gCYTB5-III

Co-immunoprecipitation coupled with mass spectrometry is commonly used to identify the interacting partners of a protein of interest. In my experiments, a custom antibody against gCYTB5-III was bound to magnetic beads and used to trap gCYTB5-III along with its interacting partners from a Giardia trophozoite protein lysate. I added an *in vivo* crosslinking step to stabilize the interaction of gCYTB5-III with its partners within Giardia trophozoites before lysing the cells. As a control for the gCYTB5-III co-IP, a parallel co-IP using the pre-immune serum rather than anti-gCYTB5-III antibody was also performed. The pre-immune serum contains all the antibodies that the animal possessed prior to its exposure to the gCYTB5-III peptide used as the immunogen. Any Giardia proteins that are recognized by these pre-immune antibodies as well as proteins that bind non-specifically to antibodies or the beads would be recovered in the pre-immune sample, but these proteins would not be enriched in the gCYTB5-III sample. Therefore, the proteins identified in the immunoprecipitants with the anti-gCYTB5-III and the pre-immune serum are compared so that only proteins unique to or enriched in the gCYTB5-III sample were further examined.

I initially selected proteins that are enriched 2-fold or more with the anti-gCYTB5-III co-IP relative to the pre-immune co-IP for further examination. Later, I included an additional three proteins that are enriched less than 2-fold but greater than 1.5-fold in the anti-gCYTB5-III co-IP for further consideration, but I added more control data sets to ensure that these proteins were not false positives. The three proteins of interests are

POB3 (GL50803_6671), Nar I (GL50803_6304), and endonuclease III (GL50803_3595), which will be discussed in the upcoming sections. The control samples added were from two previous co-IP experiments I performed for gCYTB5-III, and six control samples from pulldown experiments performed for mitosomal proteins by Pyrih et al. (2016) that are publicly available. These control samples were all crosslinked with DSP rather than BMH except for one of my co-IP samples that did not use any crosslinkers. Pyrih et al. used streptavidin coated Dynabeads while I used Protein G coated Dynabeads for my samples. As these data sets cannot be treated quantitatively because they are from different experiments, I treated them qualitatively with the assumption that proteins found in common among these samples are those that bind non-specifically to the beads. I also removed 42 proteins from the original 182 proteins that were originally thought to be unique to the gCYTB5-III sample based on comparison to the single pre-immune control sample, however, were found in at least one of the eight additional control samples.

My results from the mass spectroscopy analysis of the co-IP of gCYTB5-III showed two categories of proteins: those that are associated with chromatin in the nucleus, and those that are involved in Fe-S cluster assembly in the mitosome. In the first section below, I will discuss the co-IP data supporting a role for gCYTB5-III in the nucleus and other evidence that gCYTB5-III interacts with DNA. In the second section, I will discuss the co-IP data suggesting a role for gCYTB5-III in the mitosome. In the third section, I will discuss how gCYTB5-III could be a link between the nucleus and the mitosome due to the increased need for iron-sulfur clusters, generated in the mitosomes, that are

required for DNA damage proteins in the nucleus. Lastly, possible reasons for the lack of detection of gCYTB5-III in previous proteomic analysis of the mitosomes will also be discussed.

4.2.1 Evidence that gCYTB5-III is associated with DNA in the nucleus

Among the 140 proteins unique to the gCYTB5-III co-IP sample, I initially selected those that are likely to be nuclear proteins for further analysis, based on our IFA data which shows gCYTB5-III is in the nucleoplasm (Fig. 4). These proteins belong in the Gene Ontology (GO) category of DNA metabolism, which includes transcription, translation, and DNA repair. These proteins consist of DNA polymerase, RNA polymerase, DNA topoisomerase, DRE4 (SPT16), RNA helicase, DNA helicase, and PcnA, as well as cyclins, transcription factors, kinases, and acetyltransferases. Histones H2A, H2B and H3.3 were also found in this sample, with histone H2A as the most enriched annotated protein recovered among all nuclear proteins, with 6.1X as many peptides within the co-IP of gCYTB5-III versus the control.

A giardial protein annotated as Dre4 (GL50803_17430) is one of the most enriched proteins (4.2-fold) in the co-IP of gCYTB5-III. Dre4 is also referred to as Spt16 in human and yeasts and is one of the two core components of the FACT (facilitates chromatin transcription) complex. The other core component of the FACT complex is SSRP1 of humans, which corresponds to POB3 in yeast. Using the yeast POB3 sequence in a BLAST search, I found an ortholog of POB3 in Giardia, GL50803_6671, with 75% coverage and

19% identity. Comparison of the predicted structure of the putative Giardia POB3 to the Human SSRP1 with the I-TASSER program (Roy, Kucukural, & Zhang, 2010) resulted in a RMSD (root mean squared deviation) score of 1.03 Å, which indicates a very high match, as homology modelling of homologous proteins in the PDB yield RMSD values between 0 - 1.2 Å. This putative Giardia POB3 is found with a 1.5-fold enrichment that is below the threshold of 2-fold set in my initial analysis, but this protein is not found in any of the eight additional control samples.

The FACT complex is a type of histone chaperone with a structure and function that are highly conserved across all eukaryotes (Winkler & Luger, 2011). Histone chaperones bind histones and facilitate their removal, addition or replacement within nucleosomes (Hammond, Stromme, Huang, Patel, & Groth, 2017). FACT complexes have roles in DNA replication, transcription, and DNA repair (Hammond et al., 2017). As an example of the breadth of the FACT complex, the deletion of genes encoding CHZ1 and NAP1 in yeast are non-lethal because FACT is able to substitute them with Isw1 and Ioc3 (Luk et al., 2007). Giardia appears to have an ortholog of Isw1 (GL50803_8228) and this protein is also found in the immunoprecipitate of gCYTB5-III. However, there are no matches of Giardia genes for CHZ1, NAPI and loc3. The mechanism in which the FACT complex function in both assembly and disassembly of the nucleosomes is unknown (Liu et al., 2020). Using proteins found in FACT complexes of yeast and human as the query sequences to perform BLAST sequences on the Giardia genome database, I identified 12 proteins that may constitute a FACT complex in Giardia (Table 5). The recovery of eight

of these proteins that are either unique or enriched in the gCYTB5-III immunoprecipitate suggest that gCYTB5-III may have a role in chromatin remodeling.

Table 5: Putative Giardia FACT complex found via BLAST analysis of the Giardia genome. From left to right: the FACT component common name, the species of origin for the top BLAST alignment, the E-value of that alignment, the functional role of the ortholog in FACT, the potential Giardia ortholog, the annotation of the protein in the Giardia genome, its molecular weight, and its enrichment within the anti-gCYTB5 co-IP experiment. The yeast species is *S. cerevisiae.*

Ortholog proteins	Species	UniProt Accession number	E-Value	Function	Giardia potential orthologs	GiardiaDB Annotation	MW (kDa)	Fold enrichment
SPT16	Human	Q9Y5B9	2e-11	Core Component of FACT complex	GL50803_17430	DRE4 protein	130	4.2
POB3 (SSRP1)	Yeast	Q04636.1	4e-3	Core Component of FACT complex	GL50803_6671	hypothetical protein	73	1.5
NEK1	Human	Q96PY6.2	7e-101	DNA damage checkpoint control	GL50803_92498	Kinase, NEK	102	2.0
POL1	Human	P09884.2	3e-59	Initiation of DNA replication	GL50803_27326	DNA polymerase alpha subunit A	195	Unique
SNF2/SWI2	Human	P28370.2	5e-130	Component of NURF, CERF, & WICH chromatin remodelling complexes; facilitates perturbation of chromatin structure in an ATP-dependent manner.	GL50803_8228	DNA-dependent ATPase, putative	145	Unique
Rbbp7	Human	Q16576.1	4e-37	Core histone binding subunit that targets chromatin assembly/remodelling and histone deacetylases.	GL50803_14753	Histone acetyltransferase type B subunit 2	49	Unique
CHD3 (CHD1-5)	Human	Q12873.3	1e-121	Binds to target gene promoters, causing chromatin remodelling	GL50803_112978	Chromodomain helicase-DNA-binding protein	301	Unique
CKA1 & CKA2	Yeast	P19454.2	2e-77	Interacts with FACT, acting of transcription factors and RNA pol.	GL50803_27520	Kinase, CMGC CK2 alpha subunit	55	Unique
RFA1	Human	P27694.2	5e-2	Replication factor A, binds and stabilizes ssDNA in replication and DNA stress	GL50803_13075	hypothetical protein	53	Absent
ESA1	Yeast	Q08649.1	9e-58	Component of NuA4 complex. Histone acetylation of all histone variants contrary to being part of NuA4 (H4 specific).	GL50803_2851	Histone acetyltransferase MYST2	50	Absent
HMG2 (Hmgb2)	Human	P26583.2	1e-3	May be redox sensitive. Chromatin associated, functioning in transcription, remodeling, and V(D)J recombination. Binds ssDNA.	GL50803_14064	hypothetical protein	24	Absent
Hmg 3-4	Human	Q9HCS4.1	2e-05	Interacts with FACT complex	GL50803_3349	hypothetical protein	22	Absent

The nuclear localization of gCYTB5-III (Dayer, 2017) and its positively charged flanking domains (Alam et al., 2012) suggest that this protein could bind to DNA. Our lab has previously tested recombinant gCYTB5-III's ability to bind DNA in electrophoretic mobility shift assays (EMSAs) and in DNA affinity chromatography but could not detect any DNA-binding (unpublished). However, only a few DNA probes corresponding to specific Giardia gene promoters were tested with gCYTB5-III in EMSAs, while the DNA affinity chromatography used beads linked to single-stranded and double-stranded calf thymus DNA. In both the EMSA and DNA chromatography assays, "naked" DNA was tested with recombinant gCYTB5-III. Therefore, if gCYTB5-III could only bind to DNA organized into chromatin or it required the association with another protein to bind to DNA, the two *in vitro* assays would not be able to detect this. Another type of protein-DNA binding assay called the chromatin immunoprecipitation assay (ChIP) is more suitable for analyzing biological protein-DNA interactions since it detects these interactions within the cell. ChIP assays typically use 1% formaldehyde to crosslink target transcription factors to the DNA within cells before their lysis (Carranza et al., 2016; Tao & Hajri, 2011; Wang, Chen, Sun, & Qian, 2019). The DNA is then sheared, leaving short pieces of DNA with protein crosslinked to them. If the DNA is not completely broken up, the CHIP assay will be unsuccessful (Martin, On, Bowers, & McCullough, 2018). Chromatin, consisting of histones, non-histone proteins and DNA, will be recovered in the pellet after centrifugation of the cell lysate if the DNA is not sufficiently sheared. This may explain my observation of gCYTB5-III in the pellet fraction of lysates prepared from standard lysis buffers (Section 3.3). This could also explain why the alkaline lysis buffer

was efficient in recovering gCYTB5-III, as the alkaline pH would denature DNA and neutralize the positive charged residues on the surface of the proteins, releasing all DNA associated proteins (discussed in section 4.1.3).

To further explore the possibility that formaldehyde was directly crosslinking gCYTB5-III to DNA, I examined the effect of adding DNase I to these samples on the detection of monomeric gCYTB5-III on western blots (Fig. 16). Only the soluble fraction (supernatant) of the lysates were examined in the results shown in Figure 16. In the absence of DNase I, increasing the formaldehyde concentration resulted in decreasing recovery of monomeric gCYTB5-III in the supernatant (Fig. 16, Supernatant, highlighted by blue box). Upon DNase I treatment of the pellet from supernatant samples, the gCYTB5-III that was sequestered in the pellet with undigested chromatin is now released and recovered in the supernatant of the DNase Pellet Extract (Fig. 16, DNase Pellet Extract, highlighted by blue box). This demonstrates a correlation between DNA degradation and gCYTB5-III in the supernatant. Notably, CHIP assays are usually performed with the addition of 1 - 2 % formaldehyde as the crosslinker, and I observed a shift of the gCYTB5-III band at these concentrations that would correlate to the addition of ~200 bp of DNA. Notably, 200 bp of DNA is approximately the length of DNA that would be wrapped around one nucleosome plus the linker region in other eukaryotes (147 bp core nucleosome and 50 bp linker DNA) (Cutter & Hayes, 2015).

Although the increased recovery of gCYTB5-III in the supernatant with the incubation of DNase I may be due to an increase in cell lysis rather than the release of gCYTB5-III from large fragments of DNA, there is no gCYTB5-III found in the extracted

sample from the DNase-treated pellet without prior crosslinking with formaldehyde (0%). This shows that all gCYTB5-III was released into the supernatant with alkaline lysis in the absence of crosslinking. In addition, DNase treatment was performed in a buffer without any detergents, and my data in Section 3.3 of the Results section demonstrate it is unlikely that the incubation of Giardia in this buffer could result in cell lysis. Tubulin is also present in the DNase-treated samples, but this is expected due to the abundance of this protein within the cell and its propensity to be found within the cell pellet. The detection of tubulin in the DNase I-treated samples show the same trend as the samples without DNase I treatment (Fig. 16), suggesting that the crosslinking is maintained in these samples. If the increase in gCYTB5-III in the DNase I treated samples were caused by crosslink reversal, we would also observe an increase in the detection of tubulin in the same samples. This supports the idea that the increasing presence of gCYTb5-III in the supernatant obtained after centrifugation of a DNase-I treated resuspended pellet from formaldehyde-crosslinked samples is correlated to DNA degradation. These results suggest gCYTB5-III interacts directly with DNA, and a CHIP assay could be performed to determine if this binding is DNA-sequence specific.

4.2.2 Evidence that gCYTB5-III interacts with the Fe-S cluster assembly of the mitosome

GiOR-1 (GL50803_91252) was found within the top ten proteins unique to the gCYTB5-III immunoprecipitate. This protein has high sequence similarity to cytochrome P450 reductases, which are flavoenzymes that transfer electrons from reduced

nicotinamide cofactors to electron acceptors such as cytochromes P450 and cytochromes b_5. While GiOR-1 catalyzes the NADPH-dependent reduction of gCYTB5-III *in vitro* (Pyrih et al., 2014), it may also have a role similar to the yeast flavoenzyme Tah18, which is an enzyme involved in the insertion of iron-sulfur (Fe-S) clusters into non-heme iron metalloproteins (Jedelsky et al., 2011). In IFA experiments, the endogenous and exogenously expressed tagged versions of GiOR-1 are localized to Giardia mitosomes, which is the starting site of Fe-S assembly (Jedelsky et al., 2011; Pyrih et al., 2016). This is interesting as the canonical Tah18 protein functions in the cytosolic part of the Fe-S cluster assembly machinery (CIA) (Netz et al., 2010).

Further examination of the unique and enriched proteins in the gCYTB5-III immunoprecipitate showed the presence of several other mitosomal proteins. A list of confirmed mitosomal proteins was obtained from Dr. Pavel Dolezal, whose research group has worked extensively on the characterization of Giardia mitosomes. I used this list to compare to the proteins found from MS analysis of the co-IP of gCYTB5-III (Appendix B). Among the highest enriched proteins in the gCYTB5-III sample were mitosomal chaperone proteins that function in the transport and folding of proteins within the mitosome and the Fe-S assembly machinery. Figure 19 shows the known proteins in the Giardia mitosome and the components that are enriched in the gCYTB5-III immunoprecipitate. This figure also includes the components of the Giardia Fe-S assembly machinery (CIA) that have been identified. The information presented in Figure 19 represents the most current knowledge of the Giardia mitosomal proteome (Dagley et al., 2009; Dolezal et al., 2005; Elias et al., 2008; Jedelsky et al., 2011; Kunz et al., 2017;

Lill & Kispal, 2000; Martincová et al., 2015; Pusnik et al., 2009; Pyrih et al., 2016; Pyrihov et al., 2018; Rada et al., 2009; Regoes et al., 2005; Rout et al., 2016; Šmíd et al., 2008; Tachezy et al., 2001; Tovar et al., 2003). I have analyzed the results of all previous studies on protein interactions in the Giardia mitosome so that proteins touching each other in Figure 19 have interactions that are supported by experimental data. Furthermore, I did a cross comparison of each interactome study with my own to find which co-IP had the most proteins in common to that of gCYTB5-III (Appendix C).

The mitosomal proteome includes 42 proteins, 18 of which were found uniquely (dark red) or enriched (light red) in the co-IP of gCYTB5-III (Fig. 19). Almost all the core proteins involved in the mitosomal part of the Fe-S assembly pathway were identified in the gCYTB5-III immunoprecipitate. In addition, all but three of the core proteins are unique to the co-IP of gCYTB5-III and are absent from the additional controls, and those three that are found in both, Grx5, DnaJ III, and MOMTiP-9, have an enrichment factor of 4.9, 2.5, and 6.3, respectively. Three proteins (Mlf1, MOMTiP-1 and Nar1) found within the controls of other experiments remain in red but have an asterisk (*) added to them. One of these proteins, Mlf1, is of particular interest since it resembles a transcription factor found in the nucleus and cytosol of mammals (Wu et al., 2021). The control sample that contains Mlf1 is from a previous co-IP of gCYTB5-III that I performed without the addition of crosslinker. This experiment was successful, in isolating gCYTB5-III, but did not contain any proteins that could be used to suggest a potential function of gCYTB5-III. Mlf1 is found unique to the MS data discussed here and with a 2-fold enrichment in the previous co-IP without crosslinking. Also common to both these co-IP

was the mitosomal Hsp70 (unique to gCYTB5-III co-IP sample in both experiments). These are the only two candidate proteins common to both the crosslinked co-IP results discussed here and the non-crosslinked co-IP of gCYTB5-III, suggesting a strong interaction between Mlf1, Hsp70 and gCYTB5-III which was maintained without crosslinking.

The results of my co-IP of gCYTB5-III, identified more than 40% of the Giardia mitosomal proteome including most of the mitosomal proteins involved in the Fe-S pathway in this organelle (ISC). The maturation of the Fe-S cofactor required for proteins located in the cytosol and nucleus is completed in the cytosol, and the current understanding of this part of the pathway (the CIA) in yeast involves eight core proteins: Tah18, Dre2, CFD1, Nbp35, Nar1, Cia1, Cia2, Met18 (Fig. 20) (Netz et al., 2014). In Giardia, orthologs of four of these (Fig. 20, Giardia, proteins in blue) have been identified, while a fifth, GiOR-1, has been shown to rescue the phenotype from the knockdown of Tah18 in *Trypanosoma brucei* (Pyrih et al., 2016). The putative scaffold proteins for Giardia CIA are composed of three proteins that all resemble Nbp35, which are annotated as Nbp35-1, Nbp35-2, Nbp35-3. It has been proposed that these three proteins form the scaffold complex without a Cfd1 ortholog (Pyrih et al., 2016) because Nbp35 and Cfd1 are similar MRP-like proteins in the family of P-loop NTPase family (Lill & Mühlenhoff, 2005). Therefore, the three Nbp35 proteins in Giardia are shown in a green tetrameric complex without a Cfd1 protein (Fig. 20). The protein encoded by the gene with accession number GL50803_33030 has been suggested to be the giardial ortholog of Nar1 (Pyrih et al., 2016). However, I propose that GL50803_6304 could also

be an Nar1 ortholog because it showed 25% identity with 96% coverage of the Mouse Nar1 protein. In comparison, the protein encoded by GL50803_33030 showed 23% identity with 78% coverage of the mouse Nar1 protein. I have included both accession numbers as possible Nar1 orthologs in Fig. 20.

The formation of an Fe-S cluster on the CIA scaffold requires an electron transfer chain composed of Tah18 (GiOR-1) and Dre2. Tah18 facilitates electron transfer from NADPH to Dre2, which in turn can reduce Nbp35 to stabilize the [4Fe-4S] clusters in the heterotetrametric complex of Nbp35 and CFD1. No Dre2 ortholog has been identified in Giardia, and it has been demonstrated that GiOR-1 can facilitate an electron transfer from NADPH to gCYTB5-III. Therefore, it is possible that gCYTB5-III replaces the role of Dre2 in Fe-S cluster assembly pathway. However, if this were the case then one of the putative Nbp35 proteins would be expected within the co-IP results for gCYTB5-III but no Nbp35 proteins were detected. Furthermore, IFA of the three putative Nbp35 proteins showed that they are localized to the mitosomes and cytosol rather than nucleus (Pyrih et al., 2016). There is one exception that this paper does not discuss; the protein they have deemed Nbp35-1, when localized with an HA tag, is distinctly absent from the nuclear region. When they analyzed this protein in IFA with a custom antibody against the endogenous protein, some of the protein is detected in nucleus. However, they did not use the antibody raised against the endogenous Nbp35-1 in W. blot analysis of their subcellular fraction. Therefore, the lack of detection of Nbp35-1 in the nucleus by the addition of an epitope tag to this protein may be similar to our observation that HA-tagging of gCYTB5-III prevents it from localizing to the nucleus.

In other eukaryotes, the targeting complex of the Fe-S assembly in the cytosol that is composed of Met18, Cia1 and Cia2, delivers the Fe-S to cytosolic proteins as well as to the nuclear proteins requiring this cofactor (Fig. 20). Therefore, these three proteins are also detected in the nucleus in human and yeast (Balk et al., 2005; Ito et al., 2010). In Giardia, an ortholog of Met18 could not be identified, and the ortholog of Cia2 is localized to the mitosome but not the cytosol nor the nucleus. However, the Giardia ortholog of Cia1 is localized to the cytosol but not in the nucleus (Pyrih et al., 2016). Notably, I did not detect the Giardia Cia1 or Cia2 in the immunoprecipitate of the gCYTB5-III co-IP despite the prevalence of other nuclear proteins recovered in this experiment. Another Giardia protein with unexpected localization is the presence of GiOR-1 exclusively to the mitosome (Pyrih et al., 2016). GiOR-1 is structurally similar to Tah18 in yeast that is involved in assembling the Fe-S scaffold complex in the cytosol (Fig. 20). Furthermore, GiOR-1 is able to rescue the knockdown of Tah18 in *Trypanosoma brucei*.

In Pyrih et al. 2016 paper, they also performed pulldown experiments with biotin-tagged Cia2 and GiOR1. The results of the Cia2 pulldown experiment have only two common proteins with the co-IP of gCYTB5-III versus 13 common proteins with the GiOR-1 pulldown (Appendix C). The observation of CIA proteins (Nbp35, GiOR-1 and Cia2) within the mitosome, rather than the cytosol suggest the mitosome has a predominant role in the Fe-S cluster assembly pathway in Giardia compared to that of human and yeast. It can be noted that many of these results are based on tagged

proteins, therefore the other components of the CIA, such as Nar1 and Cia1, may be mislocalized due to tagging, and also localized to the mitosome.

Nuclear proteins with Fe/S clusters are required in DNA replication, DNA repair and the maintenance of genome stability. Knockouts of any CIA components in yeasts are associated with increased DNA lesions, mutation, and cell death (Paul & Lill, 2015). I propose that Fe/S clusters are transferred directly from the mitosomes to the nucleus in Giardia. There are two categories of mitosomes in Giardia: the peripheral mitosomes that underlie the plasma membrane and the central mitosomes that are located between the two nuclei in Giardia trophozoites (Fig. 21). Other than their differences in cellular locations, a biological difference between the peripheral and central mitosomes is shown by an experiment where the translocation of mitosomes was purposely disrupted by creating a fusion of GiMOMP35, a mitosome membrane protein and GiQb4, a SNARE protein from the PV (Voleman et al., 2017) . The expression of this fusion protein caused the aggregation of all mitosomes except the central mitosomes. This suggests that the central mitosome has a mechanism of membrane interaction that is distinct from the peripheral mitosomes, possibly interacting with the nuclear membrane instead of the ER. Another difference between the two categories of mitosomes is that the division of the peripheral mitosomes is the highest during telophase while the division of the central mitosomes is the highest during prophase (Voleman et al., 2017). During prophase, the central mitosomes appeared to be connected to the karyomastigont, which is a structural complex of the basal bodies and the nuclei (Voleman et al., 2017). This physical association between the mitosomes and

the nuclei during mitosis may be a means for the mitosome to supply Fe-S clusters for proteins that require them in the nucleus.

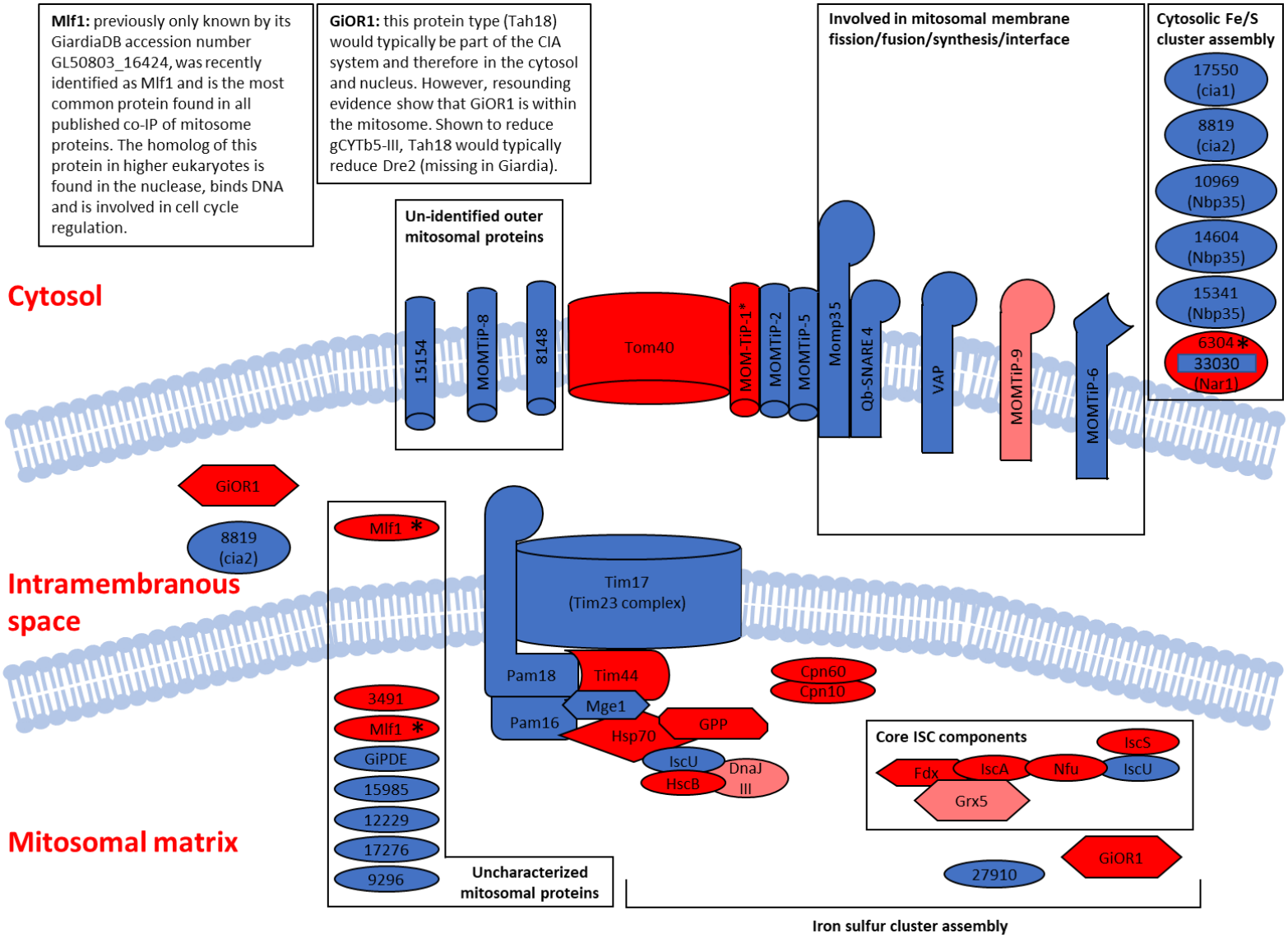

Figure 19: A diagram of the established mitosomal proteome of Giardia, showing the localization and interactions of proteins within the organelle. Proteins found uniquely to the gCYTB5-III co-IP sample are shown in dark red while proteins enriched in the gCYTB5-III sample are shown in lighter red. An asterisk denotes proteins found in the co-IP of gCYTB5-III, but also found in controls produced by other experiments. Proteins indicated in blue are those that were not identified in the gCYTB5-III sample.

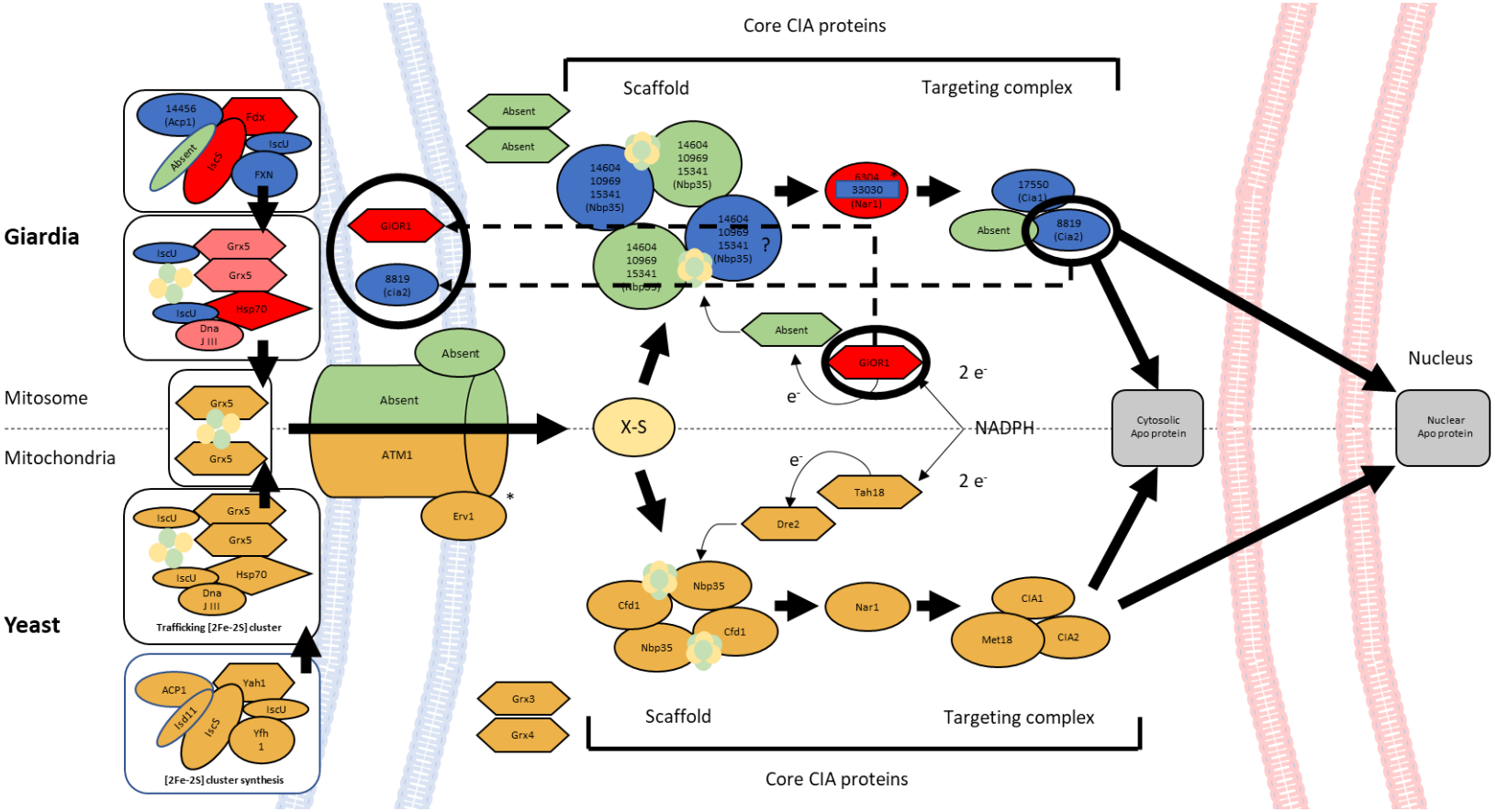

Figure 20: Representation of the cytosolic iron sulfur cluster assembly (CIA) protein in yeast and Giardia. On the left is the portion of the Fe-S cluster assembly within the mitochondria / mitosome, that is thought to supply the sulfur containing compound to the CIA. Yeast proteins involved in the maturation of cytosolic and nuclear iron sulfur clusters are shown as yellow proteins at the bottom half of the diagram. The top half on the diagram mirrors the yeast pathway with potential Giardia orthologs as indicated by their GiardiaDB accession numbers. Proteins found in the co-IP of gCYTb5-III are indicated in red, proteins not detected in the gCYTB5-III co-IP are indicated in blue, and proteins that do not have a Giardia ortholog identified are indicated in green. The dotted lines next to the Giardia Cia2 and GiOR1 are to indicate the discrepancy in localization data of these two proteins to the intramembranous space of the mitosome instead of the cytosol. I have introduced two new orthologs, not found in the literature, a paralog of the Nar1 proposed in the literature, thus the two colours and accession numbers for that protein, and an Acp1 protein that has not yet been identified in any mitosomal literature.

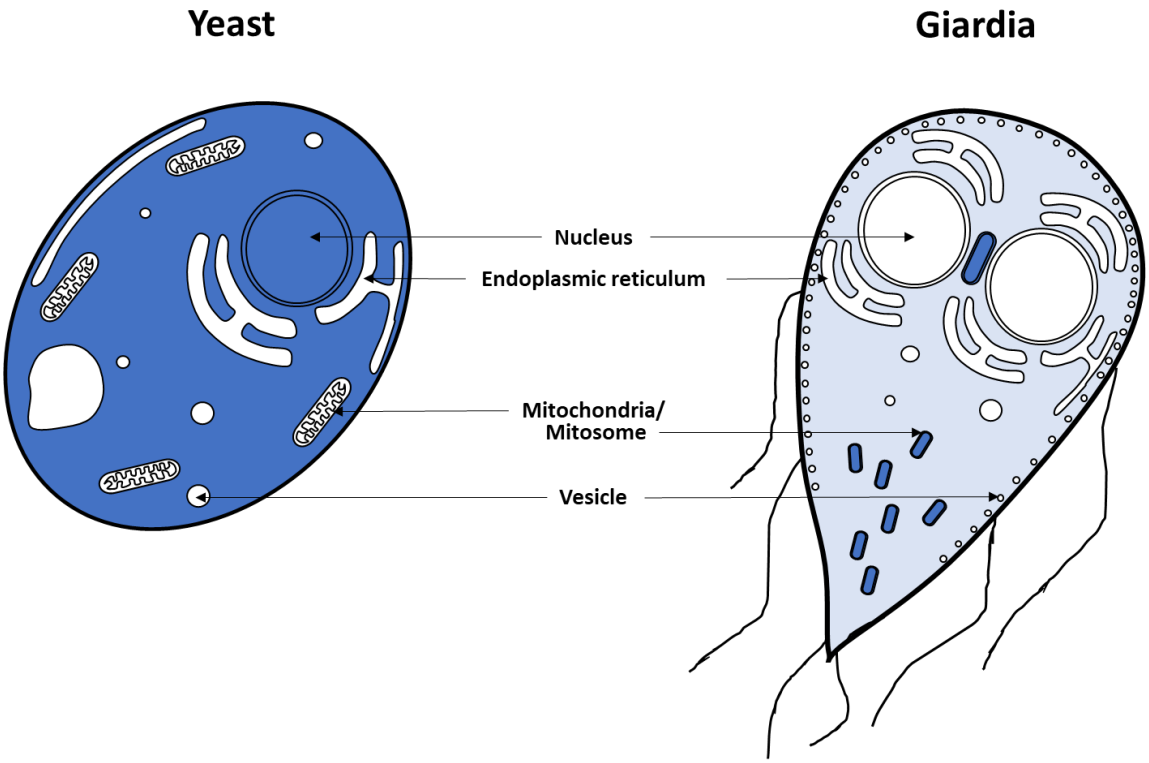

Figure 21: Representation of the cytosolic iron sulfur cluster assembly machinery (CIA) localization in yeast and what is currently known in Giardia. Protein localization of the core CIA proteins in each cell type is shown in blue. In yeast, all the CIA proteins are localized to the cytosol and nucleus (dark blue) and none in the mitochondria (white). In contrast, most of the CIA proteins in Giardia are localized to the mitosomes (dark blue), very few to the cytosol (light blue), and none in the nuclei (white).

4.2.3 Potential connection between a role of gCYTB5-III in the response to DNA damage in the nucleus to Fe-S proteins and the mitosomes

When exploring different crosslinkers for my co-IP, I tested different concentrations of formaldehyde (0.25% – 2%) in titration experiments to evaluate its efficiency in stabilizing protein complexes containing gCYTB5-III. Typically, the sample without crosslinker would show the highest intensity of the band representing the monomeric form of the protein on a western blot, and this band's intensity would decrease as crosslinker concentration increased due to the sequestering of the protein

in higher molecular weight complexes containing other proteins (see Fig. 14 for example of tubulin). However, I observed an increased intensity of monomeric gCYTB5-III upon treatment of Giardia with 0.1% and 0.2% formaldehyde. These results were observed in three independent replicates of this experiment. Formaldehyde is commonly used as a crosslinker to stabilize protein-protein and protein-DNA interactions. However, formaldehyde also causes DNA damage and has been used to induce cellular stress in experiments (Anandarajan et al., 2020; Ciftci et al., 2015; de Graaf et al., 2009; Noda et al., 2011). The apparent increased band intensity of gCYTB5-III at low levels of formaldehyde suggests a link of this protein to a DNA stress response.

To date the only DNA damage response pathway that has been analyzed in Giardia is the homologous recombination pathway (Martínez-Miguel et al., 2017; Ordoñez-Quiroz, Ortega-Pierres, Bazán-Tejeda, & Bermúdez-Cruz, 2018; Torres-Huerta, Martínez-Miguel, Bazán-Tejeda, & Bermúdez-Cruz, 2016), which is activated in response to double-stranded DNA breaks. Such breaks can be induced through oxidative stress and free radical damage, which occurs when Giardia are treated with the pro-drug metronidazole, the most commonly prescribed treatment for giardiasis. The response to metronidazole occurs over a longer time (several hours) than what I have observed with formaldehyde (1 hour), although a DNA damage response within 1 hour has been reported in Giardia using gamma radiation as shown by the increased phosphorylation of histone H2A and increased expression of DMC1B, a homologous recombinase (Martínez-Miguel et al., 2017; Torres-Huerta et al., 2016). My observation of a change in

expression of gCYTB5-III after a 30-minute exposure to formaldehyde correlates to the fast response to DNA damage from radiation in Giardia.

DNA stress due to interstrand DNA crosslinks activates the cellular excision and mismatch repair machinery (Mu et al., 2000). The Fanconi anemia pathway is required to remove such interstrand crosslinks, and it is only activated during S-phase of the cell cycle (Knipscheer et al., 2009). The increase in expression of gCYTB5-III under formaldehyde treatment occurs within 1 hour, which corresponds more closely to the time response of the excision and mismatch repair machinery and not to the longer time required for the activation of the Fanconi anemia pathway. Interestingly, many of the enzymes that are involved in DNA repair, such as DNA endonucleases, DNA helicases, and DNA glycosylases, contain Fe-S clusters (Stehling et al., 2012). Therefore, the rapid increase in gCYTB5-III levels from exposure to formaldehyde could be due to a direct role of this protein in DNA repair, or its role in Fe-S assembly that provides Fe-S cofactors for DNA repair enzymes in the nucleus.

The TFIIH protein complex is required for the nucleotide excision repair mechanism (Compe & Egly, 2012). No components of this complex, and only one mismatch repair protein (GL50803_34058) are found in the co-IP of gCYTB5-III, which argues against a direct role of gCYTB5-III in the repair of DNA damage in Giardia. Other proteins involved in this base excision process such as DNA polymerase delta and beta (Sattler, Frit, Salles, & Calsou, 2003) are also absent from the gCYTB5-III immunoprecipitate. However, it is possible that gCYTB5-III, via its association with the FACT chromatin remodeling complex, may be involved in the activating the expression

of DNA repair proteins. The polymerase unique to the immunoprecipitate of gCYTB5-III are DNA polymerase alpha, which is involved in DNA replication, as well as two subunits of RNA polymerase I (GL50803_10055 & GL50803_23496) and two subunits of RNA polymerase II (GL50803_7474 & GL50803_89347), which are involved in transcription. All these polymerases are unique to the co-IP results and are not found in any of the controls from previous experiments, except for a single peptide of RNA polymerase II (GL50803_7474) in one of the six controls of Pyrih et, al. (2016). These findings support the proposal that gCYTB5-III may be involved in upregulating the transcription of the Fe-S assembly machinery, or the nuclear Fe-S containing proteins that are found in some DNA repair enzymes, rather than responding directly to DNA damage.

For this conclusion to be valid, Giardia would need to possess the Fe-S proteins that function in DNA repair. Therefore, I have conducted a search of the Giardia genome for orthologs of known Fe-S containing DNA repair proteins. The Fe-S proteins involved in DNA repair include adenine DNA glycosylase (MUTY), endonuclease III, and DNA helicases. I found an ortholog for endonuclease III and three DNA helicases with conserved Fe-S coordinating cysteine residues within the Giardia genome (Fig. 22). Of these proteins, only endonuclease III is found enriched in the co-IP of gCYTB5-III. This is interesting, because the Fe-S in endonuclease III is known to function as a redox-sensitive responder to DNA damage (Fuss, Tsai, Ishida, & Tainer, 2017). The presence of these proteins and their conserved coordinating cysteine residues fortifies the notion that DNA stress would increase the need for nuclear Fe-S clusters in Giardia. Therefore, gCYTB5-III may be responding to this need.

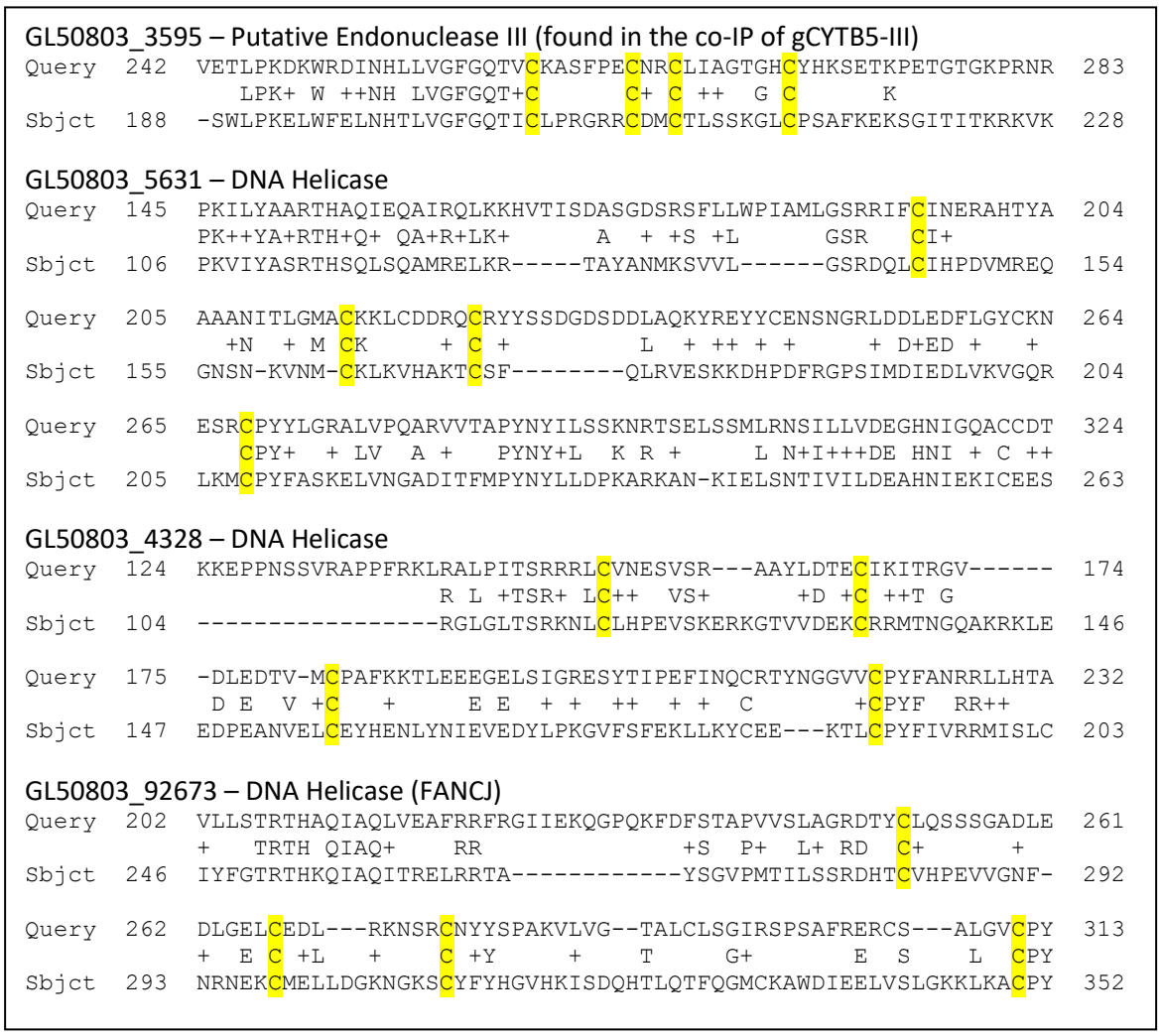

Figure 22: Alignment of Fe-S cluster containing DNA damage repair machinery. The conserved Fe-S coordinating cysteines are highlighted in yellow.

Future experiments to examine the induction of gCYTB5-III could be performed with other reagents that induce DNA damage. In Giardia the commonly used treatments are metronidazole or gamma radiation (Martínez-Miguel et al., 2017; Ordoñez-Quiroz et al., 2018; Torres-Huerta et al., 2016). These stressors can be used on the cells under conditions previously established (7 µM metronidazole and 100 Gy for gamma radiation (Ansell et al., 2016; Torres-Huerta et al., 2016)) and protein expression can be monitored

over time by western blot. The change in expression can be compared to the phosphorylation of histone H2a, a marker for double-stranded DNA breaks, which increases 4-fold upon gamma irradiation when compared to the approximately 2.5-fold increase of DMC1, another marker for DNA damage. A TUNEL assay may also be used to directly monitor DNA damage. This would allow us to compare the expression changes seen in gCYTB5-III to the changes that occur upon DNA damage. Using both stressors will also allow for observations under different types of DNA damage, single stranded breaks from gamma radiation, versus double stranded breaks from MTZ. In addition, performing a knockdown of gCYTB5-III would also assist in illuminating its function.

4.2.4 Discussion on the discrepancy of gCYTB5-III interacting with the mitosomal proteome without co-localization

The main issue with my co-IP data suggesting that gCYTB5-III interacts with nuclear and mitosomal proteins is that IFA performed with the custom gCYTB5-III antibody shows the gCYTB5-III exclusively in the nucleus (Dayer, 2017). Another issue is that previous co-IP and pulldown experiments performed with different mitosomal proteins as baits have never detected gCYTB5-III among the immunoprecipitants (Dagley et al., 2009; Dolezal et al., 2005; Martincová et al., 2015; Pyrih et al., 2016; Pyrihov et al., 2018; Rada et al., 2009; Rout et al., 2016). Proteomic analysis of semi-purified mitosomes have also not identified this protein among the results (Jedelsky et al., 2011). One possible explanation for the lack of detection of gCYTB5-III in the previous studies of the

mitosomes is that these studies all involved mass spectroscopy (MS) analysis of trypsin generated peptides to identify the proteins. These conditions do not permit a high recovery of gCYTB5-III peptides for several reasons. First, gCYTB5-III is a small protein (129 amino acids), so protease digestion of this protein does not yield as many peptides compared to similar digestions of larger proteins. Second, trypsin digestion of gCYTB5-III yields only five peptides, all from the N-terminus, that are within the size range (7 – 50 amino acids) that could be analyzed by MS (Fig. 23). The peptides generated from the trypsin digestion of the C-terminal half of the protein are either too small or too large for MS analysis.

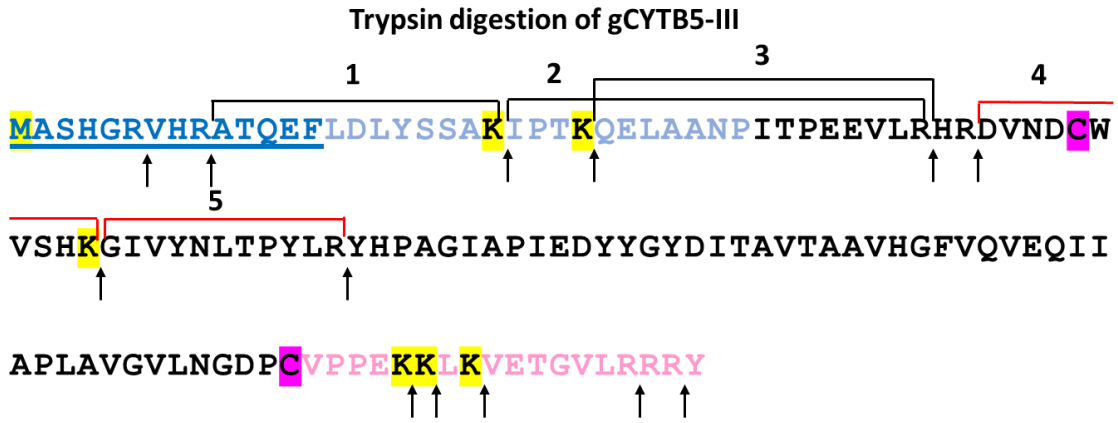

Peptide	Found in HA-tagged system	Found in CL endogenous system	Peptides
1	1	1	ATQEFLDLYSSAK
2	2	1	IPTKQELAANPITPEEVLR
3	1	1	QELAANPITPEEVLR
4	1	n/a	DVNDcWVSHK
5	2	n/a	GIVYNLTPYLR

Legend

Underlined: epitope representing 1st 14 amino acids at N-terminal

Yellow highlight: lysine (K) and primary amine crosslinking sites for NHS

Pink highlight: cysteine (C) crosslinking sites for BMH

↑ Arrows: trypsin cleavage sites

Figure 23: Diagram displaying potential peptides generated by trypsin digestion of gCYTB5-III. The cleavage sites for trypsin within the protein are indicated by the arrows. Previous co-IP in our lab by Guillem Dayer with an over expressed HA-tagged CYTb5-III identified a total of 7 sequences representing 5 different peptides (indicated by brackets labeled 1 – 5) of gCYTB5-III. MS analysis of my co-IP results identified three sequences corresponding to three different peptides (1 – 3). The lack of detection of peptide 4 is likely due to the presence of the cysteine (pink highlight) that would result in the crosslinking of this site to another protein by the BMH crosslinker. Peptide 5 would not be able to be detected due to possible steric hinderance of the crosslinked adjacent peptide 4.

Trypsin is the protease most commonly used for proteomic analysis because it is very efficient, specific, and yields peptides with a basic arginine or lysine at the C-terminus, which are all qualities amenable to MS analysis (Tsiatsiani & Heck, 2015). I investigated the possibility of using other proteases (chymotrypsin, Lys-N, Lys-C) for MS analysis of the gCYTB5-III immunoprecipitate, but trypsin was ultimately chosen since this is the protease commonly used to generate a good coverage of peptides for the detection of other giardial proteins that may be potential interactors of gCYTB5-III.

Another possible explanation for the lack of detection of gCYTB5-III in previous MS data is that that its peptides may not be well ionized. If the peptides do not efficiently take on a charge, then the peptide will not "fly well" within the MS instrument and cannot be detected. More importantly, if the peptide does not take on a charge in a predictable manner to give a MS spectrum that matches the corresponding protein, then this protein will not be identified. For example, MS analysis could not detect the presence of exogenously expressed transcription factors, CEBPG and HMGA1, in cell lysates despite their high abundance in the cells and confirmation of adequate protease digestion (Stergachis, Maclean, Lee, John, & Maccoss, 2012). The authors concluded that some transcription factors are not amenable to proteomic analysis following trypsin-based digestion. This may also be the case for gCYTB5-III which could explain its low detection rates in co-IP and pulldown experiments, and its absence in proteomic analysis of Giardia mitosomes.

The poor detection of gCYTB5-III with MS analysis of trypsin peptides is supported by results from a previous co-IP in our lab on lysates prepared from Giardia trophozoites overexpressing an HA-tagged version of the gCYTB5-III (Dayer, 2017). This previous analysis detected only seven sequences representing five different peptides (Fig. 23) despite the overexpression of gCYTB5-III from a promoter from the ornithine carbamoyltransferase gene (GL50803_10311), which is one of the highest expressed genes in Giardia (Pham et al., 2017). In comparison, the co-IP I performed with endogenous gCYTB5-III, yielded three sequences representing three different peptides in MS analysis (Fig. 12 and 23).

Conclusion

I have shown evidence that gCYTB5-III is associated with chromatin, interacts with a putative FACT complex that is involved in epigenetic regulation of transcription, and increases in expression when the cell is subjected to DNA stress. Furthermore, I found 43% of the known Giardia mitosomal proteome within the co-IP of gCYTB5-III. As certain Fe-S-containing proteins are required for DNA scanning and repair within the nucleus, this suggests that gCYTB5-III may act as a link between Fe-S assembly in the mitosome and proteins requiring Fe-S clusters in the nucleus.

Future Directions

Future work to characterize the function of gCYTB5-III could involve the following experiments:

1. The interaction of gCYTB5-III with mitosomal proteins could be confirmed by performing a reverse co-IP with one of the mitosomal proteins, such as mHSP70 or GiOR-1, as the bait. The immunoprecipitate could then be analyzed for the presence of gCYTB5-III with the custom antibody we have in our lab. Western blot analysis would allow the identification of gCYTB5-III in the immunoprecipitate without the inherent problems of detecting this protein by MS.

2. The expression of gCYTB5-III in Giardia's response to other inducers of DNA stress could be studied. Metronidazole or gamma radiation can be used to induce DNA damage in Giardia cultures, and DNA damage could be monitored through TUNEL assays, or by the phosphorylation of histone H2a.
3. The effect of a knockdown on the expression of gCYTB5-III could be studied. The successful application of CRISPR interference (CRISPRi) in Giardia was recently described (McInally et al., 2019). A gCYTB5-III knockdown in Giardia should be more sensitive to DNA damage, based on my hypothesis that gCYTB5-III is involved in the production of nuclear Fe-S-containing proteins, including DNA repair enzymes.
4. CHIP assays would allow us to establish if gCYTB5-III is interacting with DNA in a sequence-specific manner, and to identify this sequence.
5. The BirA/biotin-tagging system could also be used for a pulldown with Mlf1 as the bait. This is the most common enriched protein identified in mitosomal studies, and its ortholog, determined by BLAST analysis, is a transcription factor in higher eukaryotes. As Mlf1 is identified in co-IP of gCYTB5-III under non-crosslinked conditions, performing a pulldown or coIP with this protein to compare the results to gCYTB5-III would be valuable.

References

Agarwal, S., Rastogi, R., Gupta, D., Patel, N., Raje, M., & Mukhopadhyay, A. (2013). Clathrin-mediated hemoglobin endocytosis is essential for survival of Leishmania. *Biochimica et Biophysica Acta - Molecular Cell Research*, *1833*(5), 1065–1077. https://doi.org/10.1016/j.bbamcr.2013.01.006

Ageno, M., Dore, E., & Frontali, C. (1969). The Alkaline Denaturation of DNA. *Biophysical Journal*, *9*(11), 1281–1311. https://doi.org/10.1016/S0006-3495(69)86452-0

Aggarwal, A., Merritt, J. W. J., & Nash, T. E. (1989). Cysteine-rich variant surface proteins of Giardia lamblia. *Molecular and Biochemical Parasitology, 32*, 39–48.

Alam, S., Yee, J., Couture, M., Takayama, S. J., Tseng, W.-H., Mauk, A. G., & Rafferty, S. (2012). Cytochrome b 5 from Giardia lamblia. *Metallomics*, *4*(4), 1255–1261. https://doi.org/10.1039/c2mt20152f

Anandarajan, V., Noguchi, C., Oleksak, J., Grothusen, G., Terlecky, D., & Noguchi, E. (2020). Genetic investigation of formaldehyde-induced DNA damage response in Schizosaccharomyces pombe. *Current Genetics*. https://doi.org/10.1007/s00294-020-01057-z

Ansell, B. R. E., McConville, M. J., Baker, L., Korhonen, P. K., Emery, S. J., Svärd, S. G., … Jexa, A. R. (2016). Divergent transcriptional responses to physiological and xenobiotic stress in Giardia duodenalis. *Antimicrobial Agents and Chemotherapy*, *60*(10), 6034–6045. https://doi.org/10.1128/AAC.00977-16

Aoki, T., Wolle, D., Ben Noon, E. P., Dai, Q., Lai, E. C., & Schedl, P. (2014). Bi-functional cross-linking reagents efficiently capture protein-DNA complexes in Drosophila embryos. *Fly*, *8*(1), 43–51. https://doi.org/10.4161/fly.26805

Aurrecoechea, C., Brestelli, J., Brunk, B. P., Carlton, J. M., Dommer, J., Fischer, S., … Wang, H. (2009). GiardiaDB and TrichDB : integrated genomic resources for the eukaryotic protist pathogens Giardia lamblia and Trichomonas vaginalis, *37*(September 2008), 526–530. https://doi.org/10.1093/nar/gkn631

Balk, J., Aguilar Netz, D. J., Tepper, K., Pierik, A. J., & Lill, R. (2005). The Essential WD40 Protein Cia1 Is Involved in a Late Step of Cytosolic and Nuclear Iron-Sulfur Protein Assembly. *Molecular and Cellular Biology*, *25*(24), 10833–10841. https://doi.org/10.1128/mcb.25.24.10833-10841.2005

Bradford, M. M. (1976). A Rapid and Sensitive Method for the Quantitation Microgram Quantities of Protein Utilizing the Principle of Protein-Dye Binding. *ANALYTICAL BIOCHEMISTRY*, *72*, 248–254. https://doi.org/10.1016/j.cj.2017.04.003

Carranza, P. G., Gargantini, P. R., Prucca, C. G., Torri, A., Saura, A., Svärd, S., & Lujan, H. D. (2016). Specific histone modifications play critical roles in the control of encystation and antigenic variation in the early-branching eukaryote Giardia lamblia. *International Journal of Biochemistry and Cell Biology*, *81*, 32–43. https://doi.org/10.1016/j.biocel.2016.10.010

Cherry, J. M., Hong, E. L., Amundsen, C., Balakrishnan, R., Binkley, G., Chan, E. T., … Wong, E. D. (2012). Saccharomyces Genome Database: The genomics resource of budding yeast. *Nucleic Acids Research*, *40*(D1), 700–705. https://doi.org/10.1093/nar/gkr1029

Ciccia, A., McDonald, N., & West, S. C. (2008). Structural and Functional Relationships of the XPF/MUS81 Family of Proteins. *Annual Review of Biochemistry*, *77*(1), 259–287. https://doi.org/10.1146/annurev.biochem.77.070306.102408

Ciftci, G., Aksoy, A., cenesiz, S., sogut, M. unlu, Yarim, G. F., Nisbet, C., … Ertekin, A. (2015). Therapeutic role of curcumin in oxidative DNA damage caused by formaldehyde. *Microscopy Research and Technique*, *78*(5), 391–395. https://doi.org/10.1002/jemt.22485

Compe, E., & Egly, J. M. (2012). TFIIH: When transcription met DNA repair. *Nature Reviews Molecular Cell Biology*, *13*(6), 343–354. https://doi.org/10.1038/nrm3350

Cutter, A. R., & Hayes, J. J. (2015). A brief review of nucleosome structure. *Federation of European Biochemical Societies Letters*, *589*, 2914–2922.

Dagley, M. J., Dolezal, P., Likić, V. A., Smid, O., Purcell, A. W., Buchanan, S. K., … Lithgow, T. (2009). The protein import channel in the outer mitosomal membrane of Giardia intestinalis. *Molecular Biology and Evolution*, *26*(9), 1941–1947. https://doi.org/10.1093/molbev/msp117

Datta, S. P., Jana, K., Mondal, A., Ganguly, S., & Sarkar, S. (2018). Multiple paralogues of α -SNAP in Giardia lamblia exhibit independent subcellular localization and redistribution during encystation and stress. *Parasites & Vectors*, *11*(539), 1–16.

Dayer, G. (2017). *Interaction study of Giardia Intestinalis Cytochrome B5*. *Trent University*. Trent University. Retrieved from http://digitalcollections.trentu.ca/objects/etd-556?solr_nav%5Bid%5D=bd774a6529a0a068dd1c&solr_nav%5Bpage%5D=0&solr_nav%5Boffset%5D=0

de Graaf, B., Clore, A., & McCullough, A. K. (2009). Cellular pathways for DNA repair and damage tolerance of formaldehyde-induced DNA-protein crosslinks. *DNA Repair*, *8*(10), 1207–1214. https://doi.org/10.1016/j.dnarep.2009.06.007

Deans, A. J., & West, S. C. (2011). DNA interstrand crosslink repair and cancer. *Nature Reviews Cancer*, *11*(7), 467–480. https://doi.org/10.1038/nrc3088

Dejaegere, A., Choulier, L., Lafont, V., De Genst, E., & Altschuh, D. (2005). Variations in antigen-antibody association kinetics as a function of pH and salt concentration: A QSAR and molecular modeling study. *Biochemistry*, *44*(44), 14409–14418. https://doi.org/10.1021/bi050986v

Dolezal, P., Smíd, O., Rada, P., Zubácová, Z., Bursać, D., Suták, R., … Tachezy, J. (2005). Giardia mitosomes and trichomonad hydrogenosomes share a common mode of protein targeting. *Proceedings of the National Academy of Sciences of the United States of America*, *102*(31), 10924–10929. https://doi.org/10.1073/pnas.0500349102

Elias, E. V, Quiroga, R., Gottig, N., Nakanishi, H., Nash, T. E., Neiman, A., & Lujan, H. D. (2008). Characterization of SNAREs Determines the Absence of a Typical Golgi Apparatus in the Ancient Eukaryote, *283*(51), 35996–36010. https://doi.org/10.1074/jbc.M806545200

Figueroa-Angulo, E. E., Rendón-Gandarilla, F. J., Puente-Rivera, J., Calla-Choque, J. S., Cárdenas-Guerra, R. E., Ortega-López, J., … Arroyo, R. (2012). The effects of environmental factors on the virulence of Trichomonas vaginalis. *Microbes and Infection*, *14*(15), 1411–1427. https://doi.org/10.1016/j.micinf.2012.09.004

Fink, D., Nebel, S., Aebi, S., Zheng, H., Cenm, B., Nehmã, A., … Howell, S. B. (1996). The Role of DNA Mismatch Repair in Platinum Drug Resistance. *Cancer Research*, *56*, 4881–4886.

Flannery, A. R., Renberg, R. L., & Andrews, N. W. (2013). Pathways of iron acquisition and utilization in Leishmania. *Current Opinion in Microbiology*, *16*(6), 716–721. https://doi.org/10.1016/j.mib.2013.07.018

Free, R. B., Hazelwood, L. A., & Sibley, D. R. (2009). Identifying Novel Protein-Protein Interactions Using Co- Immunoprecipitation and Mass Spectroscopy. *Current Protocols in Neuroscience*, (5), 1–19. https://doi.org/10.1002/0471142301.ns0528s46.Identifying

Fuss, J. O., Tsai, C., Ishida, justin P., & Tainer, J. A. (2017). Emerging critical roles of Fe-S clusters in DNA replication and repair. *Physiology & Behavior*, *176*(3), 139–148. https://doi.org/10.1016/j.physbeh.2017.03.040

Gaechter, V., Schraner, E., Wild, P., & Hehl, A. B. (2008). The single dynamin family protein in the primitive protozoan giardia lamblia is essential for stage conversion and endocytic transport. *Traffic*, *9*(1), 57–71. https://doi.org/10.1111/j.1600-

0854.2007.00657.x

Gillin, F. D., Reiner, D. S., & Boucher, S. E. (1988). Small-intestinal factors promote encystation of Giardia lamblia in vitro. *Infection and Immunity*, *56*(3), 705–707. https://doi.org/10.1128/iai.56.3.705-707.1988

Gingras, A. C., Gstaiger, M., Raught, B., & Aebersold, R. (2007). Analysis of protein complexes using mass spectrometry. *Nature Reviews Molecular Cell Biology*, *8*(8), 645–654. https://doi.org/10.1038/nrm2208

Hagen, K. D., Hirakawa, M. P., House, S. A., Schwartz, C. L., Pham, J. K., Cipriano, M. J., … Dawson, S. C. (2011). Novel structural components of the ventral disc and lateral crest in giardia intestinalis. *PLoS Neglected Tropical Diseases*, *5*(12). https://doi.org/10.1371/journal.pntd.0001442

Hammond, C. M., Stromme, C. B., Huang, H., Patel, D. J., & Groth, A. (2017). Histone chaperone networks shaping chromatin function. *Nature Reviews Molecular Cell Biology*, *18*(3), 141–158. https://doi.org/10.1016/j.physbeh.2017.03.040

Hamza, I., & Dailey, H. A. (2012). One ring to rule them all: Trafficking of heme and heme synthesis intermediates in the metazoans. *Biochimica et Biophysica Acta - Molecular Cell Research*, *1823*(9), 1617–1632. https://doi.org/10.1016/j.bbamcr.2012.04.009

Henshall, D. C., Bonislawski, D. P., Skradski, S. L., Araki, T., Lan, J. Q., Schindler, C. K., … Simon, R. P. (2001). Formation of the Apaf-1/cytochrome c complex precedes activation of caspase-9 during seizure-induced neuronal death. *Cell Death and Differentiation*, *8*(12), 1169–1181. https://doi.org/10.1038/sj.cdd.4400921

Holberton, D. V. (1981). Arrangement of Subunits in Microribbons from Giardia. *Journal of Cell Science*, *47*, 167–185.

Huynh, C., Sacks, D. L., & Andrews, N. W. (2006). A Leishmania amazonensis ZIP family iron transporter is essential for parasite replication within macrophage phagolysosomes. *Journal of Experimental Medicine*, *203*(10), 2363–2375. https://doi.org/10.1084/jem.20060559

Invitrogen. (2016). Protein G Dynabeads. Retrieved from https://www.thermofisher.com/document-connect/document-connect.html?url=https%3A%2F%2Fassets.thermofisher.com%2FTFS-Assets%2FLSG%2Fmanuals%2FMAN0015809_Dynabeads_Protein_G.pdf

Ito, S., Tan, L. J., Andoh, D., Narita, T., Seki, M., Hirano, Y., … Tanaka, K. (2010). MMXD, a TFIIH-Independent XPD-MMS19 Protein Complex Involved in Chromosome

Segregation. *Molecular Cell*, *39*(4), 632–640. https://doi.org/10.1016/j.molcel.2010.07.029

Jedelsky, P. L., Dolezal, P., Rada, P., Pyrih, J., Ondrej, S., Hrdy, I., … Tachezy, J. (2011). The minimal proteome in the reduced mitochondrion of the parasitic protist Giardia intestinalis. *PLoS ONE*, *6*(2), 15–21. https://doi.org/10.1371/journal.pone.0017285

Kassebaum, N. J., Jasrasaria, R., Naghavi, M., Wulf, S. K., Johns, N., Lozano, R., … Murray, C. J. L. (2014). A systematic analysis of global anemia burden from 1990 to 2010. *Blood Journal*, *123*(5), 615–625. https://doi.org/10.1182/blood-2013-06-508325.The

Keister, D. B. (1983). Axenic culture of Giardia lamblia in TYI-S-33 medium supplemented with bile. *Transactions of The Royal Society of Tropical Medicine and Hygiene*, *77*(4), 487–488. https://doi.org/10.1016/0035-9203(83)90120-7

Knipscheer, P., Räschle, M., Smogorzewska, A., Enoiu, M., Ho, T. V., Schärer, O. D., … Walter, J. C. (2009). The fanconi anemia pathway promotes replication-dependent DNA interstrand cross-link repair. *Science*, *326*(5960), 1698–1701. https://doi.org/10.1016/j.jsbmb.2011.07.002.Identification

Kořený, L., Oborník, M., & Lukeš, J. (2013). Make It, Take It, or Leave It: Heme Metabolism of Parasites. *PLoS Pathogens*, *9*(1), e1003088. https://doi.org/10.1371/journal.ppat.1003088

Krishnamurthy, G., Vikram, R., Singh, S. B., Patel, N., Agarwal, S., Mukhopadhyay, G., … Mukhopadhyay, A. (2005). Hemoglobin receptor in Leishmania is a hexokinase located in the flagellar pocket. *Journal of Biological Chemistry*, *280*(7), 5884–5891. https://doi.org/10.1074/jbc.M411845200

Krtkova, J., Xu, J., Lalle, M., Steele-Ogus, M., Alas, G. C. M., Sept, D., & Paredez, A. R. (2017). 14-3-3 Regulates Actin Filament Formation in the Deep-Branching Eukaryote Giardia lamblia. *MSphere*, *2*(5), 1–16.

Kunz, S., Balmer, V., Sterk, G. J., Pollastri, M. P., Leurs, R., Muller, N., … Spycher, C. (2017). The single cyclic nucleotide-specific phosphodiesterase of the intestinal parasite Giardia lamblia represents a potential drug target. *PLoS Neglected Tropical Diseases*, *11*(9).

Lederer, F. (1994). The cytochrome b5-fold: An adaptable module. *Biochimie*, *76*, 674–692.

Lill, R., & Freibert, S. (2020). Mechanisms of Mitochondrial Iron-Sulfur Protein Biogenesis. *Annual Review of Analytical Chemistry*, *89*(4), 71–99.

Lill, R., & Kispal, G. (2000). Maturation of cellular Fe-S proteins: An essential function of mitochondria. *Trends in Biochemical Sciences*, *25*(8), 352–356. https://doi.org/10.1016/S0968-0004(00)01589-9

Lill, R., & Mühlenhoff, U. (2005). Iron-sulfur-protein biogenesis in eukaryotes. *Trends in Biochemical Sciences*, *30*(3), 133–141. https://doi.org/10.1016/j.tibs.2005.01.006

Liu, Y., Zhou, K., Zhang, N., Wei, H., Tan, Y. Z., Zhang, Z., … Luger, K. (2020). FACT caught in the act of manipulating the nucleosome. *Nature*, *577*(7790), 426–431. https://doi.org/10.1038/s41586-019-1820-0

Lubec, G., & Afjehi-Sadat, L. (2007). Limitations and pitfalls in protein identifications by mass spectrometry. *Chemical Reviews*, *107*(8), 3568–3584. https://doi.org/10.1021/cr068213f

Lujan, H. D. (1995). Identification of a Novel Giardia lamblia Cyst Wall Protein with Leucine-rich Repeats. *Journal of Biological Chemistry*, *270*(49), 29307–29313. https://doi.org/10.1074/jbc.270.49.29307

Lujan, H. D., & Svärd, S. G. (2011). *Giardia A Model Organism*. *Springer Wien New York*. https://doi.org/10.1017/CBO9781107415324.004

Luk, E., Vu, N. D., Patteson, K., Mizuguchi, G., Wu, W. H., Ranjan, A., … Wu, C. (2007). Chz1, a Nuclear Chaperone for Histone H2AZ. *Molecular Cell*, *25*(3), 357–368. https://doi.org/10.1016/j.molcel.2006.12.015

Mach, J., & Sutak, R. (2020). Iron in parasitic protists-from uptake to storage and where we can interfere. *Metallomics*, *12*(9), 1335–1347. https://doi.org/10.1039/d0mt00125b

Margulis, L., & Bermudes, D. (1985). Symbiosis as a mechanism of evolution: status of cell symbiosis theory. *Symbiosis*, *1*, 101–124.

Martin, E. M., On, D. M., Bowers, E. C., & McCullough, S. D. (2018). *Chromatin immunoprecipitation: An introduction, overview, and protocol? Toxicoepigenetics: Core Principles and Applications*. Elsevier Inc. https://doi.org/10.1016/B978-0-12-812433-8.00014-9

Martincová, E., Voleman, L., Pyrih, J., Žárský, V., Vondráčková, P., Kolísko, M., … Doležal, P. (2015). Probing the Biology of Giardia intestinalis Mitosomes Using In Vivo Enzymatic Tagging . *Molecular and Cellular Biology*, *35*(16), 2864–2874. https://doi.org/10.1128/mcb.00448-15

Martínez-Miguel, R. M., Sandoval-Cabrera, A., Bazán-Tejeda, M. L., Torres-Huerta, A. L.,

Martínez-Reyes, Di. A., & Bermúdez-Cruz, R. M. (2017). Giardia duodenalis Rad52 protein: Biochemical characterization and response upon DNA damage. *Journal of Biochemistry*, *162*(2), 123–135. https://doi.org/10.1093/jb/mvx009

McInally, S. G., Hagen, K. D., Nosala, C., Williams, J., Nguyen, K., Booker, J., … Dawson, S. C. (2019). Robust and stable transcriptional repression in Giardia using CRISPRi. *Molecular Biology of the Cell*, *30*(1), 119–130. https://doi.org/10.1091/mbc.E18-09-0605

Mense, S. M., & Zhang, L. (2006). Heme: A versatile signaling molecule controlling the activities of diverse regulators ranging from transcription factors to MAP kinases. *Cell Research*, *16*(8), 681–692. https://doi.org/10.1038/sj.cr.7310086

Meyer, T. E., Shirabe, K., Yubisui, T., Takeshita, M., Bes, M. T., Casanovich, M. A., & Tollin, G. (1995). Transient kinetics of intracomplex electron transfer in the human cytochrome b5 reductase-cytochrome b5 system: NAD+ modulates protein-protein binding and electron transfer. *Archives of Biochemistry and Biophysics*, *318*(2), 457–464.

Mu, D., Bessho, T., Nechev, L. V., Chen, D. J., Harris, T. M., Hearst, J. E., & Sancar, A. (2000). DNA Interstrand Cross-Links Induce Futile Repair Synthesis in Mammalian Cell Extracts. *Molecular and Cellular Biology*, *20*(7), 2446–2454. https://doi.org/10.1128/mcb.20.7.2446-2454.2000

Munakata, H., Sun, J. Y., Yoshida, K., Nakatani, T., Honda, E., Hayakawa, S., … Hayashi, N. (2004). Role of the heme regulatory motif in the heme-mediated inhibition of mitochondrial import of 5-aminolevulinate synthase. *Journal of Biochemistry*, *136*(2), 233–238. https://doi.org/10.1093/jb/mvh112

Netz, D. J. A., Mascarenhas, J., Stehling, O., Pierik, A. J., & Lill, R. (2014). Maturation of cytosolic and nuclear iron-sulfur proteins. *Trends in Cell Biology*, *24*(5), 303–312. https://doi.org/10.1016/j.tcb.2013.11.005

Netz, D. J. A., Stümpfig, M., Doré, C., Mühlenhoff, U., Pierik, A. J., & Lill, R. (2010). Tah18 transfers electrons to Dre2 in cytosolic iron-sulfur protein biogenesis. *Nature Chemical Biology*, *6*(10), 758–765. https://doi.org/10.1038/nchembio.432

Noda, T., Takahashi, A., Kondo, N., Mori, E., Okamoto, N., Nakagawa, Y., … Ohnishi, T. (2011). Repair pathways independent of the Fanconi anemia nuclear core complex play a predominant role in mitigating formaldehyde-induced DNA damage. *Biochemical and Biophysical Research Communications*, *404*(1), 206–210. https://doi.org/10.1016/j.bbrc.2010.11.094

Nunez-quintana, M., Truan, G., & Van Heijenoort, C. (2006). *RCSB PDB - 2I96: Solution*

structure of the oxidized microsomal human cytochrome b5. Retrieved from https://www.rcsb.org/structure/2I96

Ordoñez-Quiroz, A., Ortega-Pierres, M. G., Bazán-Tejeda, M. L., & Bermúdez-Cruz, R. M. (2018). DNA damage induced by metronidazole in Giardia duodenalis triggers a DNA homologous recombination response. *Experimental Parasitology*, *194*(March), 24–31. https://doi.org/10.1016/j.exppara.2018.09.004

Park, E., Kim, J., Shin, M. Y., & Park, S.-J. (2020). A polo-like kinase modulates cytokinesis and agella biogenesis in Giardia lamblia. *Parasites & Vectors*, 1–30.

Patel, N., Singh, S. B., Basu, S. K., & Mukhopadhyay, A. (2008). Leishmania requires Rab7-mediated degradation of endocytosed hemoglobin for their growth. *Proceedings of the National Academy of Sciences of the United States of America*, *105*(10), 3980–3985. https://doi.org/10.1073/pnas.0800404105

Paul, V. D., & Lill, R. (2015). Biogenesis of cytosolic and nuclear iron-sulfur proteins and their role in genome stability. *Biochimica et Biophysica Acta - Molecular Cell Research*, *1853*(6), 1528–1539. https://doi.org/10.1016/j.bbamcr.2014.12.018

Pazdzior, R., Yang, Z., Mesbahuddin, M. S., Yee, J., van der Est, A., & Rafferty, S. (2015). Low reduction potential cytochrome b5 isotypes of Giardia intestinalis. *Experimental Parasitology*, *157*, 197–201. https://doi.org/10.1016/j.exppara.2015.08.004

Pchelintsev, N. A., Adams, P. D., & Nelson, D. M. (2016). Critical parameters for efficient sonication and improved chromatin immunoprecipitation of high molecular weight proteins. *PLoS ONE*, *11*(1), 1–11. https://doi.org/10.1371/journal.pone.0148023

Pham, J. K., Nosala, C., Scott, E. Y., Nguyen, K. F., Hagen, K. D., Starcevich, H. N., & Dawson, S. C. (2017). Transcriptomic Profiling of High-Density Giardia Foci Encysting in the Murine Proximal Intestine. *Frontiers in Cellular and Infection Microbiology*, *7*(May), 1–17. https://doi.org/10.3389/fcimb.2017.00227

Pusnik, M., Charrie, F., Ma, P., Waller, R. F., Dagley, M. J., & Lithgow, T. (2009). The Single Mitochondrial Porin of Trypanosoma brucei is the Main Metabolite Transporter in the Outer Mitochondrial Membrane. *Molecular Biology and Evolution*, *26*(3), 671–680. https://doi.org/10.1093/molbev/msn288

Pyrih, J., Harant, K., Martincová, E., Sutak, R., Lesuisse, E., Hrdý, I., & Tachezy, J. (2014). Giardia intestinalis incorporates heme into cytosolic cytochrome b5. *Eukaryotic Cell*, *13*(2), 231–239. https://doi.org/10.1128/EC.00200-13

Pyrih, J., Pyrihová, E., Kolísko, M., Stojanovová, D., Basu, S., Harant, K., … Tachezy, J.

(2016). Minimal cytosolic iron-sulfur cluster assembly machinery of Giardia intestinalis is partially associated with mitosomes. *Molecular Microbiology*, *102*(4), 701–714. https://doi.org/10.1111/mmi.13487

Pyrihov, E., Motyckova, A., Voleman, L., Wandyszewska, N., Fiser, R., Seydlov, G., … Doležal, P. (2018). GBE A Single Tim Translocase in the Mitosomes of Giardia intestinalis Illustrates Convergence of Protein Import Machines in Anaerobic Eukaryotes. *Genome Biology and Evolution*, *10*(10), 2813–2822. https://doi.org/10.1093/gbe/evy215

Rada, P., Šmíd, O., Sutak, R., Doležal, P., Pyrih, J., Žárský, V., … Tachezy, J. (2009). The monothiol single-domain glutaredoxin is conserved in the highly reduced mitochondria of giardia intestinalis. *Eukaryotic Cell*, *8*(10), 1584–1591. https://doi.org/10.1128/EC.00181-09

Rafferty, S., & Dayer, G. (2015). Experimental Parasitology Heme proteins of Giardia intestinalis. *Experimental Parasitology*, *159*, 13–23. https://doi.org/10.1016/j.exppara.2015.08.001

Regoes, A., Zourmpanou, D., León-Avila, G., Van Der Giezen, M., Tovar, J., & Hehl, A. B. (2005). Protein import, replication, and inheritance of a vestigial mitochondrion. *Journal of Biological Chemistry*, *280*(34), 30557–30563. https://doi.org/10.1074/jbc.M500787200

Rivero, M. R., Miras, S. L., Feliziani, C., Zamponi, N., Quiroga, R., Hayes, S. F., … Touz, M. C. (2012). Vacuolar Protein Sorting Receptor in Giardia lamblia, *7*(8). https://doi.org/10.1371/journal.pone.0043712

Rivero, M. R., Miras, S. L., Quiroga, R., Ropolo, A. S., & Touz, M. C. (2011). Giardia lamblia low-density lipoprotein receptor-related protein is involved in selective lipoprotein endocytosis and parasite replication. *Molecular Microbiology*, *79*(5), 1204–1219. https://doi.org/10.1111/j.1365-2958.2010.07512.x.Giardia

Rout, S. (2015). *Functional analysis of structurally diverged and reduced organelles in Giardia*. University of Zurich.

Rout, S., Zumthor, J. P., Schraner, E. M., Faso, C., & Hehl, A. B. (2016). An Interactome-Centered Protein Discovery Approach Reveals Novel Components Involved in Mitosome Function and Homeostasis in Giardia lamblia, 1–32. https://doi.org/10.1371/journal.ppat.1006036

Roy, A., Kucukural, A., & Zhang, Y. (2010). I-TASSER : a unified platform for automated protein structure and function prediction. *Nature Protocols*, *5*(4), 725–738. https://doi.org/10.1038/nprot.2010.5

Russev, G., Venkov, C., & Tsanev, R. (1974). Stepwise Dissociation of Histones from Rat-Liver Chromatin in Alkaline Solutions. *European Journal of Biochemistry*, *43*, 253–256.

Sajer, B. H. (2019). *The Effect of Nitrosative Stress on Heme Proteins Expression and Localization in Giardia Intestinalis*. Trent Univeristy.

Sattler, U., Frit, P., Salles, B., & Calsou, P. (2003). Long-patch DNA repair synthesis during base excision repair in mammalian cells. *EMBO Reports*, *4*(4), 363–367. https://doi.org/10.1038/sj.embor.embor796

Severance, S., & Hamza, I. (2009). Trafficking of Heme and Porphyrins in Metazoa Scott. *Chemical Reviews*, *109*(10), 4596–4616. https://doi.org/10.1021/cr9001116.Trafficking

Singh, S. B., Tandon, R., Krishnamurthy, G., Vikram, R., Sharma, N., & Basu, S. K. (2003). 2003 Singh Rab5mediated endosome_endosome fusion, *22*(21).

Šmíd, O., Matušková, A., Harris, S. R., Kučera, T., Novotný, M., Horváthová, L., … Tachezy, J. (2008). Reductive evolution of the mitochondrial processing peptidases of the unicellular parasites Trichomonas vaginalis and Giardia intestinalis. *PLoS Pathogens*, *4*(12). https://doi.org/10.1371/journal.ppat.1000243

Smith, A. L., Friedman, D. B., Yu, H., Carnahan, R. H., & Reynolds, A. B. (2011). ReCLIP (Reversible Cross-Link Immuno-Precipitation): An Efficient Method for Interrogation of Labile Protein Complexes, *6*(1). https://doi.org/10.1371/journal.pone.0016206

Stehling, O., Vashisht, A. a, Mascarenhas, J., Jonsson, Z. O., Sharma, T., Netz, D. J. a, … Lill, R. (2012). MMS19 assembles iron-sulfur proteins required for DNA metabolism and genomic integrity. *Science*, *337*(July), 195–199. https://doi.org/10.1126/science.1219723.MMS19

Stergachis, A. B., Maclean, B., Lee, K., John, A., & Maccoss, M. J. (2012). Rapid empirical discovery of optimal peptides for targeted proteomics. *Nature Methods*, *8*(12), 1041–1043. https://doi.org/10.1038/nmeth.1770.Rapid

Swenson, S. A., Moore, C. M., Marcero, J. R., Medlock, A. E., Reddi, A. R., & Khalimonchuk, O. (2020). From Synthesis to Utilization: The Ins and Outs of Mitochondrial Heme. *Cells*, *9*(3), 10–19. https://doi.org/10.3390/cells9030579

Tachezy, J., Sánchez, L. B., & Müller, M. (2001). Mitochondrial type iron-sulfur cluster assembly in the amitochondriate eukaryotes Trichomonas vaginalis and Giardia intestinalis, as indicated by the phylogeny of IscS. *Molecular Biology and Evolution*, *18*(10), 1919–1928. https://doi.org/10.1093/oxfordjournals.molbev.a003732

Tao, H., & Hajri, T. (2011). Very low density lipoprotein receptor promotes adipocyte differentiation and mediates the proadipogenic effect of peroxisome proliferator-activated receptor gamma agonists. *Biochemical Pharmacology*, *82*(12), 1950–1962. https://doi.org/10.1016/j.bcp.2011.09.003

Torres-Huerta, A. L., Martínez-Miguel, R. M., Bazán-Tejeda, M. L., & Bermúdez-Cruz, R. M. (2016). Characterization of recombinase DMC1B and its functional role as Rad51 in DNA damage repair in Giardia duodenalis trophozoites. *Biochimie*, *127*, 173–186. https://doi.org/10.1016/j.biochi.2016.05.014

Touz, M. C., Kulakova, L., & Nash, T. E. (2004). Adaptor Protein Complex 1 Mediates the Transport of Lysosomal Proteins from a Golgi-like Organelle to Peripheral Vacuoles in the Primitive Eukaryote Giardia lamblia. *Molecular Biology of the Cell*, *15*(April), 3751–3737. https://doi.org/10.1091/mbc.E03

Tovar, J., León-Avila, G., Sánchez, L. B., Sutak, R., Tachezy, J., van der Giezen, M., … Lucocq, J. M. (2003). Mitochondrial remnant organelles of Giardia function in iron-sulphur protein maturation. *Nature*, *426*(November). https://doi.org/10.1038/nature01945

Tripodi, K. E. J., Menendez Bravo, S. M., & Cricco, J. A. (2011). Role of heme and heme-proteins in trypanosomatid essential metabolic pathways. *Enzyme Research*, *2011*(1). https://doi.org/10.4061/2011/873230

Tsaousis, A. D., Gentekaki, E., Eme, L., Gaston, D., & Roger, A. J. (2014). Evolution of the cytosolic iron-sulfur cluster assembly machinery in Blastocystis species and other microbial eukaryotes. *Eukaryotic Cell*, *13*(1), 143–153. https://doi.org/10.1128/EC.00158-13

Tsiatsiani, L., & Heck, A. J. R. (2015). Proteomics beyond trypsin. *FEBS Journal*, *282*(14), 2612–2626. https://doi.org/10.1111/febs.13287

Vashisht, A. A., Yu, C. C., Sharma, T., Ro, K., & Wohlschlegel, J. A. (2015). The association of the xeroderma pigmentosum group D DNA helicase (XPD) with transcription factor IIH is regulated by the cytosolic iron-sulfur cluster assembly pathway. *Journal of Biological Chemistry*, *290*(22), 14218–14225. https://doi.org/10.1074/jbc.M115.650762

Vergeresb, G., & Waskell, L. (1995). Cytochrome bs, its functions, structure and membrane topology. *Biochimie*, *77*, 604–620.

Voleman, L., Najdrová, V., Ástvaldsson, Á., Tumova, P., Einarsson, E., Svindrych, Z., … Doležal, P. (2017). Giardia intestinalis mitosomes undergo synchronized fission but not fusion and are constitutively associated with the endoplasmic reticulum. *BMC*,

15(27), 1–16. https://doi.org/10.1186/s12915-017-0361-y

Wade, M., Li, Y.-C., & M. Wahl, G. (2013). Successful co-immunoprecipitation of Oct4 and Nanog using cross-linking. *Nature Reviews Cancer*, *13*(2), 83–96. https://doi.org/10.1002/ana.22528.Toll-like

Wang, X., Chen, X., Sun, L., & Qian, W. (2019). Canonical cytosolic iron-sulfur cluster assembly and non-canonical functions of DRE2 in Arabidopsis. *PLoS Genetics*, *15*(4), 1–23. https://doi.org/10.1371/journal.pgen.1008094

Winkler, D. D., & Luger, K. (2011). The histone chaperone FACT: Structural insights and mechanisms for nucleosome reorganization. *Journal of Biological Chemistry*, *286*(21), 18369–18374. https://doi.org/10.1074/jbc.R110.180778

Wu, J.-H., Tung, S.-Y., Ho, C.-C., Su, L.-H., Gan, S.-W., Liao, J.-Y., … Sun, C.-H. (2021). A myeloid leukemia factor homolog involved in encystation-induced protein metabolism in Giardia lamblia. *Biochimica et Biophysica Acta (BBA) - General Subjects*, *1865*(6), 129859. https://doi.org/10.1016/j.bbagen.2021.129859

Yamamoto, M., Hayashi, N., & Kikuchi, G. (1982). Evidence for the transcriptional inhibition by heme of the synthesis of δ-aminolevulinate synthase in rat liver. *Biochemical and Biophysical Research Communications*, *105*(3), 985–990. https://doi.org/10.1016/0006-291X(82)91067-1

Yamamoto, M., Hayashi, N., & Kikuchi, G. (1983). Translational inhibition by heme of the synthesis of hepatic δ-aminolevulinate synthase in a cell-free system. *Biochemical and Biophysical Research Communications*, *115*(1), 225–231.

Yang, Z. (Alice), Pazdzior, R., Yee, J., & Rafferty, S. (2016). Reduction potential and heme-pocket polarity in low potential cytochrome b 5 of Giardia intestinalis. *Journal of Inorganic Biochemistry*, *158*, 110–114. https://doi.org/10.1016/j.jinorgbio.2016.02.021

Zemskov, E. A., Kang, W., & Maeda, S. (2002). Evidence for Nucleic Acid Binding Ability and Nucleosome Association of Bombyx mori Nucleopolyhedrovirus BRO Proteins. *Journal of Virology*, *74*(15), 6784–6789. https://doi.org/10.1128/jvi.74.15.6784-6789.2000

Zumthor, J. P., Cernikova, L., Rout, S., Kaech, A., Faso, C., & Hehl, A. B. (2016). Static Clathrin Assemblies at the Peripheral Vacuole — Plasma Membrane Interface of the Parasitic Protozoan Giardia lamblia, 1–33. https://doi.org/10.1371/journal.ppat.1005756

Appendix A: Protocol for co-IP with endogenous gCYTB5-III

Prep of Giardia cells

1. Grow 40x 16 mL tubes of (640 mL total) Giardia cultures to approximately late log to early stationary phase (~8 x 10^5 cells/mL).
2. Chill cultures on ice slushy for 5 min.
3. Centrifuge culture tubes at 1200 x g for 15 min. and aspirate off supernatant leaving ~0.5 mL of media in each culture tube.
4. Resuspend cells in remaining medium, and pool into a single 50 mL Falcon tube.
5. Centrifuge 50 mL Falcon at 1200 x g for 20 min. and remove supernatant.
6. Re-suspend cells in 5 mL sterile PBS pH 7.2 for triplicate cell count in Beckman-Coulter Vi-Cell XR cell counter. A 1:20 dilution was used in each cell count (25 µL resuspended cells in 475 µL of sterile PBS). The total number of cells recovered from 40x culture tubes is ~ **5.4 x 10^8 cells**.
7. Centrifuge cells at 1200 x g for 15 min. and replace supernatant with 5 mL fresh sterile PBS.

Crosslinking

Bismaleimidohexane: BMH, non-cleavable, membrane permeable, 13 angstrom linker arms, reactive toward sulfhydryl groups (Cys-Cys X-link), MW 276.29 g/mol. ThermoFisher Cat# 22330.

1. Resuspend **4.97 mg** of BMH (bismaleimidohexane) in 500 µL of DMSO to make a 36 mM solution.
2. Add the 500 µL of 36 mM BMH to the 5 mL of PBS containing the 5.4 x 10^8 cells. Cell suspension was topped up to 6 mL with PBS. This will result in a final [BMH] = 3 mM.

NOTE:

- **All crosslinkers begin to degrade after dilution, therefore before dilution of the crosslinker, cells must be prepared for the addition.**
- **BMH is light sensitive and therefore when working with BMH light should be turned off.**

3. Incubate cells with crosslinker for 30 min.
4. Centrifuge cells at 1200 x g and remove supernatant.
5. Resuspend cells in 6 mL of PBS and quench crosslinking by addition of 240 µL of 1 M L-cysteine, pH 7.2 to achieve a [final] = 40 mM. Incubate at RT for 20 min.

6. Centrifuge cells at 1200 x g and remove supernatant.
7. Re-suspended cells in 5 mL PBS and repeated centrifugation to removed wash.
8. Re-suspended cells in 3 mL of an alkaline RIPA buffer with protease inhibitors added.
9. Pulse sonicate: 3x 1 sec. pulses until lysate becomes less opaque.
10. Incubate at 4 °C for 45 min on a rotisserie.
11. Centrifuged lysate at 14 000 x g to removed cell debris. The supernatant (refer to as the cell lysate) is used for co-IP but we also keep and store the pellet in case there is inefficient cell lysis.
12. Determine protein concentration in cell lysate (supernatant) by Bradford assay. Will obtained a concentration of **~3.6 mg/mL** or a total of **10.8 mg total** for his lysate from 40 tubes of Giardia.
13. Directly before IP, the lysate is diluted by the addition of 2 volumes of **80 mM TBS pH 7.2** with 0.01% Tween (**This is the only time 80 mM TBS is used – all other TBS is 20 mM TBS**). This dilution brings the pH down to 8.4 that is more acceptable for Co-IP.

NOTE: prior to IP, lysate is analyzed by western blot to ensure crosslinking and cell lysis was efficient. Need to see gCYTB5-III detected as ~15 kDa band on western blot but also expected to see bands of higher MW due to crosslinking of gCYTB5-III to other proteins.

Co-IP

Binding of antibody (Ab) with magnetic beads

1. Prepare four samples:
    i. Dynabeads + CYTb5-III Ab (CIII)--> for MS analysis
    ii. Dynabeads + CYTb5-III Ab (CIII) --> for SDS-PAGE analysis
    iii. Dynabeads + pre-immune serum (PI) --> for MS analysis
    iv. Dynabeads + pre-immune serum (PI) --> for SDS-PAGE analysis
2. Add 50 µL of protein G Dynabeads (ThermoFisher cat # 10003D) into each 1.5 mL low protein binding microfuge tube (Sarstedt Ref# 72.706.600).
3. Place each tube on the DynaMag magnetic stand (ThermoFisher Cat#: 12321D) so that the beads are pulled toward the magnet. Carefully remove the storage liquid at the bottom of the tube.
4. Add 200 µL of PBS + **0.02%** Tween-20 (PBS-T) and wash beads by gentle pipetting. Place tube against magnet and remove wash.

NOTE: it is essential from this point onwards that you change the pipette tip after every solution to prevent contaminating experimental samples with control samples or vice versa.

5. Re-suspended beads in 200 µL of PBS-T. For the experimental samples (CIII), add 5 µL of 2 µg / µL solution of CYTb5 III Ab yielding 10 µg total Ab on the beads. For the control samples (PI), add an equivalent volume (5 µL) of pre-immune serum. Resuspend the beads with gentle pipetting and then incubate with the antibody for 30 min. at RT.
6. Place samples on magnet and remove antibody solution.
7. Wash beads with 1 mL TBS + **0.01% Tween** to remove any residually unbound Ab.
8. Re-suspend beads in 1.2 mL of dilute lysate with gentle mixing. This diluted lysate represents 400 µL of the original lysate (3.6 mg/mL) with the addition of 800 µL of TBS-T 0.01% pH 7.2. **This is equivalent to 1.44 mg protein used per co-IP sample.**
9. Incubate beads with lysate on microfuge rotisserie overnight at 4°C.
10. Place samples on magnet stand to remove unbound protein solution. **Keep this for analysis as the unbound fraction.**
11. Re-suspend beads in 1 mL TBS **+ 0.5% Tween**. Incubate on rotisserie (for microfuge tubes) for 1 min. at RT.
12. Place samples on magnet stand to remove unbound protein solution. **Keep this for analysis as wash 1.**
13. Perform 5 more washes with 1 mL TBS 0.5% Tween. **Keep all washes for analysis.**
14. One of the two experiment samples and control samples will be eluted with 30 µL 1x SDS-PAGE loading buffer to be analyzed via western blot. This can be heated to 65 °C for 15 min. with the rest of the sample prior to loading on SDS-PAGE.
15. The other samples will be washed 3 more times with TBS **without Tween**. These 3 washes are to remove the detergent from the samples, as it is not compliant with MS analysis. These samples are frozen without liquid @ -20 ℃ to be sent for MS analysis pending western blot results.

Recipes

RIPA alkaline (pH 10.6):

Component	[Final]	Stock	Amt of stock
NaCl	150 mM	**Powder**	0.44 g
NP40	1.0 %	**100 %**	500 µL
SDS	0.1 %	**10 %**	50 µL
Glycine	80.0 mM	**Powder**	0.30 g
NaOH	75.0 mM	**Powder**	0.15 g
		Final volume	50 mL

*Adjust pH accordingly

*Additional components	[Final]	Stock	Amt of stock
EDTA	1 mM	**100 mM**	30 µL
PIC (BioShop Cat# PIC001)	1 x	**100x**	30 µL
Leupeptin	1.0 mg/mL	**100 mg/mL**	30 µL
		Lysis Buffer volume	**3 mL**

*The alkaline RIPA can be made up in 50 mL and store at RT. A 3-mL aliquot is removed and supplemented with the additional components immediately for each co-IP experiment.

TBS – pH to desired pH and add appropriate Tween content.

Chemical	Concentration
Tris	20 mM (or 80 mM where noted)
NaCl	150 mM

PBS - pH 7.2, add appropriate Tween content.

Chemical	Concentration
KH2PO4	1.7 mM
Na2HPO4	5 mM
NaCl	150 mM

Appendix B: Current list of mitosomal proteins

Table developed from a list supplied by Dr. Pavel Dolezal, whose lab has extensively studied the Giardia mitosome. From left to right, are the Giardia data base accession number for each of the proteins, annotation for the proteins with their orthologs in other eukaryotes, the function of those proteins in other eukaryotes, the citation is the first that described the protein as a mitosomal proteins, IP-gCYTB5-III status describe whether the protein is found in the co-IP of gCYTB5-III, the peptides are how many peptides were found within the MS analysis of the gCYTB5-III eluate and the control sample is noted if the sample was not found unique to the experimental, and finally Experimental evidence of mitosomal localization describes what has been done in addition to co-IP experiments to demonstrate mitosomal localization.

Giardia DB accession #	**Annotation**	**Putative function and data for mitosomal protein**	**Citation**	**IP-gCYTb5-III status**	**Peptides**	**Experimental evidence in mitosomes**
GL50803_10452	Tim17	Convergence of mitochondrial Tim17 and Tim22. solely responsible for transport into the inner membrane on the mitosome.	Pyrih et al., 2018			IFA with overexp. HA-tagged
GL50803_17161	Tom40	Channel-forming protein essential for import of protein precursors into mitochondria	Dagley et al., 2009	Unique	2	IFA with polyclonal rabbit anti-Tom40
GL50803_300001	Pam18	Essential component of the PAM complex, a complex required for the translocation of transit peptide-containing proteins from the inner membrane into the mitochondrial matrix in an ATP-dependent manner. In the complex, it is required to stimulate activity of mtHSP70	Doležal et al., 2005			IFA with overexp. HA-tagged

Giardia DB accession #	Annotation	Putative function and data for mitosomal protein	Citation	IP-gCYTb5-III status	Peptides	Experimental evidence in mitosomes
GL50803_29500	Cpn10	Seems to function only as a co-chaperone, along with CPN60, and in certain cases is essential for the discharge of biologically active proteins from CPN60. Binds to Cpn60 in the presence of Mg-ATP and suppresses the ATPase activity of the latter	Jedelský et al., 2011	Unique	2	IFA with overexp. HA-tagged
GL50803_1376	GrpE (Mge1)	Essential component of the PAM complex, a complex required for the translocation of transit peptide-containing proteins from the inner membrane into the mitochondrial matrix in an ATP-dependent manner. Seems to control the nucleotide-dependent binding of SSC1 (HSP70) to substrate proteins and the association of SSC1 (HSP70) with TIM44	Jedelský et al., 2011			IFA with overexp. HA-tagged
GL50803_17030	HscB (Jac 1)	Co-chaperone required for the assembly of iron-sulfur (Fe/S) clusters in mitochondria. Stimulates the ATPase activity of its specialized Hsp70 chaperone partner SSQ1. Binds to the substrate protein ISU1 and targets it to SSQ1. May function together with SSQ1 in the dislocation of the Fe/S cluster from ISU1 and its insertion into apoproteins.	Jedelský et al., 2011	Unique	3	IFA with overexp. HA-tagged
GL50803_14821	IscA	Is able to transfer iron-sulfur clusters to apo-ferredoxin. Multiple cycles of [2Fe2S] cluster formation and transfer are observed, suggesting that	Jedelský et al., 2011	Unique	4	IFA with overexp. HA-tagged

Giardia DB accession #	Annotation	Putative function and data for mitosomal protein	Citation	IP-gCYTb5-III status	Peptides	Experimental evidence in mitosomes
		IscA acts catalytically. Recruits intracellular free iron so as to provide iron for the assembly of transient iron-sulfur cluster in IscU in the presence of IscS, L-cysteine and the thioredoxin reductase system TrxA/TrxB (thioredoxin / thioredoxin reductase).				
GL50803_32838	Nfu	Also a Fe/S cluster scaffold with IscU and IscA	Jedelský et al., 2011	Unique	3	IFA with overexp. HA-tagged
GL50803_9751	chaperone DnaJ, type III	Proteins of this type, involved in Fe/S cluster assembly is called HscB. This protein has already been assigned to the gene 17030.	Jedelský et al., 2011	2.5x enrichment	5 vs. 2 in control	IFA with overexp. HA-tagged
GL50803_91252	GiOR-1	Component of the cytosolic iron-sulfur (Fe-S) protein assembly (CIA) machinery. Required for the maturation of extramitochondrial Fe-S proteins. Part of an electron transfer chain functioning in an early step of cytosolic Fe-S biogenesis. Transfers electrons from NADPH to the Fe-S cluster of DRE2. Positively controls H_2O_2-induced cell death.	Jedelský et al., 2011	Unique	8	IFA with custom antibody
GL50803_19230	Pam16	Regulates ATP-dependent protein translocation into the mitochondrial matrix. Inhibits DNAJC19 stimulation of HSPA9/Mortalin ATPase activity.	Jedelský et al., 2011			IFA with overexp. HA-tagged

Giardia DB accession #	Annotation	Putative function and data for mitosomal protein	Citation	IP-gCYTb5-III status	Peptides	Experimental evidence in mitosomes
GL50803_15985	VAP (VAMP associated protein)	Vesicle associated membrane proteins.	Jedelský et al., 2011			IFA with overexp. HA-tagged
GL50803_9296	Hypothetical protein (MOMTiP-4)	A soluble globular protein in the mitsomes with an unknown function. An antibody against this protein is commonly used as a marker for the mitosome in IFA and subcellular fractionation studies.	Jedelský et al., 2011			IFA with rabbit pAb
GL50803_15985	Hypothetical protein	Possible DNA repair protein	Jedelský et al., 2011			IFA with overexp. HA-tagged
GL50803_14058	GiPDE	Hydrolyzes the second messenger cAMP, which is a key regulator of many important physiological processes (By similarity). Antagonizes dorsal D (DD) motor neuron respecification by reducing levels of cAMP. Assuming this is true it insinuates that some sort of cAMP communication is used in the mitosome as seen in the mitochondria.	Kunz et al., 2017			
GL50803_14845	Tim44	Tethers the PAM complex with the Tim23 complex (Tim17 and Tim23)	Martincová et al., 2015 (Pyrihova 2018?)	Unique	3	IFA with overexp. HA-tagged

Giardia DB accession #	Annotation	Putative function and data for mitosomal protein	Citation	IP-gCYTb5-III status	Peptides	Experimental evidence in mitosomes
GL50803_14939	Momp35	Is anchored by two N-terminal transmembrane domains in the outer mitosomal membrane and its C-terminal domain is in the cytosol. Whether the transmembrane domains of GiMOMP35 are also responsible for its mitosomal targeting was tested by analyzing the expression of an N-terminally truncated version of the protein. Indeed, the removal of the transmembrane domains resulted in the cytosolic localization of the truncated GiMOMP35. Overexpression of this protein caused mitosomal matrix like aggregations that did not contain any proteins that would be found within the mitosomal matrix.	Martincová et al., 2015			IFA with overexp. HA-tagged
GL50803_27910	Hypothetical protein	Possible sulfurtransferase	Martincová et al., 2015			IFA with overexp. HA-tagged
GL50803_22587	Hypothetical protein (MOMTiP-6)	Localized to the mitosomes and ER. Thought to support fission of the ER and mitosome (Rout thesis 2015) possibly like yeast Gem1 GTPase that regulates the ERMES complex	Martincová et al., 2015			IFA with overexp. HA-tagged

Giardia DB accession #	Annotation	Putative function and data for mitosomal protein	Citation	IP-gCYTb5-III status	Peptides	Experimental evidence in mitosomes
GL50803_16386	Hypothetical protein	No info and IFA data from Martincova 2015 is the only paper that discussed this protein but does not make a strong argument that this is a mitosomal protein.	Martincová et al., 2015			IFA with overexp. HA-tagged
GL50803_12229	Hypothetical protein	Only data suggesting this is a mitosomal protein is from IFA.	Martincová et al., 2015			IFA with overexp. HA-tagged
GL50803_17276	Hypothetical protein	Found in Tim17 IP (pyrihov 2018) and clear IFA localization (Martincova 2015)	Martincová et al., 2015			IFA with overexp. HA-tagged
GL50803_10971	Hypothetical protein (MOMTiP-2)	Identifed in IP or pulldown with Momtip-1,3,5 Tom40 and Momp35 (Rout 2016)	Martincová et al., 2015			IFA with overexp. HA-tagged
GL50803_4852	Hypothetical protein	IFA in "probing" is not good (Martinocova 2015). Candidate PV protein (Wampfler 2014)	Martincová et al., 2015			IFA with overexp. HA-tagged
GL50803_8148	Hypothetical protein	Clear IFA localization in mitosomes (Martinocova, 2014), and discussed in Routs' thesis without giving a function.	Martincová et al., 2015			IFA with overexp. HA-tagged

Giardia DB accession #	Annotation	Putative function and data for mitosomal protein	Citation	IP-gCYTb5-III status	Peptides	Experimental evidence in mitosomes
GL50803_7035	Hypothetical protein	Dawson lab GiardiaDB IFA show this as a nuclear protein. This is also possible in the IFA found in Martincova 2015.	Martincová et al., 2015			IFA with overexp. HA-tagged
GL50803_7188	Hypothetical protein (MOMTiP-9)	Also been found to localize within PV. Suggests functional receptor-mediated endocytosis. Putative receptor found in AP2 co-IP (Zumthor 2016). Glycine rich repeat protein found as an abundant cyst protein (Ratner 2008)	Martincová et al., 2015	6.3x enriched	19 vs. 3 in control	IFA with overexp. HA-tagged
GL50803_3491	Hypothetical protein	Inner mitosomal protein	Martincová et al., 2015	Unique	2	IFA with overexp. HA-tagged
GL50803_8358	Hypothetical protein	Dawson lab on GiardiaDB IFA show this protein associates with the axoneme. If we consider this when looking at Martincova 2015 IFA, both at HA tagged and appear as if they could be axoneme associated.	Martincová et al., 2015			IFA with overexp. HA-tagged
GL50803_16424	Mlf1	**Binds DNA, binds chaperones, potential transcription factor. ** Involved in lineage commitment of primary hemopoietic progenitors by restricting erythroid formation and enhancing myeloid formation. Interferes with erythropoietin-induced erythroid terminal differentiation by	Jedelský et al., 2011	Unique	3	

Giardia DB accession #	Annotation	Putative function and data for mitosomal protein	Citation	IP-gCYTb5-III status	Peptides	Experimental evidence in mitosomes
		preventing cells from exiting the cell cycle through suppression of CDKN1B/p27Kip1 levels. Suppresses COP1 activity via CSN3 which activates p53 and induces cell cycle arrest. Binds DNA and affects the expression of several genes so may function as a transcription factor in the nucleus. Dawson GFP IFM demonstrated ventral disc lateral crest, basal bodies, cytoplasmic anterior axonemes localization.				
GL50803_2013	Grx5	Monothiol glutaredoxin involved in iron-sulfur biogenesis (PubMed:11950925, PubMed:12730244). Required for normal iron homeostasis (PubMed:11950925, PubMed:12730244). Protects cells against oxidative damage due to reactive oxygen species (PubMed:12730244). Collaborates with BOL1 in iron-sulfur protein assembly when the iron-sulfur cluster is inserted into the target protein	Rada et al., 2009	4.9x enrichment	10 vs. 2 in control	IFA with overexp. HA-tagged
GL50803_103891	Cpn60	Implicated in mitochondrial protein import and macromolecular assembly. May facilitate the correct folding of imported proteins. May also prevent misfolding and promote the refolding and proper assembly of unfolded polypeptides generated under stress conditions in the mitochondrial matrix.	Regoes et al., 2005	Unique	8	IFA with overexp. HA-tagged

Giardia DB accession #	Annotation	Putative function and data for mitosomal protein	Citation	IP-gCYTb5-III status	Peptides	Experimental evidence in mitosomes
GL50803_14581	Hsp70	Function in protein folding and assembly, and disassembly of protein complexes.	Regoes et al., 2005	Unique	24	IFA with overexp. HA-tagged
GL50803_29147	Hypothetical protein (MOMTiP-1)	N-terminal transmembrane protein of outer mitosomal membrane with c-terminus in cytosol. Expressed under the CWP1 promoter HA-tagged protein cause mitosomes to aggregate in a tube-like fashion that also stops cells from being able to divide (Rout 2016). Protein involved in DNA replication from BLAST analysis. Among the proteins associated with the outer mitosomal membrane, this one has the most common proteins between its IP and IP with gCYTB5-III	Rout et al., 2016	Unique	2	
GL50803_15154	Hypothetical protein		Rout et al., 2016			
GL50803_5785	Hypothetical protein (Qb-SNARE 4)		Rout et al., 2016			
GL50803_9503	Hypothetical protein (MOMTiP-8)		Rout et al., 2016			

Giardia DB accession #	Annotation	Putative function and data for mitosomal protein	Citation	IP-gCYTb5-III status	Peptides	Experimental evidence in mitosomes
GL50803_21943	Hypothetical protein (MOMTiP-5)		Rout et al., 2016			
GL50803_9478	GPP	Cleaves the mitochondrial sequence off newly imported precursors proteins.	Šmíd et al., 2008	Unique	7	IFA with overexp. HA-tagged
GL50803_27266	Fdx	Redox active protein functioning in the insertion of Fe/S clusters.	Tovar et al., 2003	Unique	3	IFA with overexp. HA-tagged
GL50803_14519	IscS	Scaffold protein for S in the Fe/S cluster.	Tovar et al., 2003	Unique	6	IFA with polyclonal rabbit anti-IscS
GL50803_15196	IscU	Scaffold protein for Fe in the Fe/S cluster.	Tovar et al., 2003			IFA with polyclonal rabbit anti-IscU

Appendix C: Comparing co-IP results of gCYTb5-III to co-IP of mitosomal proteins

Comparison of gCYTb5-III co-IP results to others in the literature. An "X" represents a common protein to the co-IP of gCYTb5-III, and XX mean the bait protein of the experiment was identified in the co-IP of gCYTb5-III. Bait proteins are organized in descending order left to right, and proteins are organized in descending commonality; GiOR-1 being the most common protein identified across the experiments. All protein above the thick line, are coincidently found to be mitosomal proteins.

		Tim17 (Pyrihov et al., 2018)	**GiOR-1** (Pyrih et al., 2016)	**Tim44** (Martincová et al., 2015)	**MOM TiP-1** (Rout et al., 2016)	**Pam18** (Martincová et al., 2015)	**IscS** (Rout et al., 2016)	**Hsp70** (Martincová et al., 2015)	**Tom40** (Rout et al., 2016)	**MOM P35** (Martincová et al., 2015)	**Tom40** (Martincová et al., 2015)	**MOM TiP-4** (Rout et al., 2016)	**MOM TiP-3** (Rout et al., 2016)	**Cia2** (Pyrih et al., 2016)
GL50803_91252	GiOR-1	X	XX	X	X	X	X	X	X		X		X	
GL50803_14821	IscA	X	X	X	X	X	X	X				X	X	
GL50803_16424	Mlf1	X		X	X	X		X	X	X	X			X
GL50803_14519	IscS	X	X	X	X		XX			X	X	X		
GL50803_14581	Hsp70	X	X	X	X	X	X	XX	X			X		
GL50803_17161	Tom40				X		X		XX	X	XX	X	X	
GL50803_103891	Cpn60	X	X	X	X	X	X		X					
GL50803_7188	MOMTiP-9				X				X	X	X		X	
GL50803_27266	ferredoxin	X	X	X	X		X	X						
GL50803_9478	GPP	X	X	X	X	X	X							
GL50803_29147	MOMTiP-1				XX				X			X	X	
GL50803_14845	Tim44	X	X	XX		X		X						
GL50803_2013	Grx5	X	X	X		X								
GL50803_32838	Nfu	X				X								

		Tim17 (Pyrihov et al., 2018)	**GiOR-1** (Pyrih et al., 2016)	**Tim44** (Martincová et al., 2015)	**MOM TiP-1** (Rout et al., 2016)	**Pam18** (Martincová et al., 2015)	**IscS** (Rout et al., 2016)	**Hsp70** (Martincová et al., 2015)	**Tom40** (Rout et al., 2016)	**MOM P35** (Martincová et al., 2015)	**Tom40** (Martincová et al., 2015)	**MOM TiP-4** (Rout et al., 2016)	**MOM TiP-3** (Rout et al., 2016)	**Cia2** (Pyrih et al., 2016)
GL50803_3491	hypothetical protein	X	X	X										
GL50803_22291	hypothetical protein		X							X	X			
GL50803_137745	SMC3-like protein			X										
GL50803_13922	hypothetical protein									X				
GL50803_15487	WD-40 repeat protein					X								
GL50803_16498	Nucleolar GTPase	X												
GL50803_16891	Protein C21orf2							X						
GL50803_21942	NADP-specific glutamate dehydrogenase	X												
GL50803_2338	hypothetical protein							X						
GL50803_5359	Nucleolar protein NOP5	X												

		Tim17 (Pyrihov et al., 2018)	**GiOR-1** (Pyrih et al., 2016)	**Tim44** (Martincová et al., 2015)	**MOM TiP-1** (Rout et al., 2016)	**Pam18** (Martincová et al., 2015)	**IscS** (Rout et al., 2016)	**Hsp70** (Martincová et al., 2015)	**Tom40** (Rout et al., 2016)	**MOM P35** (Martincová et al., 2015)	**Tom40** (Martincová et al., 2015)	**MOM TiP-4** (Rout et al., 2016)	**MOM TiP-3** (Rout et al., 2016)	**Cia2** (Pyrih et al., 2016)
GL50803_8001	Ribosomal protein L15	X												
GL50803_7778	hypothetical protein									X				
GL50803_8471	Gp49, putative										X			
GL50803_89887	Nucleolar GTP-binding protein 2	X												
GL50803_90950	ATP-dependent RNA helicase	X												
GL50803_96818	hypothetical protein										X			
GL50803_92498	NEK Kinase		X											
GL50803_8444	MDR Permease													X
Total		**18**	**13**	**12**	**11**	**10**	**8**	**8**	**7**	**7**	**7**	**5**	**5**	**2**

Appendix D: Full list of candidate proteins in MS analysis of gCYTB5-III co-IP

This is the list of proteins found unique to the co-IP of gCYTB5-III. The Giardia DB accession number # is the unique identifier of the gene in GiardiaDB, the annotation of the protein is based on its best match in BLAST searches. IP-gCYTb5-III status is either unique to or 2- fold or higher enrichment in the immunoprecipitate for gCYTB5-III compared to the pre-immune control. The last three columns are for the presence of peptides for these proteins in controls from my previous co-IP (as well as 6 control samples from (Pyrih et al., 2016). The inclusion of these control sample in my analysis was to increase the confidence of proteins found unique to the co-IP of gCYTb5-III and to consider proteins with lower than 2-fold enrichment if they are not common contaminants in other control co-IP samples. DSP CL PI is number of peptides of proteins common to the pre-immune control of a co-IP that was crosslinked with DSP rather than the BMH of the results discussed in this thesis. Non-CL PI is number of peptides of proteins common to the pre-immune control of a co-IP that was not crosslinked prior to co-IP. Finally, Pyrih 2016 controls are qualitative and do not contain a number but rather if peptides for the protein were found in at least 1 of the 6 control samples. Proteins highlighted in green are either experimentally shown to be nuclear or anticipated to be nuclear based on their annotation. Proteins highlighted in orange are mitosomal proteins and have been extensively described as such.

Giardia DB accession #	Annotation	IP-gCYTb5-III status	DSP CL PI	Non-CL PI	Pyrih 2016 controls
GL50803_14581	Chaperone protein DnaK HSP70 (mitochondria HSP70)	Unique			
GL50803_115245	Coiled-coil protein (possible importin)	Unique			
GL50803_13922	hypothetical protein	Unique		1.0	
GL50803_9722	Protein 21.1	Unique			
GL50803_103891	Chaperonin 60	Unique			
GL50803_91252	Nitric oxide synthase, inducible (GiOR-1)	Unique			
GL50803_16975	DNA topoisomerase II	Unique			
GL50803_15587	Protein 21.1	Unique			
GL50803_9478	GPP, unique single subunit matrix processing peptidase (bMPP)	Unique			
GL50803_3762	Protein 21.1	Unique			
GL50803_17005	Protein 21.6	Unique			Y
GL50803_14519	Cysteine desulfurase (IscS)	Unique			
GL50803_15487	WD-40 repeat protein	Unique			
GL50803_5593	Ribosomal protein L11	Unique	6.0	5.0	Y
GL50803_17587	CTP synthase	Unique			

Giardia DB accession #	Annotation	IP-gCYTb5-III status	DSP CL PI	Non-CL PI	Pyrih 2016 controls
GL50803_6933	hypothetical protein	Unique			
GL50803_8228	[SNF2L1] DNA-dependent ATPase, putative	Unique			
GL50803_89347	DNA-directed RNA polymerase II largest subunit RPB1	Unique			
GL50803_14821	HesB domain-containing protein (IscA)	Unique			
GL50803_7309	Syntaxin-like protein 1	Unique			
GL50803_115337	hypothetical protein	Unique			
GL50803_10568	hypothetical protein (binds GTP-Rho)	Unique			
GL50803_9119	ATP-dependent RNA helicase	Unique			
GL50803_137705	hypothetical protein	Unique			
GL50803_2323	hypothetical protein	Unique			
GL50803_25238	High cysteine protein	Unique			
GL50803_32697	hypothetical protein	Unique		1.0	
GL50803_95406	hypothetical protein	Unique			
GL50803_14098	ATP-dependent RNA helicase	Unique			
GL50803_5648	hypothetical protein	Unique		1.0	Y
GL50803_90950	ATP-dependent RNA helicase	Unique			Y
GL50803_8608	hypothetical protein	Unique			
GL50803_14972	hypothetical protein	Unique			
GL50803_16037	hypothetical protein	Unique		1.0	
GL50803_101212	hypothetical protein	Unique			
GL50803_9007	hypothetical protein	Unique			
GL50803_7760	Sentrin	Unique			
GL50803_4236	Dynein light chain	Unique			
GL50803_33870	Cytochrome b5 isotype III	Unique			
GL50803_27266	[2Fe-2S] ferredoxin	Unique			
GL50803_13930	ARF3	Unique		1.0	
GL50803_4463	Dynein light chain	Unique			
GL50803_6439	hypothetical protein	Unique			
GL50803_11305	hypothetical protein	Unique			
GL50803_32838	hypothetical protein	Unique			
GL50803_14869	Ribosomal protein L24	Unique			Y
GL50803_17030	Chaperone protein dnaJ	Unique			
GL50803_4349	Endothelin-converting enzyme 2	Unique		2.0	

Giardia DB accession #	Annotation	IP-gCYTb5-III status	DSP CL PI	Non-CL PI	Pyrih 2016 controls
GL50803_10027	hypothetical protein	Unique			
GL50803_15383	Peroxiredoxin 1	Unique	9.0		
GL50803_16424	Mlf1	Unique		14.0	
GL50803_7566	hypothetical protein	Unique		1.0	Y
GL50803_14845	Tim44	Unique			
GL50803_5632	Exosome complex exonuclease, putative	Unique			
GL50803_13269	hypothetical protein	Unique	4.0	1.0	
GL50803_3977	G2/mitotic-specific cyclin B	Unique	2.0		
GL50803_16906	Phosphatidate cytidylyltransferase	Unique			Y
GL50803_9121	hypothetical protein	Unique			
GL50803_95064	tRNA-ribosyltransferase, putative	Unique			
GL50803_17298	hypothetical protein	Unique			
GL50803_5772	CDC72	Unique			
GL50803_28954	hypothetical protein	Unique			
GL50803_21803	hypothetical protein	Unique			
GL50803_13194	VSP AS8	Unique		7.0	
GL50803_16313	Hypothetical protein	Unique			
GL50803_17277	Phospholipase B	Unique	2.0		
GL50803_13791	ATP-dependent RNA helicase	Unique			Y
GL50803_21063	hypothetical protein (possible gyrase)	Unique			
GL50803_89887	Nucleolar GTP-binding protein 2	Unique			Y
GL50803_24279	hypothetical protein	Unique		1.0	
GL50803_15823	1,4-alpha-glucan branching enzyme	Unique			
GL50803_15192	hypothetical protein	Unique			
GL50803_14487	hypothetical protein	Unique			
GL50803_13875	Phosphatase	Unique			
GL50803_92031	RNA binding protein, putative	Unique			
GL50803_15344	MCM2	Unique			
GL50803_34179	hypothetical protein	Unique			
GL50803_16916	hypothetical protein	Unique			
GL50803_14593	hypothetical protein	Unique		1.0	
GL50803_39312	Midasin	Unique			
GL50803_29500	hypothetical protein	Unique			

Giardia DB accession #	Annotation	IP-gCYTb5-III status	DSP CL PI	Non-CL PI	Pyrih 2016 controls
GL50803_13575	Dynein light chain	Unique			
GL50803_29147	hypothetical protein	Unique		1.0	
GL50803_4156	HIT family protein	Unique			
GL50803_6812	hypothetical protein	Unique			Y
GL50803_24451	hypothetical protein	Unique		9.0	
GL50803_14651	Glucosamine 6-phosphate N-acetyltransferase	Unique			Y
GL50803_3367	Histone H3.3 (active chromatin or Euchromatin)	Unique			Y
GL50803_3978	Ubiquitin-conjugating enzyme E2-17	Unique		2.0	Y
GL50803_14960	hypothetical protein	Unique			
GL50803_17367	hypothetical protein	Unique			
GL50803_6366	hypothetical protein	Unique			
GL50803_17116	hypothetical protein (cytochrome b5)	Unique			
GL50803_17261	hypothetical protein	Unique			
GL50803_7873	Yip interacting protein, putative	Unique			
GL50803_14841	Phosphoglycolate phosphatase	Unique			
GL50803_5786	Ribosome biogenesis protein NEP1, putative	Unique			
GL50803_11434	20S proteasome alpha subunit 2	Unique	3.0		
GL50803_9060	hypothetical protein	Unique			
GL50803_27059	Proteasome subunit beta type 7 precursor	Unique	2.0		
GL50803_3491	hypothetical protein	Unique			
GL50803_4059	5-methylthioadenosine nucleosidase, S-adenosylhomocysteine nucleosidase	Unique			
GL50803_9594	Heat shock 70kD protein binding protein	Unique			
GL50803_10856	Alpha-snap	Unique			
GL50803_6170	Coatomer delta subunit	Unique			
GL50803_17278	hypothetical protein	Unique			
GL50803_8037	Kinase, CMGC CDK	Unique		4.0	
GL50803_2053	Serine/threonine protein phosphatase 4	Unique			
GL50803_10612	Phosphotyrosyl phosphatase activator protein, putative	Unique			
GL50803_7474	DNA-directed RNA polymerase RPB3	Unique			Y
GL50803_7018	hypothetical protein	Unique			
GL50803_10221	hypothetical protein	Unique			
GL50803_13661	Eukaryotic translation initiation factor 3 subunit 2	Unique			
GL50803_17161	Tom40, hypothetical protein	Unique			

Giardia DB accession #	Annotation	IP-gCYTb5-III status	DSP CL PI	Non-CL PI	Pyrih 2016 controls
GL50803_5615	hypothetical protein	Unique			
GL50803_10055	DNA-directed RNA polymerase subunit D	Unique			
GL50803_11206	unspecified product	Unique			
GL50803_24372	ENC6 protein	Unique			
GL50803_16127	Replication factor C, subunit 5	Unique			
GL50803_114623	hypothetical protein	Unique			
GL50803_12109	hypothetical protein	Unique			
GL50803_4331	26S proteasome non-ATPase regulatory subunit 6	Unique		1.0	
GL50803_8524	Transitional endoplasmic reticulum ATPase	Unique		2.0	
GL50803_4026	Alpha-19 giardin	Unique			
GL50803_14753	Histone acetyltransferase type B subunit 2	Unique			
GL50803_32399	hypothetical protein	Unique			
GL50803_8189	Ubiquitin carboxyl-terminal hydrolase 14	Unique			
GL50803_137603	TMP52	Unique			
GL50803_16882	Bystin	Unique			
GL50803_27520	Kinase, CMGC CK2	Unique			
GL50803_7021	Protein 21.1	Unique			
GL50803_2483	Kinase, NEK	Unique	3.0	1.0	
GL50803_10162	hypothetical protein	Unique			
GL50803_17308	mRNA capping enzyme alpha subunit	Unique			
GL50803_14856	Signal recognition particle receptor	Unique		1.0	
GL50803_6615	hypothetical protein	Unique			
GL50803_13836	hypothetical protein	Unique			
GL50803_16356	Suppressor of actin 1	Unique			
GL50803_16760	Phenylalanyl-tRNA synthetase beta chain	Unique	2.0		
GL50803_22455	hypothetical protein	Unique			
GL50803_5533	DUB-1	Unique			
GL50803_8916	Signal recognition particle 68	Unique			
GL50803_14200	Molybdenum cofactor sulfurase	Unique			
GL50803_6492	hypothetical protein	Unique			
GL50803_32571	hypothetical protein	Unique			
GL50803_116477	VSP	Unique		4.0	
GL50803_14181	Spindle pole protein, putative	Unique			Y

Giardia DB accession #	Annotation	IP-gCYTb5-III status	DSP CL PI	Non-CL PI	Pyrih 2016 controls
GL50803_91712	Amino acid transporter family	Unique			
GL50803_14765	hypothetical protein	Unique			
GL50803_88071	Protein 21.1	Unique			
GL50803_8589	Suppressor of actin 1	Unique			
GL50803_15573	hypothetical protein	Unique		1.0	
GL50803_4498	Cleavage and polyadenylation specificity factor, 73 subunits	Unique			
GL50803_8035	Block of proliferation 1, BOP1	Unique		1.0	
GL50803_95549	Kinase, NEK	Unique			
GL50803_101955	hypothetical protein	Unique			
GL50803_4371	Kinesin-8	Unique			
GL50803_14916	Kinase, NEK	Unique			
GL50803_14167	hypothetical protein	Unique			
GL50803_16230	Hypothetical protein	Unique			
GL50803_14158	Protein 21.1	Unique			
GL50803_3146	hypothetical protein	Unique			
GL50803_16264	WD-40 repeat protein	Unique			
GL50803_102248	Coiled-coil protein	Unique			
GL50803_34058	Mismatch repair protein	Unique			
GL50803_94762	hypothetical protein	Unique			
GL50803_14346	hypothetical protein	Unique			
GL50803_112489	hypothetical protein	Unique			
GL50803_137745	SMC3-like protein	Unique			
GL50803_92739	ATP-dependent RNA helicase A	Unique			
GL50803_102722	Ribosome biogenesis protein BMS1	Unique			Y
GL50803_113522	Kinase, AGC MAST (likely FUS3 homolog)	Unique			
GL50803_17123	hypothetical protein	Unique			
GL50803_17362	hypothetical protein	Unique			
GL50803_27326	DNA polymerase alpha subunit A	Unique			
GL50803_103838	Kinase, ULK	Unique			
GL50803_34701	hypothetical protein	Unique			
GL50803_23634	hypothetical protein	Unique			
GL50803_23496	RNA polymerase AI large subunit	Unique			
GL50803_113740	hypothetical protein	Unique			

Giardia DB accession #	Annotation	IP-gCYTb5-III status	DSP CL PI	Non-CL PI	Pyrih 2016 controls
GL50803_112978	Chromodomain helicase-DNA-binding protein, putative	Unique			
GL50803_91324	hypothetical protein	Unique			
GL50803_5359	Nucleolar protein NOP5	1.9	3.0	7.0	Y
GL50803_2098	ATP-dependent RNA helicase p54, putative	1.9	4.0	2.0	
GL50803_10608	hypothetical protein	1.9		1.0	
GL50803_16311	Centromere/microtubule binding protein CBF5	1.8			Y
GL50803_113554	26S proteasome ATPase subunit S4, putative	1.8			
GL50803_16891	Protein C21orf2	1.8		1.0	
GL50803_10661	Ubiquitin-conjugating enzyme E1	1.8	2.0	1.0	Y
GL50803_27925	Protein 21.1	1.8	21.0	16.0	Y
GL50803_17337	Ribosomal protein P1B	1.8	7.0	1.0	
GL50803_4197	Phosphatidylinositol transfer protein alpha isoform	1.8	5.0	3.0	Y
GL50803_16575	ABC transporter family protein	1.8			
GL50803_16588	hypothetical protein	1.7	15.0	6.0	
GL50803_9062	Long chain fatty acid CoA ligase 5	1.7	4.0	6.0	
GL50803_10919	Ribosomal protein S10B	1.7		2.0	
GL50803_13747	C4 group specific protein	1.7		5.0	
GL50803_21942	NADP-specific glutamate dehydrogenase	1.7	40.0		Y
GL50803_9117	CAMP-dependent protein kinase regulatory chain	1.7		3.0	Y
GL50803_9011	Glycyl-tRNA synthetase	1.7	5.0	2.0	
GL50803_9508	Metalloprotease, insulinase family	1.7	6.0	1.0	Y
GL50803_12091	Macrophage migration inhibitory factor	1.7			Y
GL50803_10524	hypothetical protein	1.7		9.0	Y
GL50803_14311	Serine/threonine protein phosphatase PP-X isozyme 2	1.7	6.0		Y
GL50803_8172	Dynein heavy chain	1.7			
GL50803_15514	Kinase, STE STE20	1.7			Y
GL50803_16326	Protein 21.1	1.7			
GL50803_104031	Glycogen synthase, putative	1.7			
GL50803_21474	hypothetical protein	1.7			
GL50803_9808	Chaperone protein DnaJ	1.6	11.0	4.0	Y
GL50803_14859	Protein 21.1	1.6	6.0	7.0	Y
GL50803_3595	Endonuclease III	1.6			
GL50803_5659	S-adenosylmethionine synthetase	1.6	3.0	2.0	Y

Giardia DB accession #	Annotation	IP-gCYTb5-III status	DSP CL PI	Non-CL PI	Pyrih 2016 controls
GL50803_6304	Fe-hydrogenase-1 (Nar1)	1.6	3.0		
GL50803_40067	hypothetical protein	1.6	2.0	1.0	
GL50803_10843	Thymus-specific serine protease precursor	1.6			
GL50803_17627	hypothetical protein	1.6			
GL50803_12216	Vacuolar ATP synthase subunit B	1.6	17.0	8.0	Y
GL50803_8001	Ribosomal protein L15	1.6	6.0	8.0	Y
GL50803_93294	hypothetical protein	1.6	3.0	5.0	
GL50803_16717	hypothetical protein	1.5	5.0	2.0	Y
GL50803_14702	RRNA biogenesis protein RRP5	1.5			
GL50803_15228	Ribosomal protein S15A	1.5	13.0	11.0	Y
GL50803_15048	ATP-dependent RNA helicase-like protein	1.5	8.0	23.0	Y
GL50803_97219	Fibrillarin-like pre-rRNA processing protein Narcisi et al	1.5	4.0	11.0	Y
GL50803_7662	RNase L inhibitor	1.5	3.0	1.0	
GL50803_17165	ABC transporter, ATP-binding protein	1.5			
GL50803_92246	Cation-transporting ATPase 2, putative	1.5			
GL50803_9355	hypothetical protein	1.5		1.0	
GL50803_7778	hypothetical protein	1.5			
GL50803_8235	Protein 21.1	1.5		1.0	
GL50803_17579	Inositol-3-phosphate synthase	1.5			
GL50803_6671	hypothetical protein	1.5			
GL50803_17119	hypothetical protein	1.5			
GL50803_17411	TCP-1 chaperonin subunit gamma	1.5	9.0	4.0	
GL50803_17054	Acidic ribosomal protein P0	1.5	22.0	10.0	Y
GL50803_3896	Sec61-gamma	1.5		2.0	
GL50803_34093	hypothetical protein	1.5	3.0	1.0	Y
GL50803_17163	Peptidyl-prolyl cis-trans isomerase B precursor	1.5	16.0		Y
GL50803_14874	hypothetical protein	1.5			
GL50803_100955	Mitotic spindle checkpoint protein MAD2	1.5			
GL50803_7323	hypothetical protein	1.5			
GL50803_10299	hypothetical protein	1.5			
GL50803_15127	Deoxyribose-phosphate aldolase lateral transfer candidate	1.5	4.0	1.0	Y
GL50803_4204	MutT/nudix family protein	1.5			
GL50803_17617	hypothetical protein	1.5			

Giardia DB accession #	Annotation	IP-gCYTb5-III status	DSP CL PI	Non-CL PI	Pyrih 2016 controls
GL50803_11486	20S proteasome alpha subunit 7	1.5	2.0		
GL50803_96264	hypothetical protein	1.5	2.0		
GL50803_10341	hypothetical protein	1.5		1.0	
GL50803_15538	Eukaryotic translation initiation factor 5	1.5	3.0		
GL50803_6120	hypothetical protein	1.5		2.0	Y
GL50803_7950	26S protease regulatory subunit 6B	1.5			
GL50803_14434	Protein 21.1	1.5	3.0		
GL50803_8471	Gp49, putative	1.5			
GL50803_22291	hypothetical protein	1.5		2.0	
GL50803_13962	Hydroxymethylglutaryl-CoA synthase	1.5			
GL50803_96818	hypothetical protein	1.5			
GL50803_86683	26S protease regulatory subunit 7	1.5		3.0	
GL50803_16894	hypothetical protein	1.5			
GL50803_12235	N2,N2-dimethylguanosine tRNA methyltransferase, putative	1.5			
GL50803_8886	Kinesin-14	1.5			
GL50803_96537	ATP-dependent RNA helicase	1.5			Y
GL50803_13315	hypothetical protein	1.5			
GL50803_9430	hypothetical protein	1.5			
GL50803_32676	hypothetical protein	1.5			
GL50803_113133	hypothetical protein	1.5			
GL50803_17164	Sec24-like	1.5		2.0	
GL50803_17110	hypothetical protein	1.5			
GL50803_5784	hypothetical protein	1.5			
GL50803_94653	Periodic tryptophan protein 2-like protein	1.5			
GL50803_21411	ABC transporter, ATP-binding protein	1.5			
GL50803_10813	hypothetical protein	1.5			
GL50803_16915	Protein 21.1	1.5			
GL50803_16652	Ribosomal protein S13	1.5	2.0	5.0	Y
GL50803_96460	Alanyl-tRNA synthetase	1.5	10.0		Y